Topochemistry of Zeolites and Related Materials. 1. Topology and Geometry

JOSEPH V. SMITH

Department of Geophysical Sciences and Materials Research Laboratory, The University of Chicago, Chicago, Illinois 60637

Received July 17, 1987 (Revised Manuscript Received November 2, 1987)

Contents

I. Introduction

Zeolites provide a nice example of the fruitful symbiosis between mineralogists, structural crystallographers, inorganic chemists, and materials scientists.[1–15a] Indeed, joint professorships of chemistry and mineralogy were typical in the U.S. during the early 19th century,[16] and mineralogists were listed as one of the six subcategories of chemists in 1870.[17] Many zeolites were first described as minerals, and the chemical substitutions in the frameworks of synthetic zeolites and the new related microporous aluminophosphate-based materials[18] were known earlier in the feldspar[19] and feldspathoid groups of minerals.[19a] The mathematical concepts used to describe the topology of frameworks in zeolites have developed from ones known to Greek philosophers and from ones used to such stunning effect in Romanesque and Islamic decorations. In this 20th century, development of crystallographic and spectroscopic techniques has led to spectacular discoveries about the topochemistry of zeolites. Deliberate control of crystallization processes has produced many materials not known in Nature. Controlled chemical and physical treatments have been used to tailor valuable new products for industry, including shape-selective molecular sieve catalysts. This triumphant application of observations and theoretical concepts to the material needs of the human race is a testimony to the power

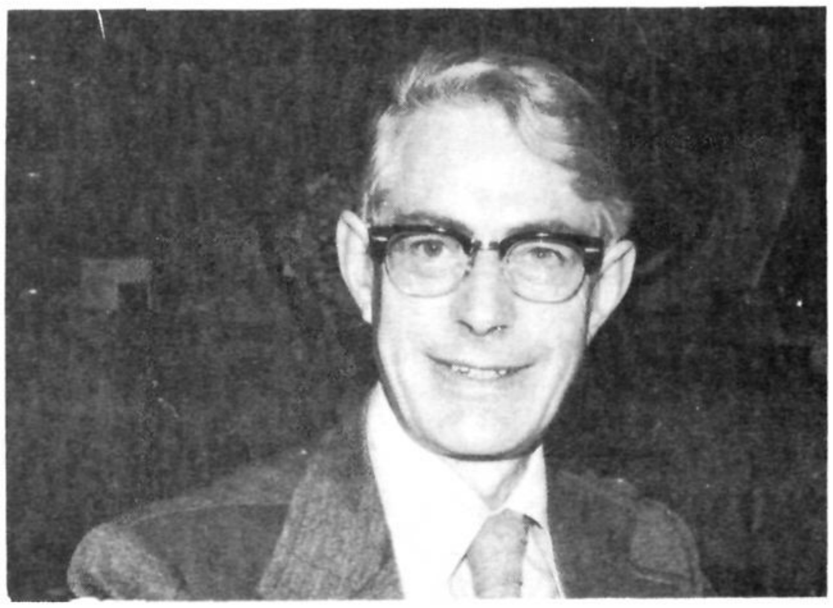

Joseph V. Smith was born in Crich, Derbyshire, England, in 1928 and is a naturalized U.S. citizen. He obtained a B.A. degree (1948, First Class Honors, Natural Sciences) and a Ph.D. degree (1951, Physics, Crystallography) from Cambridge University. After spending 3 years as Postdoctoral Fellow at the Geophysical Laboratory of the Carnegie Institution of Washington, he spent 2 years as Demonstrator in the Department of Mineralogy and Petrology at Cambridge University and 4 years in the Department of Geology and Mineralogy at The Pennsylvania State University. In 1960, he joined The University of Chicago, where he is Louis Block Professor of Physical Sciences. Professor Smith applies mathematical, physical, and chemical concepts to inorganic materials, especially those occurring in rocks. His work on feldspar, zeolite, and other framework minerals has been carried out in parallel with structural studies of molecular sieves and catalysts. Professor Smith collaborates closely with scientists in the chemical and petroleum industries and is currently determining the structures of new aluminophosphate molecular sieves invented by Union Carbide scientists. He uses X-ray and neutron diffraction techniques to elucidate the structural properties of a range of oxygen-based inorganic materials and is taking advantage of new synchrotron and pulsed-neutron techniques. Professor Smith has pioneered microanalytical techniques based on the electron microprobe (1961), ion microprobe (1974), and synchrotron X-ray fluorescence microprobe (1985). He has made numerous studies of minerals in lunar rocks and meteorites as well as in upper mantle and early crustal rocks of the Earth. His chemical and mineralogical studies led to a model of heterogeneous accretion and early melting of the Earth and Moon. Professor Smith is a member of the National Academy of Sciences and a Fellow of the Royal Society of London, the American Academy of Arts and Sciences, the Mineralogical Societies of America and Great Britain, the Geological Society of America, the American Geophysical Union, and the Meteoritical Society. He received the Murchison Medal of the Geological Society of London and the Roebling Medal of the Mineralogical Society of America. Professor Smith served on the Seitz–Eastman Committee of the National Academy of Sciences and is currently on the Board of Earth Sciences. He has written two books, *Feldspar Minerals* (two volumes, revised edition in press) and *Geometrical and Structural Crystallography*, and over 320 refereed papers.

0009-2665/88/0788-0149$06.50/0

of interdisciplinary research.

The topological and geometrical properties of zeolites and related microporous materials are covered in the first part of this review. Topochemical properties, including chemical substitutions, order–disorder, and topotactic reactions, will be covered in the second part.

The word zeolite (boiling stone) was created by the Swedish scientist A. F. Cronstedt[20] in 1756 after heating stilbite in a blowpipe flame. Reversible dehydration of zeolites without loss of crystalline integrity,[21] together with absorption of liquids[22] and gases,[23] implied that zeolites have a microporous continuous framework.[22] This was confirmed by the X-ray structure analyses of natural and ion-exchanged analcime and the fibrous zeolites.[24–28] Selective adsorption of molecules smaller than 5 Å in diameter by chabazite[29] led to the concept of a molecular sieve by J. W. McBain.[30] Reversible ion-exchange is a property of various types of minerals and synthetic materials, including zeolites, as discovered for chabazite and natrolite in 1858.[31] However, most ion exchangers lack the additional property of reversible loss of water;[1] indeed ion exchange can occur in anhydrous systems.

Currently, the term zeolite has and is being used in many inconsistent ways for a wide range of materials with either ion-exchange or adsorption properties, or both.[32–35] The mineralogical community tends to adhere to a usage consistent with a loose definition:[36] "a zeolite is an aluminosilicate with a framework structure enclosing cavities occupied by large ions and water molecules, both of which have considerable freedom of movement, permitting ion-exchange and reversible dehydration". Since the term "framework" is used imprecisely in descriptions of crystal structures,[37] the foregoing definition should be amended to specify that the Al and Si atoms occupy 4-connected vertices of a three-dimensional net, and the oxygen atoms occupy 2-connected positions between the 4-connected vertices. Thus each tetrahedral (T) vertex is surrounded by four oxygen positions, and each oxygen is chemically bonded to two (Si, Al) atoms in T sites. The designation (4;2) specifies this type of connection and provides a clear mathematical distinction[38] from other types of aluminosilicate frameworks in which an oxygen atom is chemically bonded to either one or three tetrahedral atoms and from frameworks in which Si and Al atoms have five or six oxygen neighbors.[39–42] The term "analogue" is typically used in the mineralogical literature for a material that is isostructural except for a chemical substitution; e.g., the gallium analogue of analcime $NaAlSi_2O_6{\cdot}H_2O$ would be $NaGaSi_2O_6{\cdot}H_2O$. The adjective zeolitic is often used loosely for materials, not necessarily with a (4;2)-3D net, that show ion exchange, or reversible dehydration, or both.

The nonmineralogical community uses the term zeolite in diverse and partly inconsistent ways. At one extreme, some chemists tend to follow the practice of mineralogists, as exemplified by the late D. W. Breck (pp 4–5 of ref 1). At the other extreme, various microporous materials are classified as zeolites even though they lack one or more of the properties listed above.

Some synthetic polymorphs of silica have the same type of (4;2) framework topology as zeolites that obey the mineralogical criteria. Thus the synthetic silica polymorph silicalite[43] has the same framework topology as the synthetic zeolite ZSM-5,[44] and no gap in the range of Si/Al ratios has been demonstrated in chemically zoned synthetic materials.[45] The highest Si/Al ratios of silicalites and high-silica ZSM-5 are smaller than the lowest values found in naturally occurring silica polymorphys such as quartz, which lacks the physical and chemical features of a zeolite.[46] Silicalite is definitely a molecular sieve, but various other microporous silicas lack windows large enough for reversible sorption of water molecules, except perhaps under extreme conditions. The term clathrasil[35] is more appropriate than zeolite for these materials.

Some structures listed in compilations of zeolites are based on an interrupted tetrahedral framework, in which one or more oxygen atoms are bonded to only one T atom; commonly the local ionic charge is balanced by attachment of a hydrogen. Actually, some synthetic zeolites contain a considerable fraction of framework hydroxyl groups, as exemplified by studies on ZSM-5 samples with excess ion-exchange capacity,[47–49] and all zeolites may have terminal hydroxyls at internal defects and the external surface.[50] Hence study of materials with interrupted frameworks is relevant to research on zeolites (sensu stricto).

After calcination to remove encapsulated organic species, some of the microporous aluminophosphates with Al/P = 1 are molecular sieves,[51] but they do not obey the mineralogical definition of a zeolite. However, some have the same framework topology as found in zeolites (sensu stricto).[52] The relationship is even more complex for metal-substituted aluminophosphates,[18] especially for the silicoaluminophosphates.

There is a host of materials with 3D frameworks in which each oxygen is connected to two metal atoms in 3-, 5-, or 6-coordination (this includes some of the as-synthesized aluminophosphates before calcination). Again, these materials are not zeolites in the mineralogical sense, but all are valuable from the theoretical viewpoint, and some might become commercially useful.

Finally, some natural materials included in lists of zeolites are anhydrous and can be considered as inclusion complexes of salts inside aluminosilicate frameworks. The best example is sodalite, $Na_6Al_6Si_6O_{24}{\cdot}2NaCl$, which is classed as a feldspathoid by mineralogists. However, there is a complex group[53] of hydrated and hydroxylated synthetic sodalites, $Na_8Si_6Al_6O_{24}(OH)_2{\cdot}0\text{–}8H_2O$, including one labeled as zeolite Zh.[54] Furthermore, a pure silica-sodalite with encapsulated ethylene glycol has been synthesized,[55] and classified as a clathrasil.[35]

It seems best in this review to consider the topochemistry of all the above microporous, and even some nonmicroporous, inorganic materials that are useful from the theoretical and practical viewpoints. In order to avoid nomenclature problems, the term "zeolites and related materials" will be used. Table I summarizes the essential topochemical features of selected structural types. Figure 1 shows stereoplots of the T–T linkages of those frameworks that best represent the topological principles to be discussed in the next section. A more comprehensive atlas of stereoplots together with crystallographic and geometrical information is being prepared by W. M. Meier and D. H. Olson with the assistance of the Structure Commission of the International Zeolite Association. It will be about twice as large as the first atlas[33] published in 1978. Also useful are ref 56 and 57.

Because many noncrystallographers have difficulty with stereoplots of T–T linkages, some advice may be helpful. Make sure that the lenses of the stereoviewer are exactly over the center of each stereoview. If the 3D image does not pop into place, make a copy of the stereoview and put a mark on a corresponding point of each stereoview. Now swivel your eyes to merge the marks. Of course, the stereoview should be flat. Some people can manage without a stereoviewer, especially if marks are used. Reduction from the usual 6.3 cm distance to about 5.8 cm may help.

Part II of this review considers general topological features of zeolites and related materials, and part III lists the crystallographic data for each structure type.

II. Topology and Geometry of (4;2)-Connected Regular 3D Nets

A. Mathematical Concepts

Technical descriptions of the topology of regular nets aree given in ref 58 and 59 and an introduction to the crystallographic applications is provided in ref 60.

From the strictly topological viewpoint, only the connectivity of a (4;2)-3D net is important. Because each oxygen atom of a (4;2)-connected TO_2 framework structure lies between two T atoms, it is sufficient to consider only the connectivity of the T atoms. Each T position becomes the vertex of a 3D net and each vertex lies at the intersection of four T–T edges to adjacent T positions. The resulting 3D net, which must be infinite if it is to be regular, is described as 4-connected. The family of different types of 4-connected 3D nets is distinct from the infinite families with a different order of connectivity, such as the 3-connected family or families with more than one type of connectivity.

There is an infinity of 4-connected 3D nets and there is no known systematic procedure for deriving all of them. At the current state of mathematical knowledge, the only successful systematic way to classify known 3D nets and to invent new ones is to look for common subunits, to find out whether such subunits can be linked together in new ways, and to investigate whether the subunits can be modified. As new nets are discovered in new crystal structures, the inventory of subunits increases. Currently, the first steps are being taken to establish a systematic hierarchy of subunits. Still pending is an attempt to build all possible topologies by a systematic search in 3D space for all ways to fasten edges together into a continuous net. In practice, such an attempt must necessarily be limited to nets with a small repeat unit. To the regular nets must be added the irregular ones which are relevant to zeolites with topological disorder.

Several types of subunits can be found in 3D nets. The simplest is an edge (Figure 2) between two vertices. Others are rings (Figure 2), polyhedra (Figure 3 and 4), coplanar and noncoplanar chains (Figure 5), and 2D nets (Figure 6–14). All of these types of subunits are useful for classification, and all can be linked together in various ways to make 3D nets. Table I lists selected subunits in the 3D nets of zeolites and related materials.

Extremely important is the distinction between the topological connectivity and the geometrical relationships in a 4-connected 3D net. Topology takes no account of the relative length of T–T edges or of the magnitude of the T–T–T angles. All zeolites (sensu stricto) have all the (Si,Al)–O distances between 1.58 and 1.78 Å, most of the O–(Si,Al)–O angles within 5° of the ideal tetrahedral angle of 109.46°, and most of the (Si,Al)–O–(Si,Al) angles between 130 and 160° when corrections are made for thermal and positional disorder. In consequence, all T–T edges are within a few percent of 3.1 Å, and it is possible to build a useful model from tetrahedral stars and plastic tubes cut to one length. Such a model has T positions that correspond fairly closely with those in the crystal structure of an actual zeolite. The computer program[61] DLS-76 will generate a least-squares fit for the T and O positions of a particular topology when given the relative deviations from assumed reference values for distances and angles; essentially the algorithm is building a bridge with the least deviation from spans of a constant size fastened together at constant angles. Only some connectivities yield a geometry that is reasonable from the viewpoint of chemical bonding in a zeolite.[62] This geometrical approach does not work so well for the 4-connected 3D frameworks of the vanadyl silicate hydrates cavansite (Figure 1a, stereoplot) and pentagonite, in which the vanadium is nearly in square-planar coordination to four oxygens, each of which is linked to one silicon. Actually, each vanadium is also bonded to one hydroxyl to give overall square-pyramidal coordination.

A complete mathematical description of a regular 4-connected 3D net consists of the cell dimensions, space group symmetry, and fractional atomic coordinates of the vertices. A thorough description of the connectivity could be given as a matrix array listing the number of edges between each pair of vertices in the repeat unit, thereby extending the idea of a matrix array of adjacent tetrahedral vertices used for enumeration of ordering schemes of Al and Si in feldspar.[63]

A useful but nonunique description is to specify the circuit symbol for each T vertex. There are six T_i–T–T_j angles to each T vertex, and for each angle there is a shortest circuit of edges T–T_i...T_j–T. The set of six numbers is the circuit symbol of the vertex.[59] Following Wells, the circuit symbol was given for each of the nets so far enumerated by Smith and collaborators.[64–76] The circuit symbol is useful because it gives information on the local compactness of the net; thus the presence of many 3-, 4-, 5-, and 6-circuits implies compact building units, whereas 10- and 12-circuits are present in the circuit symbols of open nets with low-framework density. See ref 65 for a technical choice for branched circuits.

A further description, which may be unique, is to determine the coordination sequence,[77,77a] which counts the number N_k of vertices at k edges away from a chosen vertex. For k = 1–5, the set of five N_k is different for the nets of most zeolites but is identical for several pairs of nets with similar subunits such as those in Rho and Linde Type A,[78] which have the sequence 4–9–17–28–42.

As soon as the first crystal structures of silicates were discovered, classifications were based on subunits. The

TABLE I. Properties of Selected Microporous Materials

IUPAC code[a]	type species	chemical composition[b]	framework density[c]	types of rings[d]	types of chains[e]	types of 2D nets[f]	types of polyhedra[g]	type of access[h]
(a) Natural Zeolites and Related Aluminosilicates with a (4;2)·3D Net								
AFG	afghanite	$Na_{12}Al_{24}Si_{24}O_{96}\cdot 12NaCl\cdot 2H_2O$	15.9	4, 6		4.6.12	canc	6·rings
ANA	analcime	$Na_{16}Al_{16}Si_{32}O_{96}\cdot 16H_2O$	18.6	4, 6, 8	ts			3D·8,8,8
BIK	bikitaite	$Li_2Al_2Si_4O_{12}\cdot 2H_2O$	20.2	5, 6, 8	c, s, z	6^3; (5^28)		1D·8
BRE	brewsterite	$Sr_2Al_4Si_{12}O_{32}\cdot 10H_2O$	17.5	4, 5, 6, 8	br, 4.6		brew	2D·8,8
——	buddingtonite	$(NH_4)_4Al_4Si_{12}O_{32}\cdot 2H_2O$	21.6	4, 6, 8	cc, bs	4.8^2		1D·8
CAN	cancrinite	$Na_6Al_6Si_6O_{24}\cdot CaCO_3\cdot 2H_2O$	16.7	4, 6, 12	zz	4.6.12	canc	1D·12
CHA	chabazite	$Ca_6Al_{12}Si_{24}O_{72}\cdot 40H_2O$	14.6	4, 6, 8, 12		4.6.12	hp, chab	3D·8
——	cowlesite	$Ca_6Al_{12}Si_{18}O_{60}\cdot 33H_2O$		*i*				
DAC	dachiardite	$Na_5Al_5Si_{19}O_{48}\cdot 12H_2O$	17.3	4, 5, 6, 8, 10	c, s, z	6^3; (4.5.10); (5^28)	test	2D·8,10
EDI	edingtonite	$Ba_2Al_4Si_6O_{20}\cdot 8H_2O$	16.6	4, 8	fi			3D·8,8,8
EPI	epistilbite	$Ca_3Al_6Si_{18}O_{48}\cdot 16H_2O$	18.0	4, 5, 6, 8, 10	c, z	6^3; (4.5.10); (5^28)	test	2D·8,10
ERI	erionite	$NaK_2MgCa_2Al_9Si_{27}O_{72}\cdot 27H_2O$	15.6	4, 6, 8, 12		4.6.12	hp, canc, erio	3D·8,8,8
FAU	faujasite	$Na_{58}Al_{58}Si_{134}O_{384}\cdot 240H_2O$	12.7	4, 6, 12			hp, to, fauj	3D·12,12,12
FER	ferrierite	$Na_2Mg_2Al_6Si_{30}O_{72}\cdot 20H_2O$	17.7	5, 6, 8, 10	c, s	6^3; $(5.6.10)_1$	test	2D·8,10
GIS	gismondine	$Ca_4Al_8Si_8O_{32}\cdot 18H_2O$	15.4	4, 8	cc, bs	4.8^2		3D·8,8,8
GME	gmelinite	$Na_8Al_8Si_{16}O_{48}\cdot 24H_2O$	14.6	4, 6, 8, 12	cc	4.6.12	hp, gmel	3D·8,8,12
GOO	goosecreekite	$Ca_2Al_4Si_8O_{32}\cdot 10H_2O$	17.6	4, 5, 6, 8	bs			3D·8,8,8
HEU	heulandite	$NaCa_4Al_9Si_{27}O_{72}\cdot 24H_2O$	17.0	4, 5, 8, 10	he, 4.5^2			2D·8,10
LAU	laumontite	$Ca_4Al_8Si_{16}O_{48}\cdot 16H_2O$	17.7	4, 6, 10			laum	1D·10
LEV	levyne	$Na_3Ca_8Al_{19}Si_{35}O_{108}\cdot 50H_2O$	15.2	4, 6, 8		4.6.12	hp, levy	2D·8,8
LIO	liottite	$Ca_9Al_{18}Si_{18}O_{72}\cdot (CaSO_4)_n\cdot 2H_2O$	15.7	4, 6		4.6.12	canc, liot, loso	6·rings
MAZ	mazzite	$K_3Mg_2Ca_{1.5}Al_{10}Si_{26}O_{72}\cdot 28H_2O$	16.1	4, 6, 8, 12	c, ss	4.6.8.12	gmel	1D·12
MER	merlinoite	$K_5Ca_2Al_9Si_{23}O_{64}\cdot 23H_2O$	16.0	4, 8	cc, bs	4.8^2	op	3D·8,8,8
MOR	mordenite	$Na_4Ca_2Al_8Si_{40}O_{90}\cdot 24H_2O$	17.2	4, 5, 6, 8, 12	c, s	6^3; (4.5.8.12)	test	2D·8,12
NAT	natrolite	$Na_{16}Al_{16}Si_{24}O_{80}\cdot 16H_2O$	17.8	4, 8	fi			3D·8,8,8
OFF	offretite	$KCaMgAl_5Si_{13}O_{36}\cdot 15H_2O$	15.5	4, 6, 8, 12	ss	4.6.12	hp, canc, gmel	3D·8,8,12
PAU	paulingite	$(K,Ca,Na)_nAl_{160}Si_{512}O_{1344}\cdot 700H_2O$	15.5	4, 6, 8			op, grco, paul, plgt	3D·8,8,8
PHI	phillipsite	$K_2CaNaAl_5Si_{11}O_{32}\cdot 12H_2O$	15.8	4, 8	cc, bs	4.8^2		3D·8,8,8
SOD	sodalite (hydro·)	$Na_6Al_6Si_6O_{24}(OH)_2\cdot 2H_2O$	17.2	4, 6	ts		to	6·rings
STI	stilbite	$Na_4Ca_8Al_{20}Si_{52}O_{144}\cdot 56H_2O$	16.9	4, 5, 6, 8, 10	st, 4^26		brew	2D·8,10
THO	thomsonite	$Na_4Ca_8Al_{20}Si_{20}O_{80}\cdot 24H_2O$	17.7	4, 8	fi			3D·8,8,8
YUG	yugawaralite	$Ca_2Al_4Si_{12}O_{32}\cdot 8H_2O$	18.3	4, 5, 8	ts, bs	4.8^2; 4.5^2	yug	2D·8,8
(b) Synthetic Aluminosilicates with a (4;2)·3D Net								
ABW	Li·A(BW)	$Li_4Al_4Si_4O_{16}\cdot 4H_2O$	19.0	4, 6, 8	c, zz	6^3; 4.8^2		1D·8
EAB	TMA·E(AB)	$(Me_4N)_2Na_7Al_9Si_{27}O_{72}\cdot 26H_2O$	15.4	4, 6, 8, 12	distorted s	4.6.12	hp, gmel, eab	2D·8,8
KFI	ZK·5	$Na_{30}Al_{30}Si_{66}O_{192}\cdot 98H_2O$	14.7	4, 6, 8			hp, grco, paul	3D-8,8,8
LOS	losod	$Na_{12}Al_{12}Si_{12}O_{48}\cdot 18H_2O$	15.8	4, 6		4.6.12	canc, loso	6·rings
LTA	Linde A	$Na_{12}Al_{12}Si_{12}O_{48}\cdot 27H_2O$	12.9	4, 6, 8			cu, to, grco	3D·8
LTL	Linde L	$K_6Na_3Al_9Si_{27}O_{72}\cdot 21H_2O$	16.4	4, 6, 8, 12	ss	4.6.8.12	hp, canc	3D·8,8,12
LTN	Linde N	$Na_{384}Al_{384}Si_{384}O_{1536}\cdot 520H_2O$	15.2	4, 6, 8			hp, canc, to, grco	6·rings
MEL	ZSM·11	$(organic)Na_3Al_3Si_{93}O_{192}\cdot 16H_2O$	17.7	4, 5, 6, 7, 8, 10	p	$(5.6.10)_2$	test, mel, pent	3D·10,10,10
MFI	ZSM·5	$(organic)Na_3Al_3Si_{93}O_{192}\cdot 16H_2O$	17.9	4, 5, 6, 7, 8, 10	p	$(5.6.10)_2$	test, pest, pent	3D·10,10,10
MTN	ZSM·39	$(organic)(Si_{0.997}Al_{0.003})_{136}O_{272}$	18.7	5, 6			rd, mtn	6·rings
MTT	ZSM·23	$(organic)(Si_{0.99}Al_{0.01})_{24}O_{48}$	20.0	5, 6, 8, 10	z	6^3; $(5.6.10)_3$	pest, hest	1D·10
MTW	ZSM·12	$(organic)(Si_{0.997}Al_{0.003})_{28}O_{56}$	19.4	4, 5, 6, 7, 8, 12	z	6^3; (4.5.6.12)	mtw, hest	1D·12
——	nepheline hydrate I	$Na_{12}Al_{12}Si_{12}O_{48}\cdot 6H_2O$	18.6	4, 6, 8	s, z, zz	6^3; 4.6.8	hest	1D·8
RHO	Rho	$Na_{12}Al_{12}Si_{36}O_{96}\cdot 44H_2O$	14.3	4, 6, 8			op, grco	3D·8,8,8
TON	Theta·1	$(organic)(Si_{0.98}Al_{0.02})_{24}O_{48}$	19.7	5, 6, 8, 10	z	6^3; $(5.6.10)_1$	pest	1D·10
——	ZSM·48	*j*						
(c) Synthetic Aluminophosphates with a (4;2)·3D Net								
AFI	$AlPO_4$·5	$(organic)Al_{12}P_{12}O_{48}$	17.5	4, 6, 12	c	4.6.12	afi	1D·12
AEL	$AlPO_4$·11	$(organic)Al_{20}P_{20}O_{80}$	19.1	4, 6, 10	c	4.6.10	afi	1D·10
AST	$AlPO_4$·16	$(organic)Al_{10}P_{10}O_{40}$	16.7	4, 6			cu, trd	6·rings
——	$AlPO_4$·21	$(organic)Al_{12}P_{12}O_{48}(OH)_4$	18.1	*k*				
ATF	$AlPO_4$·25	$Al_{24}P_{24}O_{96}\cdot nH_2O$	19.7	4, 6, 8	cc	4.6.8		2D·8,8
ATT	$AlPO_4$·33	$(organic)Al_{12}P_{12}O_{48}$	16.7	4, 6, 8	c, cc, ss	4.6.8; 4.8^2		2D·8,8
AFS	$AlPO_4$·46	$(organic)Al_{56}P_{56}O_{224}$	13.7	4, 6, 8, 12	esc	4.6.12	afo, afs, af	3D·8,8,12
AFY	$AlPO_4$·50	$(organic)Al_{16}P_{16}O_{64}$	12.5	4, 8, 12		4.6.12	cu, af	3D·8,8,12
——	$AlPO_4\cdot H_3$	$Al_{16}P_{16}O_{64}\cdot 24H_2O$	17.4	*l*				
APC	$AlPO_4$·C	$Al_{16}P_{16}O_{64}$	8.0	4, 6, 8	cc	4.8^2; 6^3		3D·8,8,8
APD	$AlPO_4$·D	$Al_{16}P_{16}O_{64}$	19.8	4, 6, 8	bhs, c	4.8^2; 6^3		2D·8,8
(d) Other Aluminophosphates That Can Be Related Geometrically to a (4;2)·3D Net								
——	$AlPO_4$·14	5· and 6·coordinated Al		4, 6, 8	odc	4.8^2	odc	
——	$AlPO_4$·15	$Al_4(OH)_2$ and $AlO_4(OH)(H_2O)$		4, 8		4.8^2	odc	
——	$AlPO_4$·EN3	AlO_4 and $AlO_4(OH)$		4, 6, 8	z	4.6.8		
——	variscite	$AlO_4(OH)_2$		4, 6	c	6^3		
——	metavariscite	$AlO_4(OH)_2$		4, 6	c	6^3	laum	

TABLE I (Continued)

IUPAC code[a]	type species	chemical composition[b]	framework density[c]	types of rings[d]	types of chains[e]	types of 2D nets[f]	types of polyhedra[g]	type of access[h]
(e) Silica Polymorphs Classified as Clathrasils								
SOD	silica-sodalite	(organic)$Si_{12}O_{24}$	17.4	4, 6	ts		to	6-rings
DOH	dodecasil 1H	(organic)$Si_{34}O_{68}$	18.4	4, 5, 6			rd, doh, dooh	5, 6-rings
DDR	decado-decasil 3R	(organic)$Si_{120}O_{240}$	17.6	4, 5, 6, 8			rd, det, detr	2D-8,8; 5-rings
MEP	melano-phlogite	$(CH_4,CO_2,N_2)Si_{46}O_{92}$	19.1	5, 6			rd, mela	5, 6-rings
NON	nonasil	(organic)$Si_{88}O_{176}$	19.3	4, 5, 6			non, nona, nonas	5, 6-rings
MTN	dodecasil 3C	(organic)$Si_{136}O_{272}$	18.6	5, 6			rd, mtn	5, 6-rings
(f) Aluminosilicates with Interrupted Frameworks based mainly on a (4;2)-3D Net								
PAR	parthéite	$Ca_8Al_{16}Si_{16}O_{60}(OH)_8 \cdot 16H_2O$	18.2	4, 6, 8, 10	[m]			
ROG	roggianite	$Ca_{16}[Al_{16}Si_{32}O_{88}(OH)_{16}] \cdot 26H_2O$	15.6	4, 6, 10, 12	[n]			
WEN	wenkite	$\sim Ba_4Ca_5Al_8Si_{12}O_{39}(OH)_2(SO_4)_3 \cdot 2H_2O$	17.0	4, 6	[o]			
—	sarcolite	$Na_2Ca_6Al_5Si_5O_{23}(H_2O,OH)(S,PO_4)$		4, 7, 8	[p]			
—	ussingite	$Na_2AlSi_3O_8(OH)$		4, 6, 8	[q]			
—	bavenite	$\sim Ca_4(BeOH)_2Al_2Si_9O_{26}$		4, 6, 8	[r]			
—	leifite	$Na_6(BeOH)_2Al_2Si_{16}O_{39} \cdot 1.5H_2O$		4, 5, 6, 7	[s]			
—	chiavennite	$CaMn(BeOH)_2Si_5O_{13} \cdot 2H_2O$	20.8	4, 5, 9	[t]			

[a] IUPAC three-letter code assigned by International Zeolite Association Structure Commission. [b] A representative idealized composition is given. Extensive substitution occurs in most natural zeolites. [c] The framework density is expressed as the number of T sites per 1000 Å³. In some zeolites, the framework density can vary several percent in response to dehydration, change of Si/Al ratio, and ion exchange. [d] Only the more obvious rings are listed in frameworks with complex connectivity. [e] Only the simpler chains are listed. [f] Only the simpler 3-connected 2D nets are listed. Some are strongly distorted from the most regular shape. Some simplified circuit symbols are used. [g] Mnemonic codes are from Figures 3 and 4 and the text. [h] Channels with access limited by 8-rings or larger windows are listed with the number of directions (1D, one-dimensional; 2D, two-dimensional; 3D, three-dimensional) and the ring size of the limiting windows. Note that some rings are strongly distorted with reduction of window size from the value in Figure 1, e.g., the boat-shaped 8-rings of LTL. [i] Structure not known. [j] Probably based on disordered crankshaft chains and ferrierite 2D net. [k] As-synthesized material has both $AlPO_4$ and $AlO_4(OH)$; calcines to $AlPO_4$-25. [l] As-synthesized material has both $AlPO_4$ and $AlO_4(OH)$; calcines to $AlPO_4$-C. [m] Interrupted at (OH) on 3-connected Al. [n] Interrupted at (OH) on 3-connected Si. [o] hp and cancrinite chains linked by 3-connected T probably with (OH). [p] Interrupted oxygen on 3-connected Si is linked to two Ca. [q] Interrupted oxygens on 3-connected Si are bridged by H. [r] Interruptions at Be(OH) and SiO. [s] Interrupted at (OH) on 3-connected Be. [t] Interrupted at (OH) on 3-connected Be.

following sections consider the possible subunits in the 3D nets of zeolites and related materials in the following sequence: rings and windows, polyhedral cages and building units, 2D nets, channel systems, and internal surfaces. These subunits are useful for several reasons: (a) any subunit is a potential candidate for synthesis during growth of a zeolite or related material; (b) any cage or channel may be the container for an encapsulated species, which may even act as a template during synthesis; (c) each channel system and window places an upper limit on the sorption of molecules; (d) each ring and internal surface provides sites for bonding of exchangeable cations to the framework oxygens; (e) each unit can be checked for possible ways of inventing new nets; (f) some units are convenient for classification.

The concept of "secondary building unit" (SBU) was invented[79] on the assumption that zeolite nets would contain only one type of SBU. Furthermore, the SBU might be a precursor in the liquid phase of reaction mixtures from which the zeolite grew. Actually, many nets can be broken down into more than one type of SBU. The original eight types of SBU (4-ring, 6-ring, 8-ring, cube, hexagonal prism, 4^3 cluster, 5-ring plus one edge, 4^25^26 cluster) required the addition of a complex 5–1 cluster[33] for the pentasil family of zeolites, and even further additions since then. The designation 4^25^26 means that there are two 4-rings, two 5-rings, and one 6-ring in the cluster, and this type of nomenclature is used in Figures 3 and 4. A set of seven structural units (chain in fibrous zeolites, vertex-shared chain of 4-rings, edge-shared chain of 4-rings, 6-ring, hexagonal prism, hexagonal sheet with handles, and 4–4–1–1 heulandite unit) was selected in ref 5. In the present review, all polyhedra and clusters that look interesting from the topological viewpoint are listed in Table I.

To complete this introduction, the following is a selection of additional papers and books that have considered the broader aspects of the topology and geometry of nets in zeolites and related materials: structural classification;[36,80] structural survey and classification;[79] comprehensive survey of structures and classification;[1] symmetry aspects;[81] structures related to mordenite;[82] σ transformation interrelating known and hypothetical nets;[83] mineralogy and crystal chemistry;[84] constituent sheets in the mordenite group;[85] new structures and zeolite minerals;[86] aluminophosphate structures;[87] structure–template specificity in aluminophosphate molecular sieves;[88] mineralogical survey;[89] framework topologies, stacking faults, twinning, intergrowths, clathrasils, lovdarite with 3-rings;[90] various concepts and new nets;[91] application of concept of coordination network to nets of framework silicates;[92] further review with comments on 3-rings in lovdarite, faulting, analogy with organic siloxanes, loop configuration, and very open networks;[93] systematic enumeration of nets containing the 4^25^4 cluster;[94] topology of frameworks of natural zeolites;[5] examples of interrupted frameworks;[95] inversion transformation interrelating nets in the pentasil family;[96] nets obtained by repetitive twinning of the unit cell of cristobalite;[96a] AB-5, AB-6, and AB-7 nets;[96b] new aluminophosphates.[96c]

B. Rings and Windows

Figure 2 summarizes the essential geometrical features of T_nO_n rings and their potential use as limiting windows in molecular sieves. Table I lists the types of rings in zeolites and related materials, and ref 33 gives

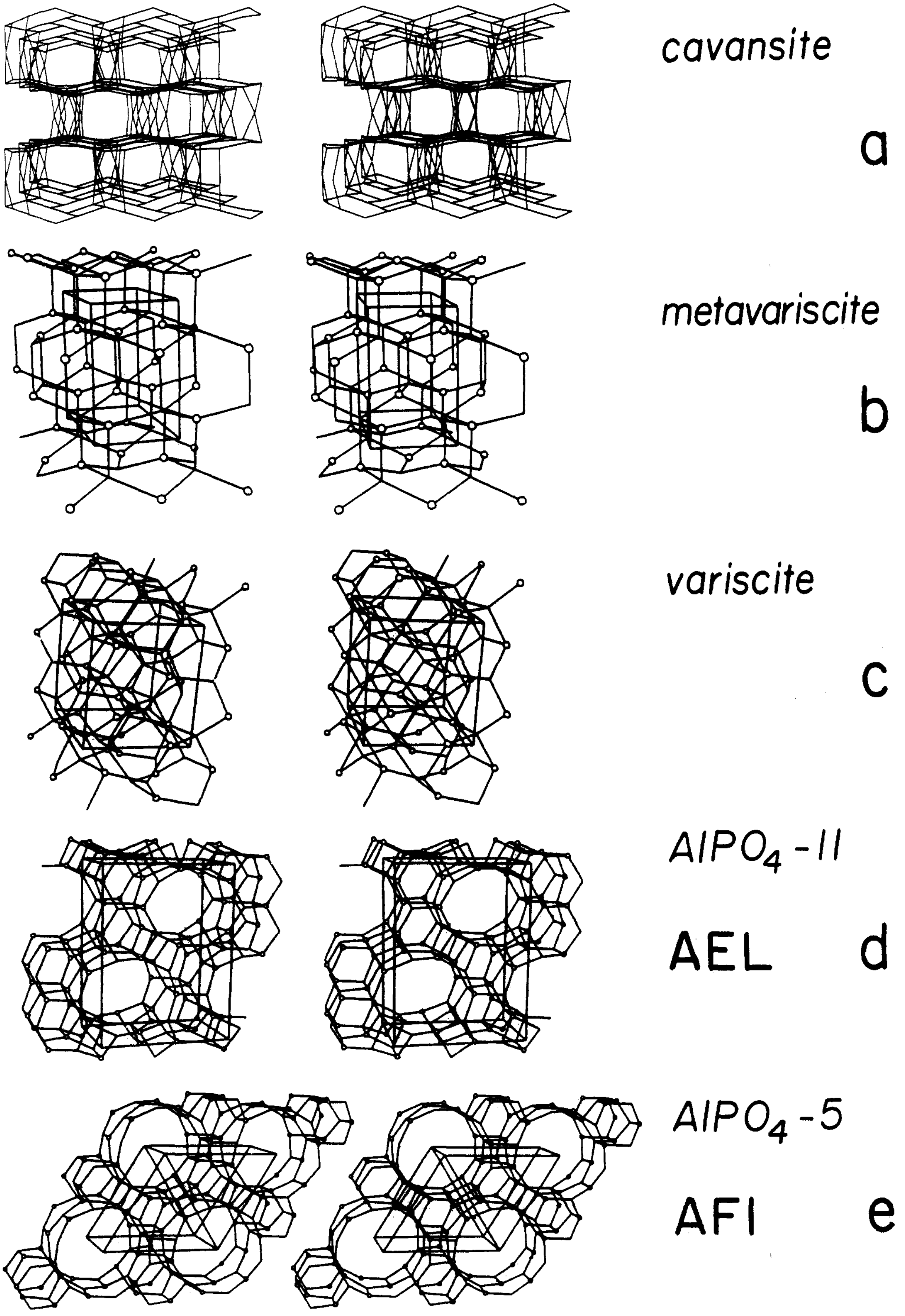

Figure 1. Stereoplots of T–T linkages of selected zeolites and related materials. (a) cavansite;[495] Si atoms occupy the vertices of the 4.8^2 2D nets, and a V atom occupies each vertex between each pair of 3-rings. (b) metavariscite; (c) variscite; (d) $AlPO_4$·11 (AEL); (e) $AlPO_4$·5 (AFI): all four diagrams[52] use a circle to distinguish between vertices occupied either by Al or P.

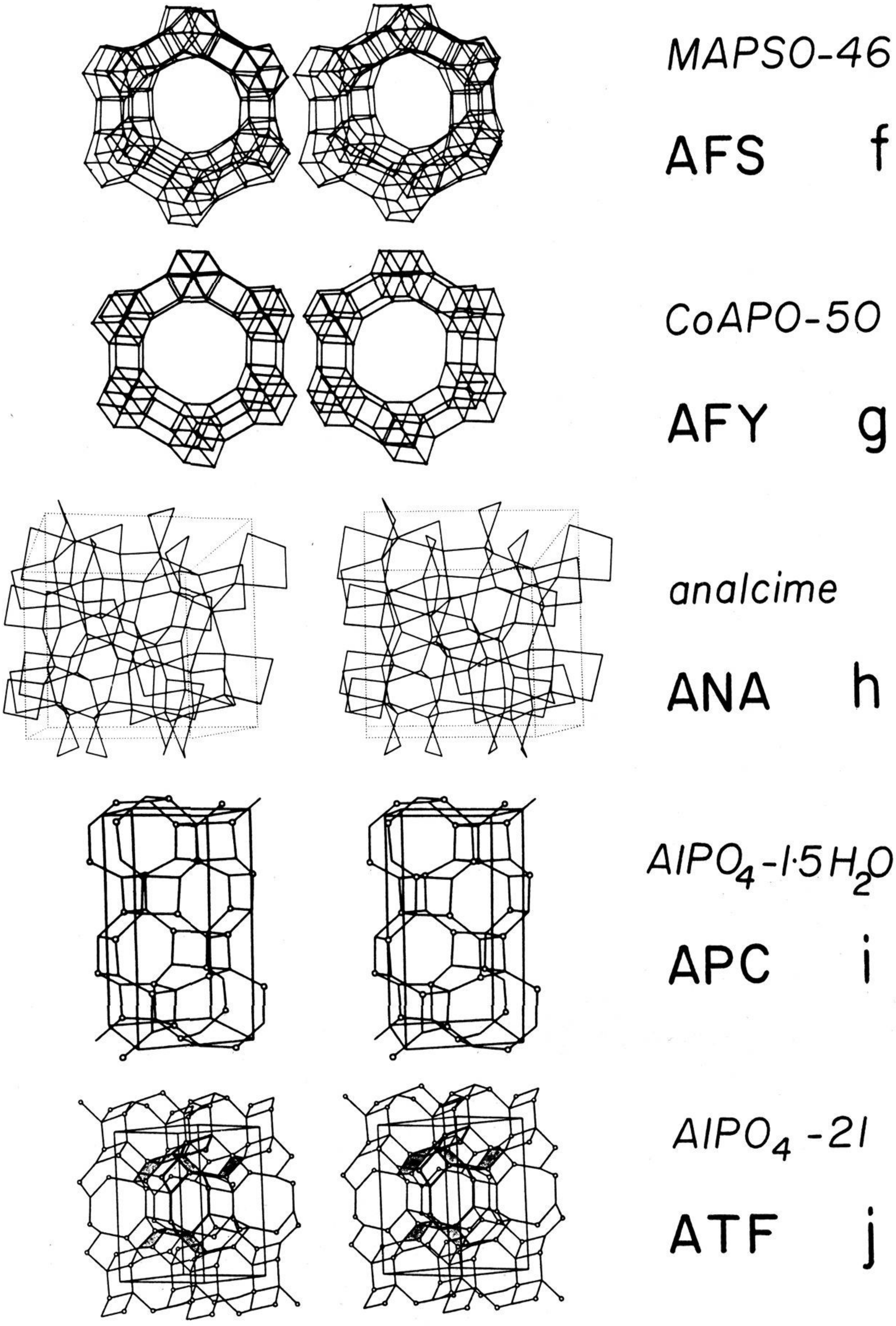

Figure 1 (*continued*). (f) MAPSO-46 (AFS); (g) CoAPO-50 (AFY): unpublished, by courtesy of J. M. Bennett and B. K. Marcus. (h) analcime (ANA): from *Atlas of Zeolite Structure Types*, 1st ed., 1978, by courtesy of W. M. Meier and D. H. Olson (reprinted with permission). (i) $AlPO_4.1.5H_2O$ (APC); (j) $AlPO_4$-21 (ATF); both diagrams[52] use a circle to show Al,P alternation; stippling shows a distorted double-crankshaft chain in j, and heavy lines outline 4-, 6-, and 8-rings.

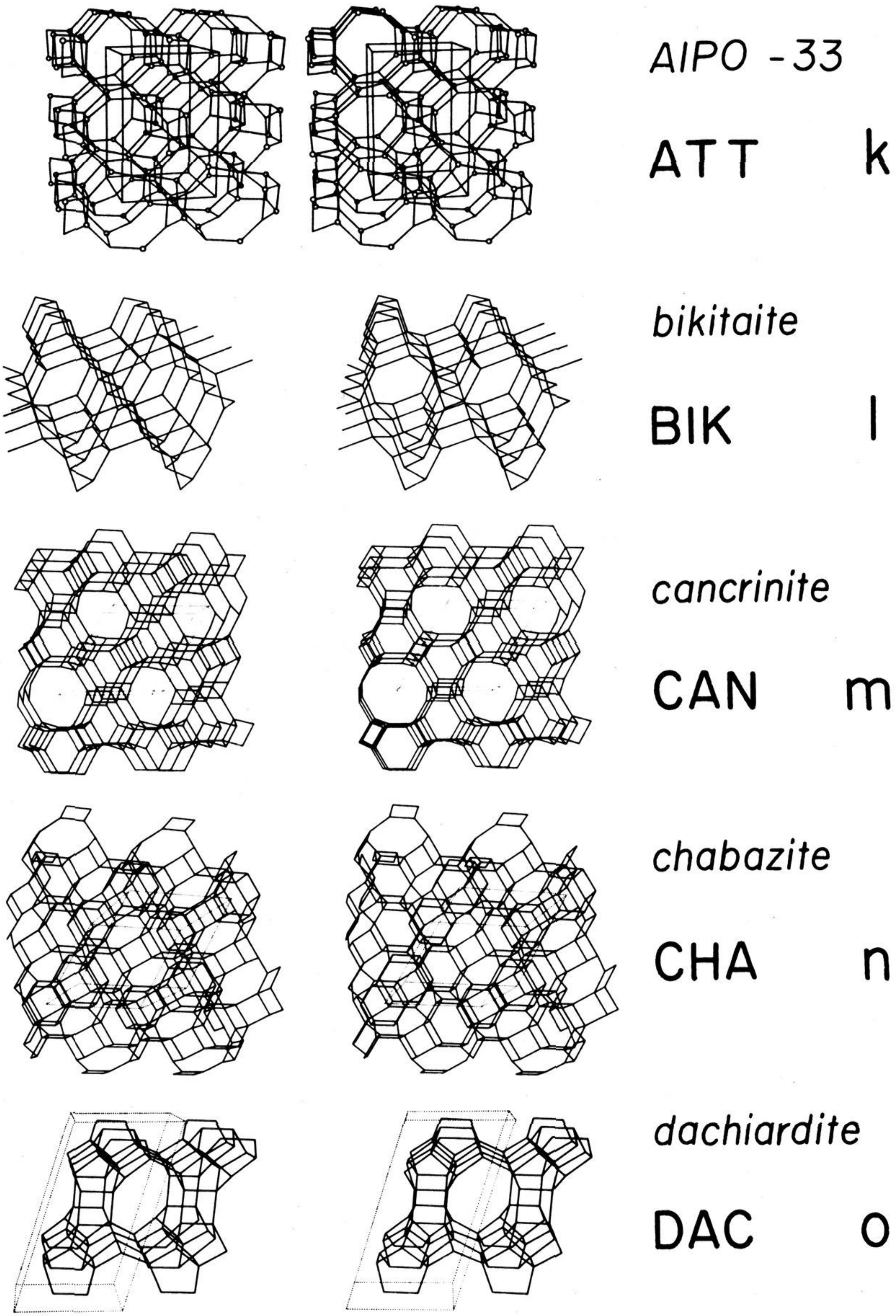

Figure 1 (*continued*). (k) $AlPO_4$-33 (ATT): unpublished, by courtesy of J. J. Pluth. (l) bikitaite (BIK); (m) cancrinite (CAN); (n) chabazite (CHA); (o) dachiardite (DAC). Stereoplots from *Atlas of Zeolite Structure Types*, 1st ed., 1978, by courtesy of W. M. Meier and D. H. Olson (reprinted with permission).

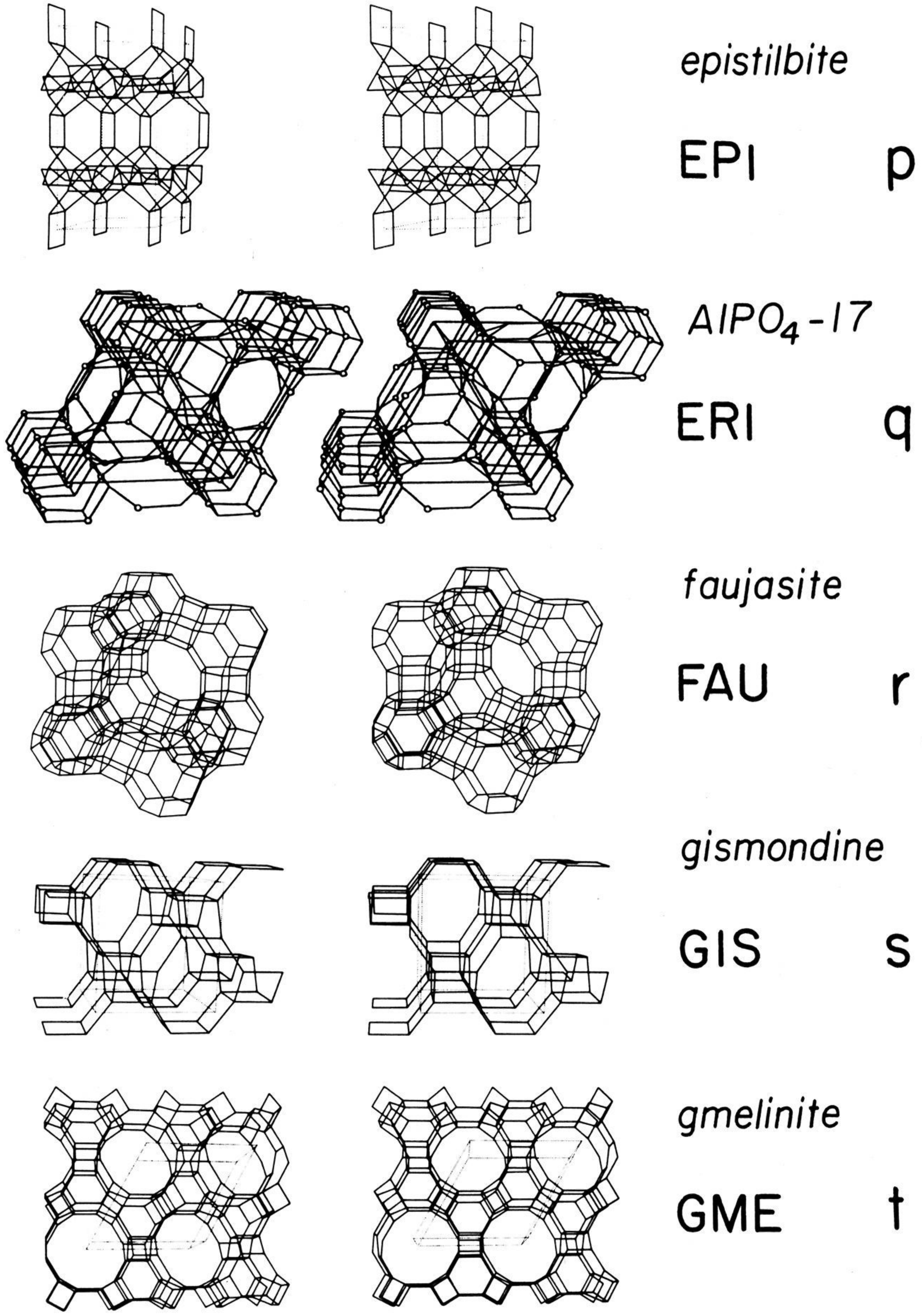

Figure 1 (*continued*). (p) epistilbite (EPI); (q) AlPO$_4$-17[52] (ERI); (r) faujasite (FAU); (s) gismondine (GIS); (t) gmelinite (GME). Stereoplots p, r, s, and t from *Atlas of Zeolite Structure Types*, 1st ed., 1978, by courtesy of W. M. Meier and D. H. Lson (reprinted with permission).

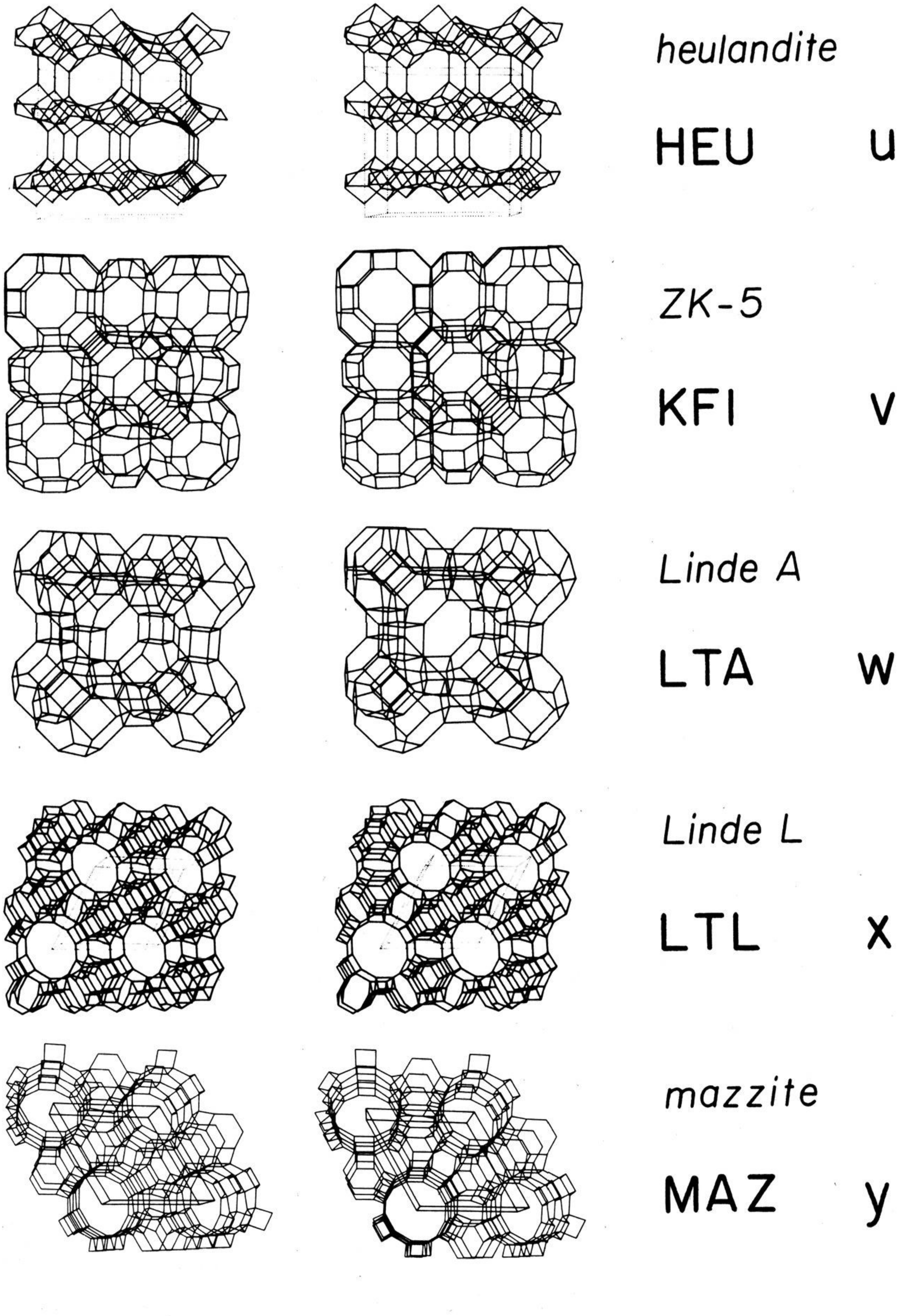

Figure 1 (*continued*). (u) heulandite (HEU); (v) ZK-5 (KFI); (w) Linde Type A (LTA); (x) Linde Type L (LTL); (y) mazzite (MAZ). Stereoplots from *Atlas of Zeolite Structure Types*, 1st ed., 1978, by courtesy of W. M. Meier and D. H. Olson (reprinted with permission).

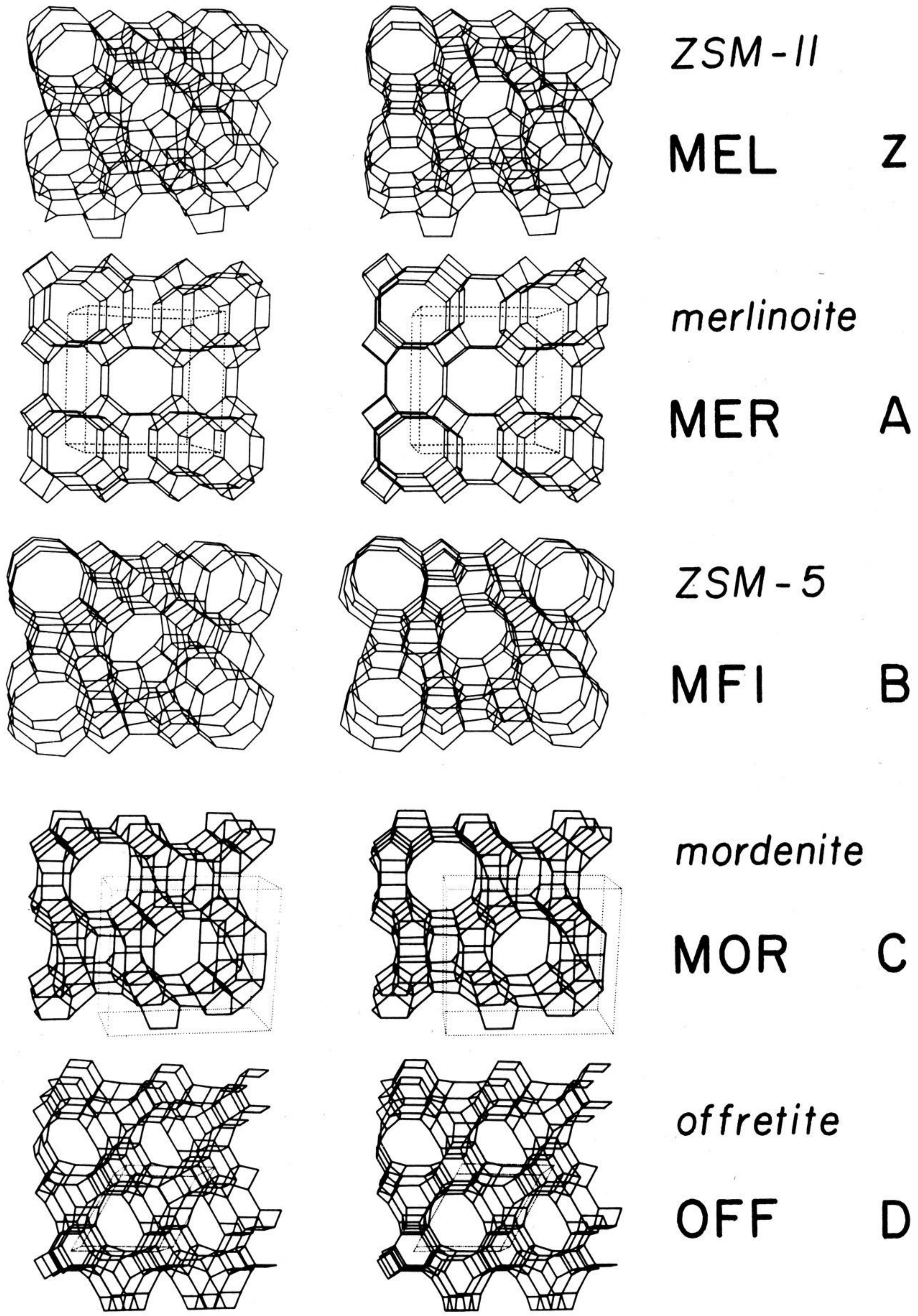

Figure 1 (*continued*). (z) ZSM-11 (MEL); (A), merlinoite (MEL); (B) ZSM-5 (MFI); (C) mordenite (MOR); (D) offretite (OFF). Stereoplots from *Atlas of Zeolites Structure Types*, 1st ed., 1978, by courtesy of W. M. Meier and D. H. Olson (reprinted with permission).

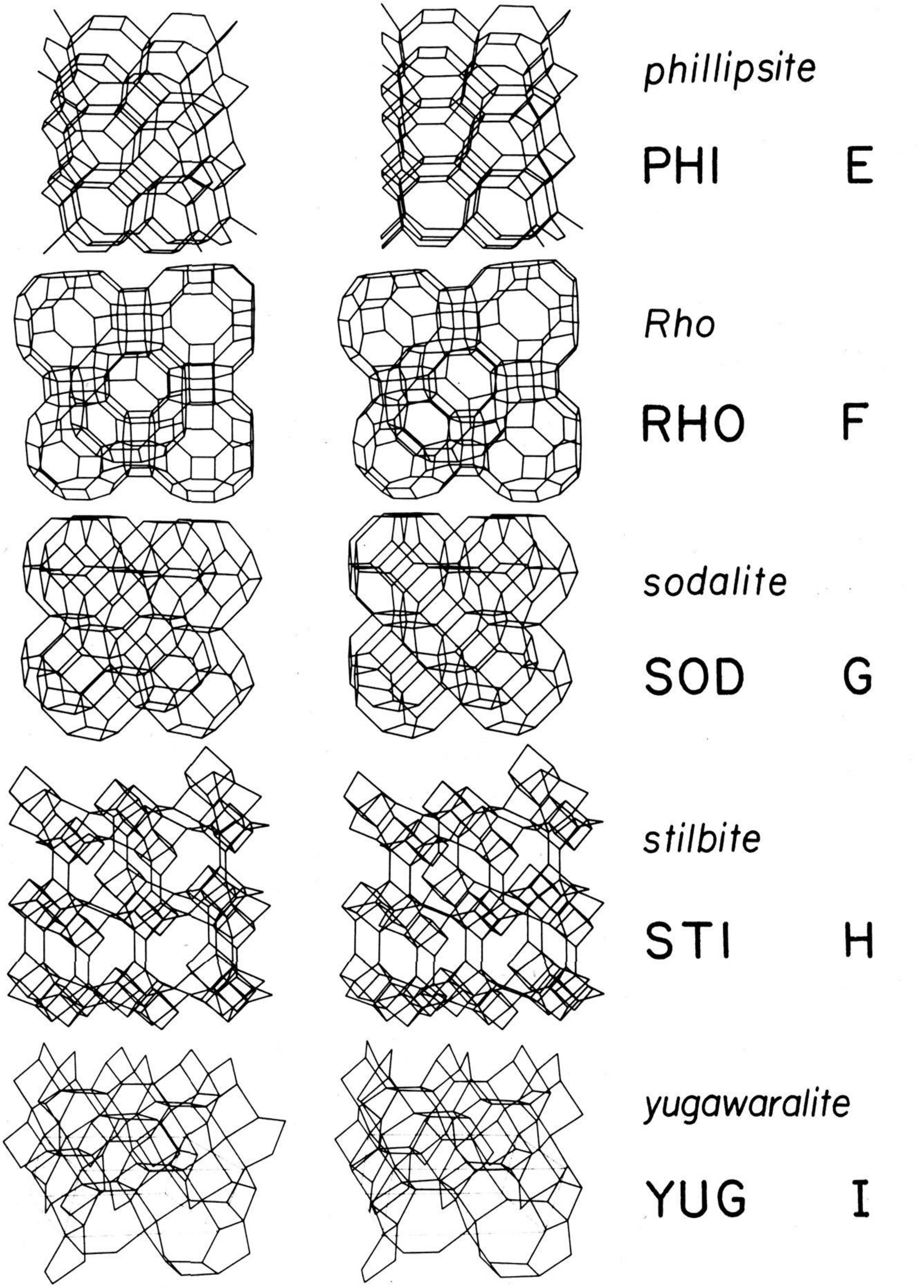

Figure 1 (*continued*). (E) phillipsite (PHI); (F) Rho (RHO); (G) sodalite (SOD); (H) stilbite (STI); (I) yugawaralite (YUG). Stereoplots from *Atlas of Zeolite Structure Types*, 1st ed., 1978, by courtesy of W. M. Meier and D. H. Olson (reprinted with permission).

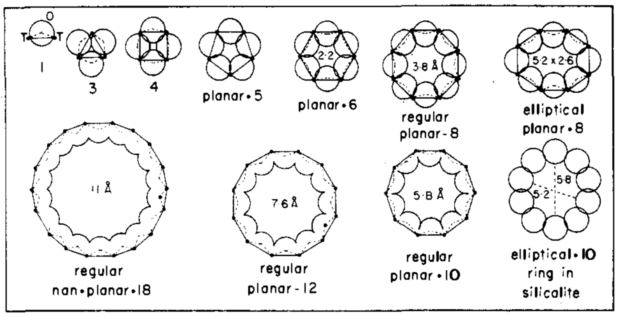

Figure 2. Geometrical properties of T–O rings and windows. Oxygen and T atoms are shown respectively by large open and small filled circles. An arbitrary value for the "free diameter" is obtained by assigning a radius of 1.35 Å to each oxygen atom and a distance of 3.1 Å between adjacent T atoms. The relative positions of the T and O atoms are chosen arbitrarily to give O–T–O angles near the tetrahedral value of 109.5°. Most rings are nonplanar in real structures with most O–T–O angles between 104 and 114° and most T–O–T angles between 130 and 160°. The importance of the regularity is shown by comparing a symmetrical planar 8-ring with an elliptical planar one. A regular planar 10-ring is compared with a nonplanar 10-ring from silicalite (MFI). Two-thirds of the T–T linkages are tilted and shortened in the projection of the 18-ring.

details of the geometry. Although atoms are not hard spheres, it turns out that the effective window size for passage of inorganic and organic molecules in zeolite molecular sieves is obtained within ~0.4 Å by assigning an arbitrary radius of 1.35 Å to each framework oxygen and the minimum kinetic diameter to the molecule (pp 633–645 of ref 1). To obtain a reliable window shape and size for a zeolite structure, the actual shape of each ring should be determined by structural analysis for the dehydrated zeolite in equilibrium with the appropriate molecule under the appropriate physical conditions. Because considerable changes of window shape can occur in some zeolites upon dehydration, it is necessary to be cautious in making predictions about the extent of molecular sorption just from the ring size of the as-synthesized zeolite or related material. This is exemplified by chabazite, whose 8-ring changes from 6.4 × 6.9 Å (hydrated) to 5.8 × 7.3 Å (dehydrated) to 6.0 × 7.4 Å (chlorine complex).[97] This change of shape results partly from movement of Ca ions to new positions during dehydration and partly from movement at the 4-ring "hinges" between the hexagonal prisms of T atoms (Figure 1n). It is impossible to pursue other details of window size here, and Figure 2 covers only the general limits.

The positions of the oxygen atoms in a ring of a zeolite (sensu stricto) depend on the topological linkage of the T atoms, the bonding to the extraframework cations, and to the water molecules. They are generally constrained by the ranges of T–O and T–T distances and of the T–O–T and O–T–O angles given earlier. An oxygen atom tends to lie about 0.3–0.7 Å from the midpoint of a T–T edge (Figure 2, upper left).

A 3-ring must be planar, and it cannot be a window for molecular adsorption. A 4-ring need not be planar, but no matter how the angles are adjusted, the T–T constraint leaves little room. A hole of ~1.5 Å diameter can be obtained for a regular planar 5-ring, but many 5-rings are strongly nonplanar in zeolite nets. A regular planar 6-ring has a hole about 2.2 Å diameter, but many 6-rings are distorted into ditrigonal or other shapes. Furthermore, many 6-rings are blocked in zeolites by cations. For a planar 8-ring, the opening can change from a circle of diameter 3.8 Å to an ellipse 2.6 × 5.2 Å; nonplanarity can further reduce the opening, while a cation can block it completely. The 5.8-Å circular hole for a planar regular 10-ring is reduced to a 5.2 × 5.8 Å hole in a 10-ring of silicalite,[97a] and as small as 3.2 × 5.3 Å in epistilbite.

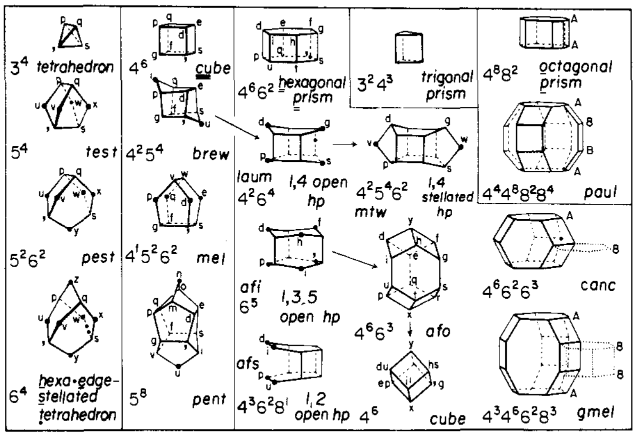

Figure 3. Selected building units and cages obtained from T–T linkages in the 3D frameworks of zeolites and related materials. Drawn with highest symmetry in clinographic projection except for some deliberate distortions to minimize overlap. Each species is labeled with the face symbol (large number = number of edges around a face; small superscript = number of faces). Vertices shown by a filled circle join only two edges; the others lie at the intersection of three edges. The mnemonic letter codes are used in Table I. The species are arranged in four groups illustrating the relationships to the tetrahedron, cube, hexagonal prism, and octagonal prism. Some corresponding vertices in each group are labeled. The trigonal prism is also shown. The following codes are from names of zeolites and related materials: *brew*sterite, *canc*rinite, *gmel*inite, *laum*ontite, *paul*ingite, *pent*asil family, *mel* (ZS*M*-*el*even), *mtw* (ZS*M*-*tw*elve), *afi* (*A*lPO$_4$-*fi*ve).

Some 12-rings in zeolites and related materials are nearly planar and have free diameters only slightly smaller than the theoretical value of 7.6 Å for a regular planar ring; however, those of offretite and gmelinite are strongly nonplanar with reduction of the free diameter to 6.4 and 7.0 Å, respectively. Nets with channels bounded by 18-rings can be invented,[71,91] but all these 18-rings are nonplanar. Theoretical net 81(1) has a nearly planar 18-ring[71] with a free diameter of 12 Å, but the diameter would drop to 11 Å for greater nonplanarity (Figure 2).

C. Polyhedral Cages and Building Units

The structural units in Figures 3 and 4 were selected for several reasons. First, the larger ones act as cages for encapsulated species in zeolites and related materials. Second, most of the smaller units occur in more than one type of 3D net and are useful for classification. Third, some of the units can be arranged in hierarchies of increasing complexity. For convenience, all the units are drawn on the same scale, and most are drawn in clinographic projection to give the best perspective. The essential topological and geometrical properties of polyhedra are summarized in ref 60.

For clarity, it is important to emphasize that each building unit is an abstract concept in which a T atom is represented by a vertex, and a T–T join by an edge. Some building units can be related to a polyhedron. The Greek concept of a polyhedron implies that faces

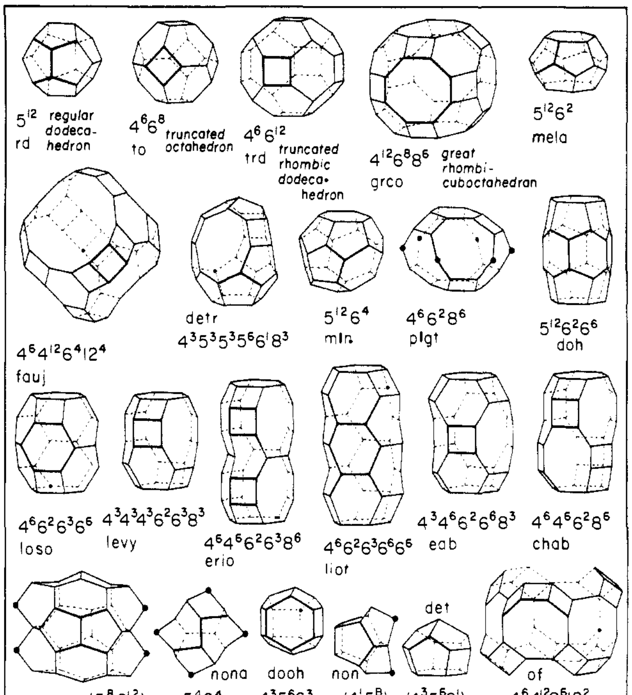

Figure 4. Selected cages and building units obtained from T–T linkages in the 3D frameworks of zeolites and related materials. Some small distortions from clinographic projection were made to reduce overlap at the boundaries. Only some of the species are planar convex polyhedra. Vertices at the intersection of only two edges are marked by small filled circles. Each species is labeled with the face symbol, and some are labeled with a specific name, or mnemonic code, or both. The following codes are from the names of zeolites: *chab*azite, *eab*, *erio*nite, *fauj*asite, *levy*nite, *liot*tite, *los*od, *paul*ingite, *mtn* (*ZSM*-*t*hirty *n*ine). Others are from clathrasils (Table I).

are enclosing a volume. The face symbol is the simplest description; thus $4^8 8^2$ for an octagonal prism specifies that there are eight quadrilaterals (actually squares when this polyhedron is regular) and two octagons. Because zeolites are based on 4-connected 3D nets, most constituent polyhedra can be chosen with three edges meeting at a vertex between polyhedra. The simplest polyhedra, such as the octagonal prism, have planar faces, but the topological relations are unchanged if the faces are made nonplanar by a continuous deformation. Actually, most polyhedra are distorted in the nets of zeolites, as seen from the stereoplots in Figure 1. Some polyhedra cannot be continuously deformed to generate planar faces. Thus the $4^6 4^6 6^2 6^3 8^6$ *erio* cage (Figure 4) must have nonplanar hexagonal faces around the waist of the double barrel. Even more extreme are the structural units that have only two edges meeting at some vertices (marked with small filled circles in Figures 3 and 4). These structural units can enclose space when bounded by nonplanar faces, as would happen if a wire model was dipped in a soap solution and pulled out to produce curved films. Hence it is convenient to use polyhedral face symbols such as $4^2 5^4$ for the *brew* structural unit (Figure 3). Cluster rather than polyhedron might be preferred for some small nonregular structural units.

The tetrahedron 3^4 does not occur in the 3D nets of zeolites and related materials, but the edge-stellated derivatives do. Complete conversion of each of the six edges into a pair of edges produces th hexa-edge-stellated tetrahedron, *hest*, in which edge pq is stellated at z to pz and zq, qr to qv and vr, and so on for the other four edges of the tetrahedron. Intermediate stages of stellation include the *t*etra- and *p*enta-*e*dge-*s*tellated *t*etrahedra, *test* and *pest*.

The cube 4^6, *cu*, can be transformed in many ways, of which several are shown in Figure 3 and one in Figure 5. The simplest product is the $4^4 6^1$ unit in *s*tilbite, for which one edge is removed. Edge-stellation of two opposing edges pq and rs gives the $4^2 5^4$ structural unit found in the 3D net of *brew*sterite; this is the 4–4–1–1 unit in ref 79. Edge-stellation of one set of four edges gives the $4^2 6^4$ unit in the *laum*ontite net. This unit can also be derived from the hexagonal prism. The $4^1 5^2 6^2$ *mel* unit in ZSM-11 is obtained from the cube by breaking the circuit of edges edpq and adding an edge vw. Even more extreme is the conversion of a cube into the torso-shaped unit 5^8, which occurs in the *pent*asil family of zeolites and related materials.[44] Another derivative is the $4^2 5^2 8$ unit (p–y) in the *yug*awaralite net (Figure 14; stereoplot, Figure 11), which is obtained by stellating two edges (pqr and vut) and opening one edge (ws).

The cube can also be transformed into a hexagonal prism either by edge-stellation, e.g., de (cube) → fgh (hexagonal prism), or by a σ transformation,[83] in which a diagonal plane such as pegs (cube) is split into two planes such as eiuq and fhtr (hexagonal prism). A further σ transformation produces the octagonal prism.

The hexagonal prism can be modified in many ways, of which eight are selected. Opening opposite edges dp and gs produces the 1,4 open hexagonal prism $4^2 6^4$ found in *laum*ontite. The 1,3,5 open hexagonal prism 6^5 occurs in $AlPO_4$-5 (*afi*), and the 1,2 open hexagonal prism $4^3 6^2 8^1$ in $AlPO_4$-46 (*afs*). Stellation of edges dp and gs produces the $4^2 5^4 6^2$ unit, which occurs ZSM-12 (*mtw*). Addition of vertices x and y to the *afi* unit produces the $4^6 6^3$ unit in $AlPO_4$-46 (*afo*). Removal of edges iu, gs, and eq and a 60° rotation recovers the cube. Conversion of three squares into double squares produces the $4^6 6^2 6^3$ unit in *canc*rinite, and a σ transformation produces the $4^3 4^6 6^2 8^3$ unit in *gmel*inite. The *canc* and *gmel* cages can be linked into 3D nets by addition of 6-rings and hexagonal prisms (dots), as discussed later. Note that there are two types of hexagons for the symbol $4^6 6^2 6^3$; this topological distinction is usually made for a face symbol given here, but is occasionally ignored for brevity.

The octagonal prism is converted into the $4^4 4^8 8^2 8^4$ cage in *paul*ingite by the same sequence of processes between the *hp* and *gmel* units.

The trigonal prism $3^2 4^3$ has not been found in 3D nets of zeolites, but a family of derivative units can be developed.

Figure 4 shows 22 more units. The *r*egular *d*odecahedron 5^{12} is a fully regular Platonic solid like the tetrahedron and cube. The *t*runcated *o*ctahedron $4^6 6^8$ and the *g*reat *r*hombi*c*ub*o*ctahedron $4^{12} 6^8 8^6$ (often called the truncated cuboctahedron; p 69 of ref 60) are Archimedean semiregular solids with congruent vertices and more than one type of regular polygon. The *t*runcated *r*hombic *d*odecahedron $4^6 6^{12}$ has two types of vertices and polygons, as does the $5^{12} 6^2$ unit in *mela*nophlogite. Six barrel-shaped cages are found in the zeolites *los*od, *levy*nite, *erio*nite, *liot*tite, TMA-*E*(*AB*), and *chab*azite, all of which belong to the ABC-6 family with parallel 6-rings.[67]

The largest cage in zeolite nets is the $4^6 4^{12} 6^4 12^4$ one in *fauj*asite. This has four hexagons at the vertices of a tetrahedron, four dodecagons at the vertices of a tetrahedron in the negative position (p 63 of ref 60), and six sets of three squares at the vertices of a cube. The $5^{12}6^4$ polyhedron *mtn* in ZSM-39 contains four hexagons at the vertices of a tetrahedron separated by twelve pentagons, three of which meet at each vertex of a negative tetrahedron. Note that the tetrahedral positions are not oriented in the conventional position of the tetrahedron in Figure 3.

The $5^{12}6^2 6^6$ *doh* polyhedron in dodecasil-1H can be obtained from a hexagonal prism as can the $4^6 6^2 8^6$ *plgt* unit which occurs in paulingite. Like the *fauj* cage, the $4^6 4^{12} 8^6 12^2$ *af* unit found in $AlPO_4$-46 and $AlPO_4$-50 has six sets of three squares. However, they are arranged at the vertices of a trigonal antiprism, while the two dodecagons are very nonplanar, as are the chair-shaped octagons.

The remaining units *det*, *detr*, *dooh*, *non*, *nona*, and *nonas* occur as cages in clathrasils. The first three units have 3-fold symmetry, *nonas* has *mmm*, *non* has *mm*2, and *nona* has 222. It is obvious that the present treatment of structural units in zeolites and related materials can be expanded. Further units may be discovered in new crystal structures. From the viewpoint of a pure mathematician, it is possible to fill in the gaps in the hierarchies, such as adding the di- and tri-edge-stellated tetrahedron to those in Figure 3, and to develop new hierarchies.

D. Chains and Linkage into Sheets

Because any sequence of edge–vertex–edge etc. is a chain, all 4-connected 3D nets contain chains. Hence, the selection of chains in the 3D nets of zeolites and related materials is arbitrary. Those given in Figure 5 were selected because they occur in more than one 3D net or because they make it easy to describe the 3D net, or both.

The simplest chains are the five coplanar ones, which are given pictorial names *z*igzag, *c*rankshaft, *s*aw, *p*entasil, and *b*ifurcated *s*quare instead of the precise abstract names in ref 42. The noncoplanar chains include the double zigzag (*zz*), the double crankshaft (cc), the double saw (*ss*), the *t*wisted *s*quare (*ts*), the *b*ifurcated *h*exagonal-*s*quare chain (*bhs*), and the chain in the *fi*brous zeolites (*fi*) which contains the 4–1 secondary building unit.[79] A chain of edge-separated-cubes (*esc*) occurs in the $AlPO_4$-46 structure (section E). A complex chain formed from edge-shared *o*pen-*d*ouble cubes occurs with considerable distortion in $AlPO_4$-14.[52] Another interesting chain composed of 4-rings is the singly-connected one in analcime (p 9 of ref 6).

Three chains contain $4^2 5^4$ clusters (*brew* unit in Figure 3) condensed in different ways. In stilbite, the *brew* units share their 2-connected vertices at p, q, r, and s, and each *brew* unit is parallel to the next in an idealized chain. In the actual stilbite net (Figure 1H), the chain is twisted. In heulandite (Figure 1u), the *brew* units again share vertices at p–s, but are flipped left for right across each shared vertex. In brewsterite, the *brew* units share edges pq, rs, tu, and vw and are parallel. The *he*, *st*, and *br* chains are linked into sheets by chains of type 4.5^2, $4^2.6$, and 4.6, respectively, and these sheets are connected into other sheets to generate 3D nets. Many other ways of cross-linking the *brew* unit were enumerated systematically.[94]

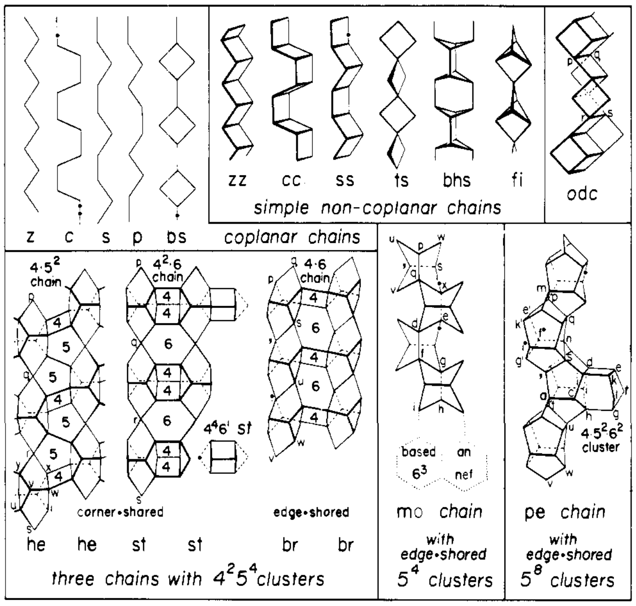

Figure 5. Some chains in zeolites and related materials. Each chain is shown by the linkages between adjacent tetrahedrally coordinated positions. Coplanar and noncoplanar chains are shown respectively in plan and near-clinographic projection. The mnemonic letter codes were assigned as follows: *z* (*z*igzag; 2-repeat), c (*c*rankshaft; 4-repeat), *s* (*s*aw; 3-repeat), *n* (*p*entasil; 8-repeat), *bs* (*b*ifurcated *s*quare; 4T in 3-repeat), *zz* (double *z*ig*z*ag), cc (double crankshaft), *ss* (double *s*aw), *ts* (*t*wisted *s*quare; 6T in 4-repeat), *bhs* (*b*ifurcated *h*exagon plus *s*quare; 8T in 4-repeat), *Fi* (chain in the *fi*brous zeolites edingtonite etc.; 5T in 3-repeat), *odc* (edge-sharing *o*pen *d*ouble cube; pq and rs are shared edges), *he* (corner-shared $4^2 5^4$ clusters with alternate clusters flipped left for right; p, q, r, and s are shared vertices; occurs in *he*ulandite, alternating with 4.5^2 chain), *st* (corner-shared parallel $4^2 5^4$ clusters; occurs in *st*ilbite, alternating with $4^2.6$ chain; $4^4 6^1$ *st* boat-shaped clusters are generated), *br* (edge-shared $4^2 5^4$ clusters; pq, rs, tu, and vw are shared edges; occurs in *br*ewsterite, alternating with 4.6 chain), *mo* (edge-shared 5^4 clusters in zigzag pattern; pw, rx, de, fg, and hi are shared edges; occurs in *mo*rdenite; the relationship to the 6^3 net is shown by dotted lines), *pe* (edge-shared 5^8 clusters in zigzag arrangement; pq, rs, tu, vw, mp, ns, and ot are shared edges; occurs in *pe*ntasil materials; a $4.5^2.6^2$ cluster is shown by d–l).

Removal of one vertex from the *brew* unit gives the 4–4–1 secondary building unit,[79] labeled as s–y in the *he* chain. This 4–4–1 unit assembles nicely into the vertex-shared *he* and *st* chains. However, this 4–4–1 unit is not applicable to the *br* chain because of the edge-sharing of the *brew* unit and is less satisfactory than the *br* unit for showing the topological relationship between the heulandite, stilbite, and brewsterite 3D nets. This distinction is important because Meier's secondary building units were invented in a search for the smallest identical pieces from which a net can be built by addition only of single edges. The structural units selected in this review were invented to be useful in describing the topology of the nets.

The 5^4 *test* unit is edge-shared at pw, qx, de, fg, and hi in the *mo* chain of mordenite. The *test* unit at the upper left is labeled as in Figure 3 to demonstrate the change of angular orientation. In the stereoplot of the mordenite net (Figure 1C), the *mo* chain is seen end-on, while the corrugated 6^3 net is edge-on in Figure 1C and in plan in Figure 5. The edges df and pq were described

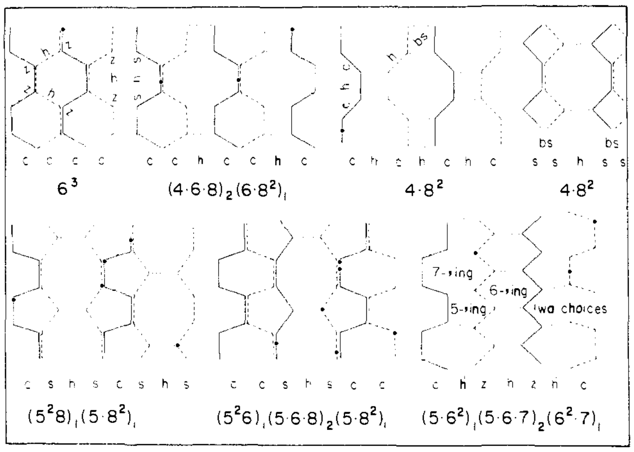

Figure 6. Some 2D nets obtained by linking simple chains.

as handles on page 23 of ref 6.

Finally, edge-sharing at mpq, nsr, otu, and vw of the 5^8 *pent* clusters (Figure 3) generates the *pe* chain in the pentasil family of zeolites. This chain can be linked by $4^15^26^2$ clusters of the *mel* type at dihcj, efglk, and e′f′g′l′k′ and equivalent positions to generate a layer in ZSM-11[98] (Figure 1z). Alternatively, the *pe* chains can be linked by two *pest* clusters condensed at a 6-ring (e.g., qxsyrv in Figure 3) to generate a layer in ZSM-5[96,99] (Figure 1B). Selection of the smallest secondary building was difficult in ZSM-5, and a chariot-shaped T_{12} unit was finally selected (Figure 2 of ref 99).

It is convenient to consider other ways of linking chains to form sheets in the next section.

E. 2D Nets and Linkage into 3D Nets

There is an infinity of topologically distinct types of 2D nets, of which some are given in reviews of plane nets in crystal chemistry.[58,100] It is appropriate here to consider only those 2D nets relevant to the classification of 3D nets in zeolites and related materials. The most obvious way to generate a 4-connected 3D net from a 2D net is to arrange one type of 3-connected 2D net into a parallel stack and to link each vertex to only one other vertex. To form a 3D net, some of the new edges must point upward and some downward from each 2D net. Otherwise a double sheet is formed, as in hexacelsian $BaAl_2Si_2O_8$ and cymrite.[64] A less obvious way is to convert a circuit of edges of a 4-connected 2D net into a helix.[66] A general review[101] of tetrahedral structures is a starting point for further ideas.

Consider first the 3-connected 2D nets, of which an infinity can be invented. There are only three types of fully regular 2D nets and equivalent tessellations (p 32 of ref 60), of which only the 6^3 net with three 6-rings meeting at each vertex is 3-connected. There are eight nets and equivalent tessellations with congruent vertices and more than one type of regular polygon, of which only the 3.12.12, 4.8.8, and 4.6.12 ones are 3-connected. None of the reciprocal tessellations are completely 3-connected, but the (3,4)-connected reciprocal nets in Figure 2.1d,e of ref 60 can be converted into 3D nets (unpublished).

Figure 6 shows how an infinity of 3-connected 2D nets can be invented from the simple coplanar chains in Figure 5. The 6^3 net can be obtained by condensation of crankshaft chains arranged back-to-back (alternate continuous and dashed lines). A second procedure is to join zigzag chains with horizontal linkages (*h*). Because of the 6-fold symmetry, a 6^3 net can be decomposed in three ways into c chains, or into *z* chains plus *h* edges. Interposition of *h* edges between alternate pairs of c chains gives the $(4.6.8)_2(6.8^2)_1$ 2D net, and addition of *h* between the remaining pairs of c chains gives the 4.8^2 2D net. This important semiregular Archimedean net can also be obtained by joining condensed pairs of *s*aw chains with *h* edges; each pair of *ss* generates a *bs* chain. There is an infinite polytypic series of 2D nets based on the condensation of c and *h*,[76] as the run lengths of c and cc are changed.

The c*shs* condensation gives the $(5^28)_1(5.8^2)_1$ 2D net, and the cc*shs* one the $(5^26)_1(5.6.8)_2(5.8^2)_1$ net. Again there is an infinite polytypic series based on varying the run lengths of c and cc.

Linkage of alternating c and *z* chains by *h* edges gives a 2D net in which a 5-, 6-, and 7-ring meet at a vertex. It is necessary to tilt half of the *h* edges to *h′* in order to obtain a regular *z* chain; alternatively, all *h* edges can be parallel if the *z* chain is distorted. Because there are two choices of position for the 5- and 7-rings across each row of 6-rings, there is an infinite polytypic series.

Two ways of converting a stack of 3-connected 2D nets into a 4-connected 3D net are shown in Figure 7. The ABW 3D net of the Li-A(BW) zeolite can be decomposed into either 6^3 or 4.8^2 2D nets. Easiest to see in the stereoview are the *zz* chains running along the c axis, with the ones at the cell edges twisted with respect to the ones running through the center of each cell. The entire set of edges at the top of the stereoview is part of a 4.8^2 net which is strongly distorted from the ideal planar shape in Figure 6. In projection (Figure 7, bottom right), each *zz* chain becomes a rectangle, and each 4.8^2 net becomes strongly corrugated.

The ABW 3D net also contains a set of crankshaft chains, which lie east–west in Figure 7, bottom right, and are horizontal in the plane of the paper. They are nearly horizontal and slightly kinked in the stereoview. Every 4.8^2 2D net must contain such a crankshaft chain (Figure 6, top right). There appears to be a second set of crankshaft chains in the c-axis projection (Figure 7, bottom right) composed of alternating *h* and *z* edges as in Figure 6, upper left. However, the tilting of the *z* edges violates the planarity condition of the ideal c chain (Figure 3) so much that the term is not used here.

The stereoview (Figure 7, top right) shows that the *h* and *z* edges combine into a nonplanar 6^3 net, which is shown in *a*-axis projection at the bottom left. Here, each pair of *z* chains overlaps to show a single zigzag, while each c chain projects as a single edge.

A third way of representing a 3D net is in a clinographic projection, as already used for polyhedra (Figure 4). Two 6^3 nets are shown at the top left of Figure 7, the one in continuous line being closer to the viewer than the one in dashed line. Each vertex marked by a filled circle has an edge pointing toward the viewer, whereas each unmarked vertex has an extra downward edge. A crankshaft chain is shown in clinographic projection at the bottom of the drawing. One of the *zz* chains which extends north–south is labeled, and a second one is unlabeled.

This example was deliberately described in detail so that the relationship between a stereoview and an abstract projection can be envisaged. From now on,

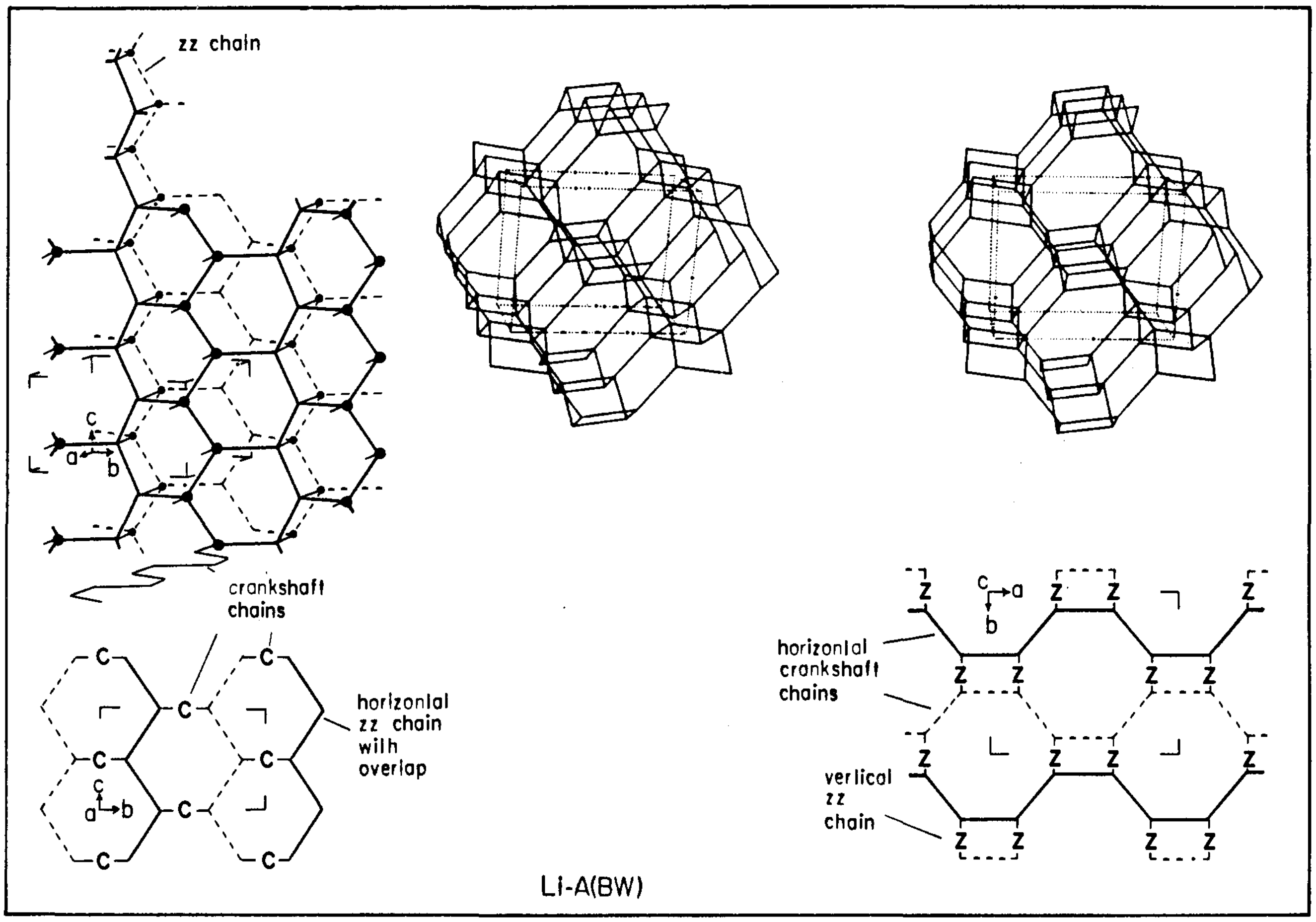

Figure 7. Four views of the ABW tetrahedral net in Li-A(BW) zeolite. Upper left: Clinographic projection with the *c* axis upward, *b* to the right, and *a* toward the left side of the viewer. Each T node is connected to the four nearest T nodes, except at the arbitrary boundary. Two 6^3 2D nets are shown by dashed and undashed lines. A double zigzag (*zz*) chain is shown parallel to the c axis. A crankshaft (c) chain, parallel to the *a* axis, is foreshortened by the perspective. Lower left: Symbolic projection down the *a* axis showing superposition of the 6^3 2D nets, of the individual *z* chains of each *zz* double chain, and of the individual branches of the c chains. Upper right: Stereoview down the c axis with *a* to the right. The *zz* chains utilize 4-rings from the nonplanar 4.8^2 2D net. Lower right: Symbolic projection down the c axis showing superposition of the 4.8^2 2D nets, a rectangular cross section of each *zz* chain, and a plan of the horizontal c chains.

whatever representation that is convenient will be used.

Figure 8 illustrates the procedure for inventing all types of 4-connected 3D nets from a particular choice of 3-connected 2D nets (here, the 6^3 net) and an extra linkage (here, an up–down edge as in Figure 7, top left). Three 2D nets are given in clinographic projection instead of just the two nets of Li-A(BW) in Figure 7. The 2D nets are idealized to the most regular shape instead of being distorted as in the actual crystal structure. The essentials of the full treatment in ref 64 are these: (a) Determine the sequence of up (U) and down (D) linkages around each 6-ring, as shown for the central 6-ring in the tridymite structure (UDUDUD) (for the ABW net the sequence would be UUUDDD). (b) Since U and D merely indicate a reversal with respect to each other, replace the sequence with S (same) and C (change) for each sequential pair of adjacent vertexes, e.g., CCCCCC for cristobalite and SSCSSC for ABW. (c) Enumerate all possible sequences in any circuit (this involves merely a systematic counting of the ways to arrange S and C; there are only 8 ways since the run lengths must be even to close the circuit; hence CCCCCC, SCCSCC, SCSCCC, SSCCCC, SSCSSC, SSSCSC, SSSSCC, SSSSSS; SSSSSS is rejected because it gives a double-sheet). (d) Since there is an infinite number of ways of combining circuits, it is useful to begin by enumerating only those simple regular nets with one type of circuit. CCCCCC leads uniquely to the tridymite net (Smith #1) if the 6^3 nets lie above each other (Figure 8, top left), and each C becomes a crankshaft chain, as for pqrs; however, the 6-fold symmetry of the CCCCCC sequence allows alternate 6^3 nets to be rotated 180° as in the 3D net of cristobalite, which has three horizontal projections A, B, and C of a sequence of three 2D nets when viewed down a triad axis of the cubic unit cell. The hydrated aluminophosphates metavariscite and variscite are based on SCCSCC and SCSCCC, respectively, when the bonding of two water molecules to each Al atom is ignored[52] (stereoviews, Figure 1b,c); the anhydrous paracelsian $BaAl_2Si_2O_8$ has SSSCSC; other nets are listed in ref 64. (e) Nets with more than one type of circuit have not been enumerated but the following occur in crystal structures: beryllonite[64] has both CCCCCC and SCSCCC, kaliophilite-01[102,103] has both SCSCCC and SSCSSC, and the $KAlGeO_4$ structure[104] has SSCSSC and CCCCCC.

Turning now to the 4.8^2 2D net, Figure 9 shows seven out of the infinity of 3D nets that can be enumerated by converting horizontal edges into chains.[65,66] The merlinoite net (stereoview, Figure 1A) retains the 4-fold symmetry of the ideal 4.8^2 net as each square is turned into the rectangular projection of a double-crankshaft

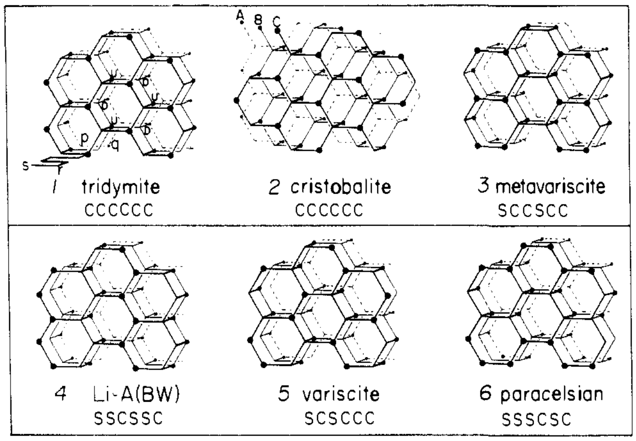

Figure 8. Six simple 3D nets using up–down linkages from a stack of parallel 6^3 2D nets. Each 3D net is represented by a stack of pieces of three 2D nets shown in clinographic projection. The numbers were assigned in a systematic enumeration.[64] Each vertex with an upward (U) branch pointing to the reader is marked with a filled circle; an unmarked vertex is attached to a downward (D) branch. The sequence UDUDUD occurs in each 6-ring of the tridymite net. It can also be represented by the sequence CCCCCC, where C represents Change between adjacent vertices. In the metavariscite net, the sequence UUDUUD gives SCCSCC, where S represents Same. A crankshaft (c) chain is produced by each pair of adjacent UD vertices, as shown by pqrs in the tridymite net. Each 6^3 net becomes nonplanar as the bond angles adjust to the chemical forces; see Figure 6 for the actual geometry of the ABW net.

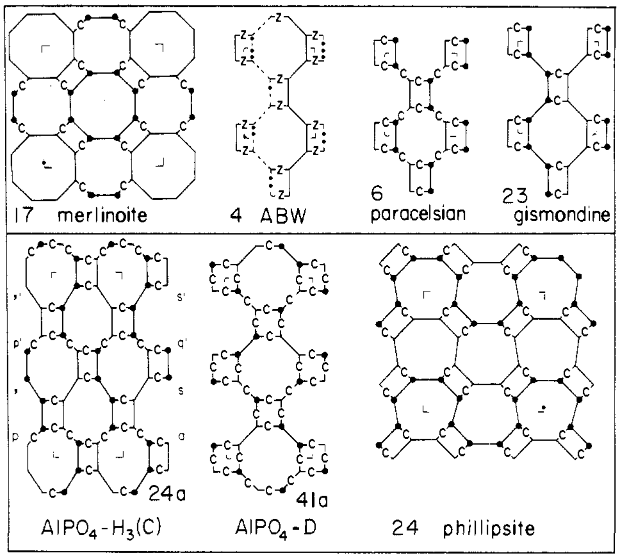

Figure 9. Seven simple 3D nets based on a stack of parallel 4.8^2 2D nets. Each 3D net is represented symbolically by labeling the nodes and branches of the 2D net. The labels c and z represent projections of crankshaft and zigzag chains (Figure 5). Net 4 (ABW) is also based on a 6^3 2D net (Figures 6 and 7). In the remaining six nets, the presence or absence of a solid circle distinguishes between vertices with an upward or a downward linkage to a vertex of an adjacent 2D net. Each row of crankshaft chains in nets 24a and 41a generates a nonplanar 6^3 net seen end-on. Corner marks show the repeat unit. The geometry of each net is idealized to give the highest symmetry for constant T–T distance. Numbers 4, 6, 17, 23, 24, and 24a were assigned in ref 65 and 105. Number 41a is newly assigned on the basis of ref 106. Its topologic description for neutral vertices is as follows: sequence ScScCcCc, $Z_t = 16$, Schläfli symbol $(4^26^28^2)_1(4.6^5)_1$, highest space group *Acam*, $Z_c = 32$, $a \sim 9.5$ Å, $b \sim 20$ Å, $c \sim 8$ Å. For alternation of Al and P, the highest space group is *Pcab*.

chain. The gismondine net (stereoview, Figure 1s) is obtained by replacing each *zz* chain of the ABW net (Figure 7, bottom right, rotated 90°) by a cc chain. Just as the ABW 3D net can be related to both a 6^3 and a 4.8^2 net (Figure 7, bottom), so can the paracelsian net (Figures 8 and 9). Conversion of all horizontal edges in the gismondine net, except for those in the *zz* chains, gives the second projection of the paracelsian net. In the phillipsite net (stereoview, Figure 1E) five adjacent edges of each 8-ring are horizontal, and these generate an infinite chain of edge-shared 4-rings (heavy lines or light lines) which is more convoluted than the chain of the edge-shared 4-rings in the gismondine net.

Two of the nets in the aluminophosphate family are also based on conversion of some of the horizontal edges of the 4.8^2 2D net into crankshaft chains. Although neither was enumerated in ref 65 because one of the cell dimensions of each crystal structure is longer than the upper limit chosen for the enumeration, both nets have only one sequence around each 4-ring and each 8-ring. The 3D net (stereoview, Figure 1i) for $AlPO_4$-H_3 (APC) is particularly interesting because it can be generated from a stack of alternating 6^3 and 4.8^2 2D nets.[105] These nets appear in projection at pq, p′q′ as cccc and at rs, r′s′ as *hchc* (cf. Figure 6). The cccc combination, which replaces each 4-ring in the 4.8^2 net of $AlPO_4$-D,[106] generates the *bhs* chain (Figure 5).

The next semiregular 3-connected 2D net, 4.6.12, is particularly useful in describing the 3D nets of zeolites and related materials (Figure 10). The cancrinite net (stereoview, Figure 1m) is obtained by replacing each 4-ring with a double-zigzag chain, which has a rectangular cross section. The 6-rings are alternately pushed upward or downward to levels A and B, and each 12-ring becomes nonplanar. The combination of six 4-rings with two 6-rings at height A and A′ gives the $4^66^26^3$ *canc* unit shown in clinographic projection in Figure 3; each pair of 4-rings is part of a *zz* chain. A 6-ring at height B is attached to each of the three edges at the waist of the *canc* unit and forms the top and bottom of two more *canc* units. The face-sharing *canc* units form a framework that is penetrated by near-cylindrical channels spanned by the nonplanar 12-rings.

Conversion of the *zz* chains into cc and *ss* chains by two or one horizontal σ transformations[83] yields the nets of gmelinite and offretite (stereoviews, Figure 1t,D), respectively. Each AA or BB corresponds to a pair of horizontal 6-rings connected by six 4-rings to give a hexagonal prism (Figure 3). The *gmel* unit is related to the *canc* unit by a horizontal σ operation. As a result of the two σ operations, the 12-ring channels are now interconnected by 8-rings instead of being separated by the 6-rings of the cancrinite net. The offretite net contains three types of polyhedral units: *hp*, *canc*, and *gmel*.

The chabazite net (Figure 10; stereoview, Figure 1n) is related to the gmelinite net by a similar mechanism as that for tridymite and cristobalite (Figure 8). Instead of a return to AA after the sequence AABB of gmelinite, the next two 6-rings occur at positions CC before the return to AA. This produces a net with rhombohedral instead of hexagonal-prismatic geometry and eliminates the cc chain of gmelinite. The *chab* polyhedral unit (Figure 4) shares an 8-ring with each of six other *chab* units in a rhombohedral arrangement, and a 6-ring with an *hp* at the top and bottom. Instead of the 12-ring near-cylindrical channels of the nets with only A and B positions, the accessible space of the chabazite net

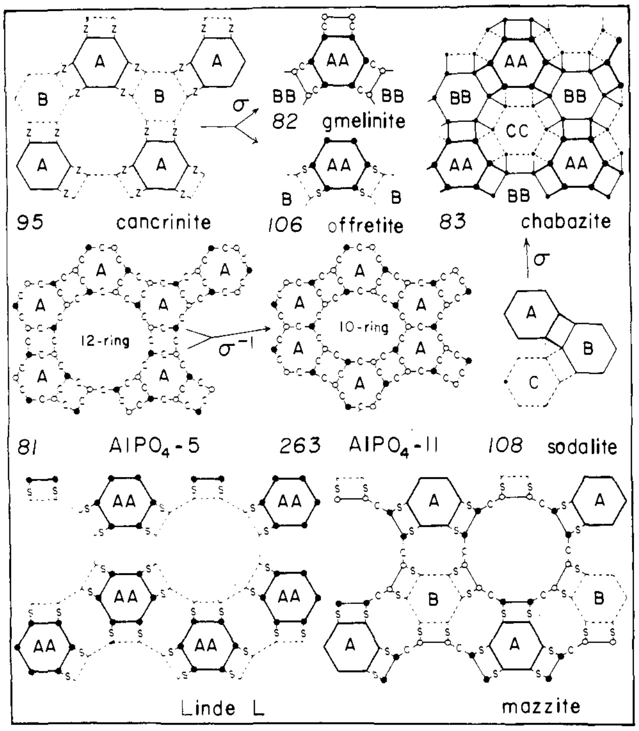

Figure 10. Six simple 3D nets based on a stack of 4.6.12 2D nets, a σ^- derivative, and two nets based on the $(4.6.8)_1(4.8.12)_1$ 2D net. The labels c, *s*, and *z* represent projections of crankshaft, saw, and zigzag chains (Figure 5). A, B, and C show different heights perpendicular to each stack of 2D nets. A solid or open circle indicates that a vertex is the projection of a vertical edge. Numbers 81, 83, 95, 106, and 108 were assigned in ref 64–67. The topologic relations of Linde L and mazzite zeolites are related to a systematic enumeration in ref 76.

consists of the 3D assemblage of *chab* cages separated by 8-ring windows.

Historically, the chabazite structure[107] was discovered before the gmelinite one, after the late D. W. Breck pointed out that the 6-ring windows in the published structure of chabazite were too small to match the sorption properties.[107a] Therefrom, the AABB sequence was proposed for the gmelinite net, and confirmed by an independent structure determination.[108] This naturally led to the recognition of the ABC-6 group of nets, which was systematically enumerated.[67] The current list of nets observed in crystal structures is as follows:[67,103] AB, cancrinite (stereoview, Figure 1m); AAB, offretite (stereoview, Figure 1D); ABC, sodalite (viewed down any triad axis of the cubic unit cell; stereoview, Figure 1G); AABB, gmelinite (stereoview, Figure 1t); ABCB, losod synthetic zeolite; AABBCC, chabazite (stereoview, Figure 1n); AABCCB, TMA-E(AB) synthetic zeolite; AABAAC, erionite (stereoview, Figure 1q); ABCBCB, liottite; ABCBCBAB, afghanite; AABCCABBC, levyne; ABCABCBACB, franzinite (probable sequence); ABABABACBABABABC, giuseppettite; also 12-, 14-, 16-, 18-, 24-, and 28-sequences indicated in complex structures. Particularly interesting are the AAB and AABAAC sequences of the offretite and erionite nets, which were confused until some nice detective work[109] sorted them out. Stacking faults are common in some members of the ABC-6 group, including gmelinite, which has AABBCC faults.[108]

Whereas all members of the ABC-6 family contain planar 6-rings in the most symmetrical geometry, the 6-rings of the net of $AlPO_4$-5 (stereoview, Figure 1e) are nonplanar, as are the 4- and 12-rings. Regular alternation of the up and down linkages[65] (Figure 10) results in every edge of the prototype 4.6.12 planar 2D net turning into the tilted linkages of a crankshaft chain. Each pair of superimposed 6-rings generates a 1,3,5 open hexagonal prism (*afi* unit, Figure 3). Condensation of one-third of the *bhs* chains (Figure 5) into crankshaft chains by a σ^- transformation[83] yields the net of $AlPO_4$-11[88] (stereoview, Figure 1d). Each cylindrical 12-ring channel becomes an elliptical 10-ring channel.

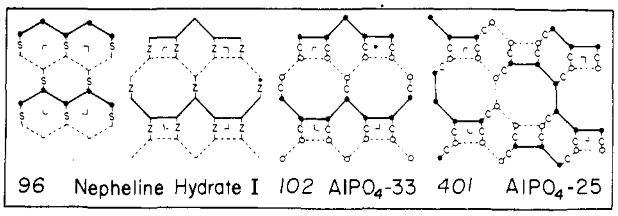

Figure 11. Three simple 3D nets based on a parallel stack of $(4.6.8)_1(6.8.8)_1$ 2D nets. The labels c, *s*, and *z* represent projections of crankshaft, saw, and zigzag chains (Figure 5). Numbers 96, 102, and 401 were assigned in ref 68 and 52. The 3D net of nepheline hydrate I can also be obtained from a 6^3 2D net (extreme left).

Another polytypic family of 3D nets is obtained from a parallel stack of 4.6.12 2D nets by linking the 1,3,5 vertices of each 6-ring of one net to the 2,4,6 vertices of the adjacent net through a two-T vertical bridge. In the $AlPO_4$-50 net (stereoview, Figure 1g), the 1,3,5 and 2,4,6 vertices of each 6-ring are linked together to form a cube, and each cube is linked to the next cube by a vertical linkage to produce a new type of chain, the *e*dge-*s*eparated-cube chain. Each 4-ring of the 2D net shares an edge with two cubes and is tilted and displaced either upward or downward. As a consequence, each 12-ring has alternate horizontal and tilted edges. The complex polyhedron *af* (Figure 4) is generated, and the polyhedral voids form a channel system limited by 12 rings in the vertical direction, and 8-rings in the horizontal one. More complex is the $AlPO_4$-46 net (stereoview, Figure 1f), in which each cube 4^6 has been transformed into the *afo* 4^66^3 structural unit by the operations shown in Figure 3. An enumeration of other ways of linking the structural units of the $AlPO_4$-46 and $AlPO_4$-50 nets into a polytypic series is being written up.

Many 3D nets can be obtained from the $(4.6.8)_1(4.8.12)_1$ 2D net,[76,110] and two have been found in the crystal structures of Linde L zeolite and mazzite (stereoviews, Figure 1x,y). Both have double-saw chains, but the Linde L net has hexagonal prisms at AA connected to planar 12-rings, whereas the mazzite net has planar 6-rings at height A or B alternately above or below each nonplanar 12-ring in which a tilted linkage of a crankshaft chain alternates with a horizontal linkage of a double-saw chain.

The $(4.6.8)_1(6.8.8)_1$ 2D net produced by a σ transformation from the 6^3 net (Figure 6) can be turned into the 3D nets of nepheline hydrate I, $AlPO_4$-33 (stereoview, Figure 1k) and $AlPO_4$-25 (Figure 11; the stereoview of the as-synthesized precursor $AlPO_4$-21 is given in Figure 1j). Both single and double zigzag chains occur in the nepheline hydrate I net, which can also be obtained from the 6^3 net by converting one-third of the edges into saw chains.[66,111] The nets of $AlPO_4$-33 and

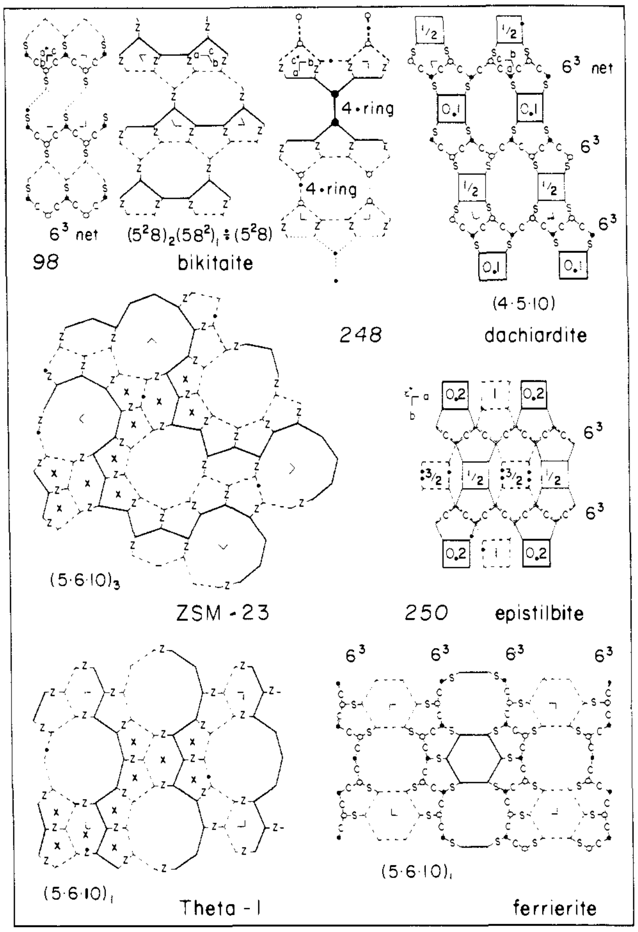

Figure 12. Six 3D nets containing several types of rings including 5-rings. The 3D net of bikitaite (Smith #98) can be obtained from parallel stacks of 2D nets, either of type 6^3 or $(5^28)_2(58^2)_1$; (5^28) for brevity. Horizontal edges of the 2D nets are replaced by crankshaft or zigzag chains. Each vertex marked by a filled or open circle is connected to a vertex either above or below by a vertical edge. The dachiardite 3D net (Smith #248) is obtained from the (5^28) net by addition of vertical 4-rings and zigzag chains, as viewed down the c axis. It can also be described by the combination of crankshaft and saw chains with a complex (4.5.10) 2D net. The numbers 0 and $^1/_2$ give heights of the 4-rings along the *b* monoclinic axis. The epistilbite 3D net (Smith #250) is related to the dachiardite net by changing from a leftward to a rightward tilt in adjacent 2D nets, as shown by the sequence of heights $b = 0, {}^1/_2, 1, {}^3/_2, 2$ referred to the dachiardite repeat $b = 7.5$ Å. This projection is viewed down the pseudoorthorhombic c axis, but epistilbite is monoclinic with c* perpendicular to the paper. The ferrierite and Theta-1 3D nets are obtained from a parallel stack of 2D nets of type $(5.5.6)_1(4.5.10)_1(5.5.10)_2(5.6.10)_2$, or briefly $(5.6.10)_1$, by converting some horizontal edges into either crankshaft and saw chains (ferrierite) or zigzag chains (Theta-1). Considerable distortion of the 2D nets occurs in both the horizontal and vertical directions. The ZSM-23 3D net is obtained by converting some horizontal edges of the $[5.6.10]_3$ 2D net into zigzag chains. It is drawn in this tilted position to show the unit of two 6-rings and eight 5-rings (marked by crosses), which is common with the Theta-1 net. Projections of some of the 6^3 2D nets are indicated; others may be found by looking for continuous strings of c chains or of *z* chains alternating with horizontal edges. Nets 98, 248, and 250 were numbered in ref 66 and 68. The other nets have not yet been classified in a systematic enumeration.

$AlPO_4$-25 utilize two different ways of converting edges into crankshaft chains.[52,66] Actually the net of $AlPO_4$-33 was first enumerated by replacing some pairs of edges of a 4.8^2 net with a double-saw chain (Figure 13 of reference 66).

Passing on now to 2D nets that contain 5-rings,[85] Figure 12 gives schematic projections of the 3D nets of six zeolites. The bikitaite net (stereoplot, Figure 11) can be obtained either from conversion of one-third each of the edges of a 6^3 net into crankshaft and saw chains[63] or from conversion of half the edges of the $(5^28)_2(58^2)_1$ net (Figure 6) into zigzag chains.[68] The dachiardite 3D net (stereoview, Figure 1o) can be obtained by replacing one-third of the *z* chains of bikitaite by a vertical string of unconnected 4-rings. Each string projects as a line segment, and the relative difference of height of the 4-rings is shown by the open and filled circles. Alternatively, the dachiardite 3D net can be projected down the monoclinic *b* axis to reveal conversion of some edges of a $(4.5.10)_1(5.5.10)_1$ 2D net (briefly (4.5.10)) into c and *s* chains. Each sequence of c chains generates a nonplanar 6^3 net, which shows up as a *zh* sequence in the left-hand drawing. The linking 4-rings alternate at heights that differ by $b/2$. An alternative description uses the concept of "handles" that straddle across vertices of the 6^3 sheet.[79] Retention of the nonplanar 6^3 net plus a left-to-right flipping of the 4-rings gives the 3D net of epistilbite (stereoview, Figure 1p). The symmetry becomes orthorhombic, and the repeat distance is doubled perpendicular to the (4.5.10) net; hence, the heights $0, {}^1/_2, 1, {}^3/_2, 2$ for the dachiardite repeat distance become $0, {}^1/_4, {}^1/_2, {}^3/_4, 1$ in the epistilbite cell.

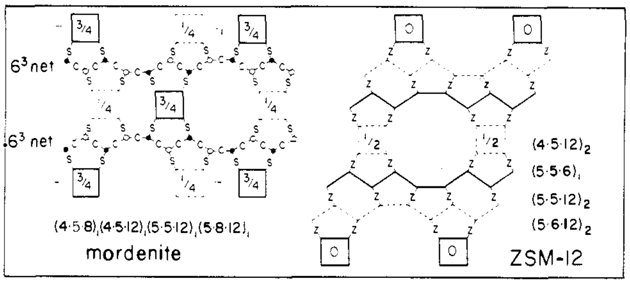

Figure 13. Projections of the 3D nets of mordenite and ZSM-12 showing projections of c, *s*, and *z* chains and of 6^3 nets.

The 3D net (TON) of the Theta-1 synthetic zeolite[112,113] is obtained by converting one-half of the edges of the $(5.5.6)_1(5.5.10)_1(5.5.10)_2(5.6.10)_2$ net (briefly $(5.6.10)_1$) into zigzag chains (note: there are two types of 5.5.10 vertices). An independent determination of the isostructural ZSM-22 synthetic zeolite[114] discussed the structural relationships between the TON 3D net and the nets of bikitaite and ferrierite. The ferrierite net is also based on the $(5.6.10)_1$ 2D net, but it contains horizontal planar 6-rings at two levels separated from vertical 6^3 nets by vertical saw chains. New nets can be developed with σ transformations. Faults occur in natural ferrierite.[114a] A systematic enumeration of all ways of converting edges of the $(4.6.10)_1$ 2D net into simple chains is under way.[115]

There is an infinity of complex 3-connected 2D nets containing 5-, 6-, and 10-rings. One of these, labeled $(5.6.10)_3$ for brevity, is the basis of the 3D net (MTT) of ZSM-23.[116] Just as for the TON net, some of the horizontal edges are converted into zigzag chains, giving the characteristic 5-Å repeat distance. A block of two 6-rings and eight 5-rings, marked by crosses, is common to the TON and MTT nets.[116]

The 3D net of mordenite (Figure 13; stereoview, Figure 1C) is based on yet another complex 3-connected 2D net containing 5-rings, here in association with 4-, 8-, and 12-rings. The 4-rings are at two levels and are

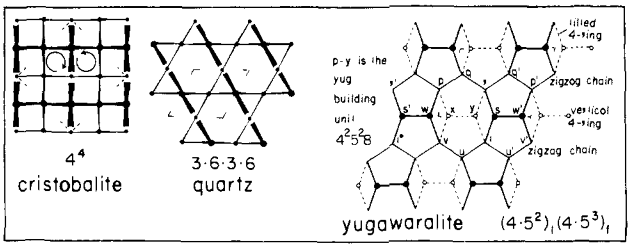

Figure 14. Three ways of converting 4- and (3,4)-connected 2D nets into 4-connected 3D nets. See ref 66 for other ways of combining helices with 2D nets.

suspended by saw chains between nonplanar 6^3 nets[85] shown in projection as a row of crankshaft chains. Some of the structural relatives of the mordenite net[90] were enumerated in ref 82, 117, and 118; see also ref 119 on the disordered svetlozarite.

Yet another complex 2D net containing 5-rings is found in the 3D net MTW of ZSM-12 (Figure 13). Fragments of this 2D net can be matched with pieces of the 2D nets in Figure 12 and in the mordenite 3D net. One-half of the edges of the 2D net (briefly (4.5.6.12)) are converted into zigzag chains in the MTW net.

This completes the description of the simplest ways in which edges of 3-connected 2D nets can be converted into simple chains to produce 4-connected 3D nets. A brief introduction is now given to an incomplete study of the conversion of 4-connected 2D nets into 4-connected 3D nets.

The 4^4 square 2D net can be converted into a 4-connected 3D net (Figure 14) by turning each circuit of four edges into a 4-fold helix.[66] Around each spiral, each vertex changes in height by $^1/_4$, as shown by the four sizes of filled circles. Adjacent circuits are forced into spirals of different parity. This procedure generates the net of cristobalite, which was derived independently from a 6^3 net in Figure 8. The net of quartz is derived by conversion of each 3-ring of a 3.6.3.6 2D net into a 3-fold helix. Two choices of parity give the left-handed and right-handed varieties. The complex 4-connected 3D net linking the Al atoms[120] of $Sr_{15}Al_{24}O_{48}(OH)_6$ can also be derived from the 3.6.3.6 2D net; some 3-rings are tilted and others are converted into 3-fold helices (not shown in Figure 14). The importance of 3- and 7-rings in this net is demonstrated by the circuit symbol $(3^267^3)_1(367^28^2)_1$.

The yugawaralite net (Figure 14; stereoview, Figure 1l) is based on the $(4.5^2)_1(4.5^3)_1$ 2D net, which is half 3-connected and half 4-connected. All the edges between the 4-connected vertices are raised (s′w and sw′) or lowered (xy) below the level of the zigzag chains and converted into vertical 4-rings. The other side of each 4-ring is then part of the next 2D net. Tilted 4-rings are generated by the edges between the zigzag chains and the vertical 4-rings. Othr (3,4)-connected 2D nets[58] can be treated in a similar manner.

This completes the description of those 3D nets in zeolites and related materials that can be readily described by linking together 2D nets. Some 3D nets are not conveniently decomposable into 2D nets. Thus the analcime net (stereoview, Figure 1h) is best described in terms of a 3D intersection of nonparallel chains of vertex-shared 4-rings spiraling around a square helix (p 9 of ref 6). Others are best described by the sharing of faces between polyhedra, as in the next section.

F. Face-Sharing of Polyhedra

This section must be restricted to some of the simplest examples. First, consider the complete filling of space with just one type of parallel polyhedron. Out of the five parallelohedra (Fedorov polyhedra) (p 77 of ref 60), only the truncated octahedron (*to*, Figure 4) fills space such that only four edges meet at each vertex. These edges generate the 3D net of sodalite (stereoview, Figure 1).

Second, consider the complete filling of space with more than one type of regular (Platonic) or semiregular (Archimedean) polyhedron. A mathematical analysis in 1907[121] was rediscovered after the related 4-connected nets had been enumerated.[67] The truncated tetrahedron and truncated cube can be combined with the truncated cuboctahedron (renamed the great rhombicuboctahedron; *grco*, Figure 4) to give a 4-connected net with some 3-rings. Of principal interest here are the cube (*cu*, Figure 3), *to*, *grco*, hexagonal prism (*hp*, Figure 3), and the octagonal prism (*op*, Figure 3). Attachment of a *cu* to each hexagonal face of a *to* leads inexorably to the net of Linde Type A zeolite (stereoview, Figure 1w). Each cubic unit cell contains a *to* at each corner, a *cu* at the center of each edge, and a *grco* at the body center. Two *to* can share an *hp* in two ways. The trans configuration in which a square of one *to* is opposite a hexagon of the next *to* leads uniquely to the net of faujasite (stereoview, Figure 1r) and generates the large *fauj* cage (Figure 4). However, the *fauj* cage contains four types of vertices and is not semiregular (Archimedean). In the faujasite net, the centers of the *hp* are topologically related to the C positions in diamond. An even better analogy is with the Si atoms in high-cristobalite, since the *hp* of faujasite correspond to the average position of the oxygen atoms. In contrast to the trans configuration, the cis configuration does not produce a regular 3D net. However, use of the trans configuration in layers of linked *to*, and the cis configuration between all or some layers, yields an infinite polytypic series. No zeolite has been identified with a fully regular structure that belongs to this polytypic series;[122] however, twinned faujasite and various synthetic zeolites may have faulted interfaces with the cis configuration.[67,123,124]

The 3D net of Mobil ZK-5 zeolite (stereoview, Figure 1v) is generated by sharing an *hp* unit between pairs of parallel *grco* units. The remaining volume is taken up by *paul* units. Sharing of an *op* unit between pairs of parallel *grco* units yields the 3D net of the Rho zeolite (stereoview, Figure 1F); there is no residual volume.

The 3D net of paulingite contains *op*, *grco*, *paul*, and *plgt* cages in a complex arrangement of shared faces; only the first two types of cages are Archimedean. Similarly, the 3D net of Linde Type N zeolite contains a complex assemblage of polyhedra, including the Archimedean units *hp*, *to*, and *grco* and the non-Archimedean *canc* unit.

σ^- derivatives of the Archimedean and paulingite nets are enumerated in ref 67 and 75.

Although the truncated rhombic dodecahedron (*trd*, Figure 4) is not Archimedean, it is highly symmetric and is the basis of the 3D net of $AlPO_4$-16. When packed together with hexagonal faces in contact, it fills space except for cubes generated from the square faces. This structure type had been predicted 30 years ago by the late D. W. Breck, on the basis of the zunyite structure, which lacks some of the edges of the 4-connected 3D net.

The members of the clathrasil group (Table If) can be represented by face-centering polyhedra.[35] The regular dodecahedron (*rd*, Figure 4) occurs in the DOH, DDR, MEP, and MTN 3D nets in association with either one or two other polyhedra listed in Table If and illustrated in Figure 4.

There is an infinity of possible nets formed by face-sharing of nonregular polyhedra, and not all the topologies found in hydrate inclusion compounds[125] have yet been found in zeolites and related materials. Furthermore, there are 92 nonuniform convex polyhedra with regular faces,[126] and there has apparently been no attempt to discover how many will lead to 4-connected 3D nets. Certainly most will not do so because of the large number of edges meeting at vertices. A general approach[127] to space-filling polyhedra should prove useful in the invention of new nets.

This section concludes the selective review of the ways in which rings, chains, sheets, and polyhedra can be regarded as building units in the 3D 4-connected nets of zeolites and related materials. Many new 3D nets can be invented simply by stacking together known structural units in new ways, and many further series of theoretical nets will be published as the tedious process of enumeration continues. Further building units will be recognized in new crystal structures, and others will be invented to fill in the obvious gaps, such as those indicated in Figure 3. Now that two 4-connected 3D nets with 3-rings are known (in $Sr_{15}Al_{24}O_{48}(OH)_6$[120] and lovdarite[90,93]) and several nets with 7-rings are recognized (e.g., $Sr_{15}Al_{24}O_{48}(OH)_6$[120]), it is important to make an effort to extend the present meager attempt to enumerate nets with 3- and 7-rings (e.g., ref 65 and 66). In addition, it is important not to rule out complex nets in the belief that the principle of parsimony applies; certainly the nets in Figure 12 are not simple. Yet again, it is important to recognize that not all chemical species occupying the vertices of 4-connected 3D nets are tetrahedrally coordinated to oxygen atoms; this is demonstrated by the presence of 4-, 5-, and 6-coordinated Al in the as-synthesized $AlPO_4$ materials.[52] Hence, caution is needed in the application of the distance-least-squares technique for testing whether a theoretical 3D net is geometrically reasonable. It is obvious that we are just beginning to explore the wide expanse of structural types that could be listed under the general classification of zeolites and related materials.

G. Micropores and Internal Surfaces

It is important to distinguish between the theoretical maximum volume of the micropores of a fully expanded (4;2)-3D net and the available volume in a corresponding zeolite or related material when account is taken of geometrical distortion, and especially of extraframework species such as cations and occluded salts. The 4-connected nets displayed in Figure 1 are somewhat misleading about the available volume because there is no precise information about the actual positions of oxygen atoms and none about the cations and any occluded salts. It is impossible to give the details here of what information is available, but they can be obtained from the specific references in section III, and from a compilation of extraframework sites.[56]

A micropore is effectively isolated from another one when a particular candidate for molecular adsorption cannot pass between the micropores. A ring or window (Figure 2) may be too small geometrically, or it may be large enough in theory, but blocked by a gatekeeper cation. Even when cations and occluded salts are ignored, some of the materials commonly listed as zeolites contain micropores whose maximum access is through 6-rings: Table I, column 9; AFG, LIO, SOD, LOS, LTN, MTN. One of the clathrasils, decadodecasil 3R, has some of the micropores accessible by a 2D system of 8-rings, whereas some of the microporosity in all of the clathrasils except SOD is accessible only through 5-rings. Although decadodecasil 3R was described[128] as the "missing link between zeolites and clathrasils", it is clear that there is a diverse range of overlapping geometrical properties between materials classified as zeolites and clathrasils.

It is important whether a micropore is accessible by only one window or by more than one window, since blockage by an occluded species is less likely for the latter. Materials based on the FAU and pentasil nets (MEL, MFI) are particularly resistant to blockage of the micropores because of the three-dimensionality of the pore system and the large size of the windows. Although there is no complete structural answer to the difference between the large- and small-pore varieties of mordenites, it is theoretically obvious that the one-dimensional 12-ring channels could be blocked by a gatekeeper cation or a trapped Al-bearing species.[129-131] Theoretically, stacking faults also could block the 12-ring channels, but apparently they are not responsible for small-pore mordenite.[131] However, stacking faults are common in natural gmelinite[108] and must block the 1D 12-ring channels.

To complete this section, the topology of the internal surface of an infinite channel system is interesting, since the surface can be treated as an infinite curved net or infinite polyhedron.[58] A systematic mathematical study of the topology of the internal surfaces of zeolites and related materials has not yet been published, but Figure 15 illustrates what might be done. The cylindrical channel of $AlPO_4$-5 can be related to two cylindrical nets. The T–T linkages form a 6^3 net, with one edge of each 6-ring parallel to the cylindrical axis. Oxygen atoms of the $AlPO_4$-5 3D net lie at the vertices of the 3.6.3.6 (kagomé) 2D net used in Figure 14. Alternatively, the oxygen positions can be expressed in terms of a 24-repeat spiral, either left-handed or right-handed.

The term "tubular building unit" was invented[62] for the assemblage of T–T linkages around linear channels. Figure 16 shows the perspective drawings[62] of tubular building units in the CAN, FER, GME, LTL, MAZ, MEL, MER, MFI, MOR, and OFF nets. A 6^3 net occurs around each cylindrical channel of the CAN net (also in the ABW net), but it is oriented with one edge perpendicular to the cylinder axis.[93] A 4.8^2 net occurs in GME, and a $(4.6.8)_1(6.8^2)_1$ net in OFF. None of the other tubular building units are based on simple 3-connected 2D nets, and some vertices are 4- or 2-connected.

A summary of the dimensionality and the ring sizes of the windows is given in column 9 of Table I, and

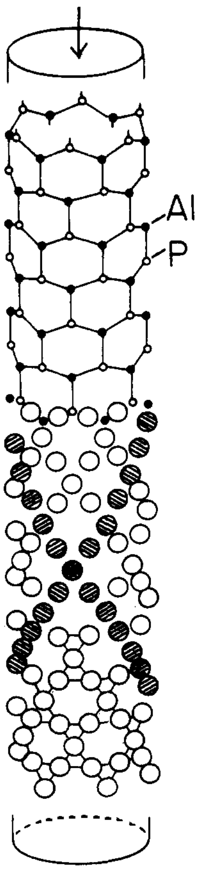

Figure 15. Three topological descriptions of the surface of a cylindrical channel in $AlPO_4$-5. The alternating Al and P positions define the vertices of a 6^3 net. The oxygen positions (open circles) can be joined into a 3.6.3.6 (kagomé) net or linked into 24-fold helices (hatched circles).

references are given in section III to the available data on detailed geometry.

H. Nets with Extremely Low Density

Although nets have been invented[71] with rings of any size up to infinity, the largest ring in an actual zeolite or related material involved 12 tetrahedra at the time of completion of this manuscript in June 1987. This limit of a 12-ring in a synthetic zeolite or related material based on a (4;2)-3D net was broken by M. E. Davis, who gave an oral report[13a] in Sept 1987 of the synthesis of a new material of unspecified chemical composition based on net 81(1) invented by Smith and Dytrych.[71] This net (Figure 18) has cylindrical channels spanned by 18-rings and is the second member of an infinite series of nets with unlimited channel diameter. The rest of this section was written in June 1987, and a detailed enumeration of many infinite series of nets is being prepared for publication.

The general problem of open packing of spheres is very difficult since the answers depend on the assumptions about the local connectivity. At the purely mathematical level, the only thing that counts is that there is continuity from one sphere to the next. From the engineering viewpoint of the stability of a pile of dust particles, or a rime of ice crystals,[132] each particle must be in contact with several other particles, but not with crystallographic regularity. For the present purpose, an open packing of spheres must be regular, at least in two dimensions, and preference is given to arrangements that are related to (4;2)-connected 3D nets.

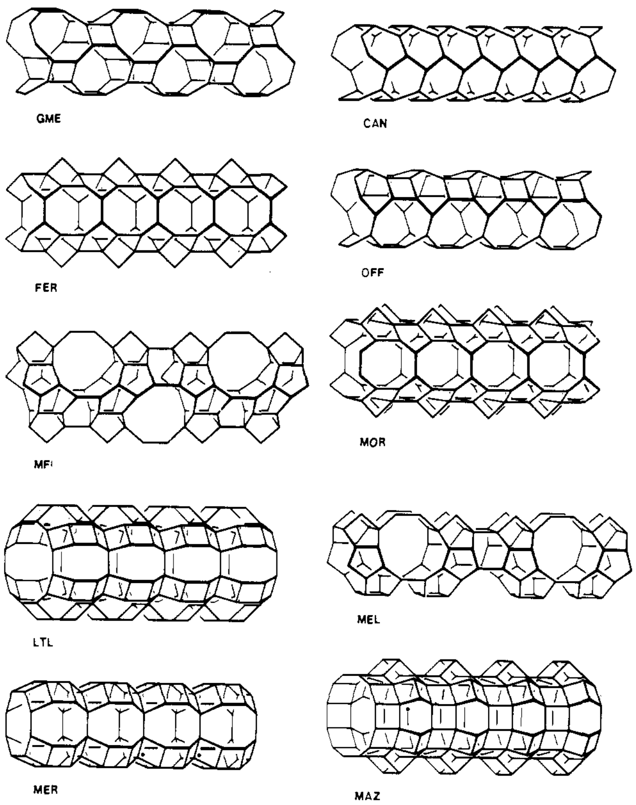

Figure 16. Ten tubular building units generated from T–T linkages in the 4-connected 3D nets of zeolites and related materials. Reassembled from Figure 3 of ref 62.

The problem of stability is a difficult one because it involves chemical bonding. From the viewpoint of simple ionic bonding, any open packing *in general* is not *electrostatically* stable with respect to a more compact one. Material encapsulated during synthesis can promote stability of open frameworks, but removal of the encapsulated material should result in collapse of the framework as the minimum of electrostatic energy is favored. From the viewpoint of ionic *plus* covalent bonding, there is a strong tendency for O–T–O and T–O–T angles to lie within the ranges given earlier for tetrahedrally bonded species, and open structures can persist metastably if bonds remain unbroken. Because some atoms in T positions have extraframework ligands which result in strong deviation of the O–T–O and T–O–T angles from those for tetrahedrally bonded species, care is needed before rejecting a geometry that does not fit with the above range of angles. Hence the safest approach in considering nets with extremely low density is to look first at all theoretical possibilities, irrespective of chemical implications, and then to look at the complex topochemical possibilities.

Low-density sphere packings were invented for a continuous, locally symmetric arrangement in which each line joining the points of contact of successive spheres passes through the centers of the spheres.[133] The most open packing has 94.4% void space. The line-center restriction is critical to *mechanical* stability of a sphere packing, but is not necessary for *chemical* stability. Replacement of one sphere by a triangle of three spheres is an important technique for creating new packings,[133] as explored later.[134] Relaxation of the above stability criterion allows invention of sphere packings of even lower density, including ones with 95.5 and 95.8% void space.[135,136]

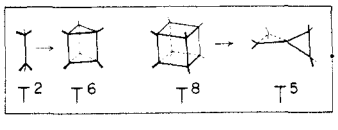

Figure 17. Two transformations that yield less-dense nets.[93]

For zeolites, each T position is surrounded by a tetrahedron of four oxygen spheres, and the condition for an open framework must be more restrictive than just for the packing of spheres. Each sphere must be in contact with four other spheres, three from the parent TO_4 group, and one from an adjacent TO_4 group. Although the three-for-one principle[133] was applied to spheres, and is not applicable to T sites, 3-rings are important in a suite of low-density frameworks.[93] A review[137] considers the effect of varying the nearest-neighbor coordination from 3 to 12.

From a consideration of coordination sequences and loop configurations, it was concluded that 4-connected zeolite-related frameworks with the lowest possible density should either contain 3-rings or have T atoms connected to more than three 4-rings.[138] Figure 17 shows two ways[93] of obtaining less dense nets by replacing a T–T dimer with a T_6 trigonal prism, and a T_8 cube by a T_5 spiro-5 unit (i.e., a vertex-shared pair of 3-rings). Figure 6 of ref 93 is a stereopair of the conversion of cubes in the Linde Type A framework to T_5 units. From Table I, cubes are available for conversion in the $AlPO_4$-16 and $AlPO_4$-50 nets; other hypothetical nets containing cubes are listed in ref 59 and 67.

An alternative approach[71] yields an infinite series of 4-connected 3D nets with channels that can be expanded to any desired diameter (Figure 18). Two series based on addition of squares to the 4.8^2 and 4.6.12 2D nets were given, and several series based on the 4.6.12 net are given in Figure 18. At the upper left is the near–near–far-facing structure,[110] which can be redescribed with saw chains, hexagonal prisms, and 4-rings. The "walls" enclose cylindrical channels bounded by nonplanar 24-rings (*not* 18-rings[110]) with a free diameter of 15 Å. Three other types of walls are shown at the bottom left. At the lower right are the walls of the first three members of an infinite series,[71] starting with the 3D net (Smith #81) of the $AlPO_4$-5 structure in which upward and downward edges alternate around each ring. Addition of each 4-ring in the wall increases the ring size of the cylindrical channel by 6. A strip of three 4-rings in each wall gives a 24-ring. For *n* squares in each wall, the ring size is $6(1 + n)$. The same idea can be applied to the nets[110] from the lower left. Adding a horizontal 4-ring (upper right) requires addition of two rectangular projections for interconnecting double chains. For *n* squares in each wall, the ring size is $12(1 + n)$.

The principle of converting single 4-rings into a chain of edge-shared 4-rings in 2D and then converting edges into c, s, and z chains yields many infinite series which will be published when detailed enumeration is completed.

Two intersecting interrupted frameworks of very low density[138a] occur in *neptunite*, $LiNa_2K(Fe,Mg)_2(TiO)_2Si_8O_{22}$.

III. Description of Specific Structures

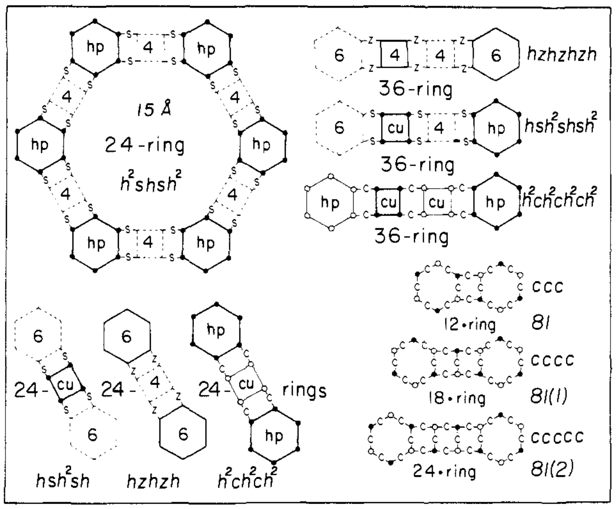

Figure 18. Projections of 3D nets that can be expanded to yield channels of unlimited size. The projection at the upper left shows how a 24-ring is generated from the sequence h^2shsh^2, which gives a hexagonal prism from the h^2, a double-saw chain from the s, and a 4-ring from the h. At the lower right is the infinite series 81(*n*). The sequence ccc gives net 81 with a 12-ring when the segment is extended by 6-fold rotation symmetry. Successive addition of c gives 81(1) with an 18-ring, 81(2) with a 24-ring, and so on. Three ways of generating 24- and 36-rings are shown at the lower left and upper right. A detailed enumeration and description of these and other infinite series of 3D nets with unrestricted ring size is being prepared for publication.

This section summarizes the important structural and chemical features of selected microporous materials and references thereto. It should be read in conjunction with the 1987 revised *Atlas of Zeolite Structure Tyes*, which contains a thorough compilation of loop configuration of T atoms, coordination sequences, channels, fault planes, type species, isotypic framework structures, selected references, stereoplot and cross sections of channels. The present treatment describes some related materials not listed in the Atlas. It also provides a guide to a reader looking for a material with a particular geometrical feature. First look at Table I for those species with the desired feature, then consult the Atlas, and finally check this review for the important structural and chemical features of materials containing the desired feature. Reference 56 lists structure determinations up to 1981.

A. Natural Zeolites and Related Aluminosilicates, Including Synthetic Analogues

AFG. Afghanite,[139] an (Na, K, Ca) aluminosilicate with micropores filled mainly by (Cl, SO_4, CO_3).

ANA. The analcime structure type is represented by *analcime*[5] (ideally $NaAlSi_2O_6{\cdot}H_2O$, but with solid solution toward SiO_2; several symmetry variants with polyhedral tilting;[140] ion exchange and reversible dehydration through highly distorted 8-rings slightly bigger than circular 6-rings[141-144]), *wairakite* (ideally $CaAl_2Si_4O_{12}{\cdot}2H_2O$, but containing Na; more tightly bonded than analcime[145]), *doranite* (an Mg-bearing mineral variety $Na_{10}Mg_3Al_{16}Si_{32}O_{96}{\cdot}25H_2O$[145a]), *synthetic aluminosilicophosphate* ($Na_{13}Al_{24}Si_{13}P_{11}O_{96}{\cdot}16H_2O$; ordered Al and Si,P[146]), various feldspathoids,[103] including *leucite* (ideally $KAlSi_2O_6$; framework crinkling at phase transition;[147-149] synthetic analogues[149,150]) and *pollucite* (near $Cs_3NaAl_4Si_8O_{24}{\cdot}H_2O$;[151] synthetic analogues $(Rb,Cs)(Be,Mg,Fe,Co,Ni,Zn,Cd)Si_5O_{12}$[152,153]), the fluoroberyllosilicate *hsianghualite*[154] ($Li_4Ca_6Be_6Si_6O_{24}F_4$), and various natural and synthetic phosphorus-bearing materials[33] lacking detailed structural data.

BIK. *Bikitaite*, $LiAlSi_2O_6 \cdot H_2O$, in partly[155] and fully Al,Si-ordered[156] types; no data on dehydration. *Synthetic* $Cs_{0.35}Al_{0.35}Si_{2.65}O_6$[157] has Cs bonded across the 8-ring.

BRE. *Brewsterite*, $(Sr,Ba)Al_2Si_6O_{16} \cdot 5H_2O$, has a 2D channel system, but the 8-rings are strongly distorted;[158,159] no data on dehydrated structure.

—. *Buddingtonite*, $NH_4AlSi_3O_8 \cdot {}^1/_2H_2O$; feldspar structure[19] with strongly distorted 8-rings.

CAN. *Cancrinite* is the general name for a family of feldspathoid minerals,[103] including *cancrinite* itself, near $Na_6Al_6Si_6O_{24} \cdot CaCO_3 \cdot 2H_2O$ with possible hydroxyl,[160–164] *microsommite*,[165] containing sulfate, etc., and *tiptopite*,[165a] $K_2(Li_{2.9}Na_{1.7}Ca_{0.7})Be_6P_6O_{24}(OH)_2 \cdot 1.3H_2O$. Synthetic varieties include a germanate analogue[166,166a] and a salt-free hydrated cancrinite.[167] Complex ABC-6 stacking varieties[168] are often listed in the cancrinite family. The ideal structure has a one-dimensional 12-ring channel, but it is blocked by salts in most cancrinites.

CHA. Represented by the minerals *chabazite*[107] (ideally $CaAl_2Si_4O_{12} \cdot 6H_2O$, but with an extensive range[5,169] of Si/Al and substitution of Na, K, Sr, and Ba; complex Al,Si order–disorder) and *willhendersonite*[170] ($KCaAl_3Si_3O_{12} \cdot 5H_2O$ with alternating Al and Si[171]). Considerable changes[172] of cation positions and framework geometry occur in chabazite during ion exchange, dehydration, and molecular sorption: *hydrated at room temperature*, natural[107,173,174] and exchanged with Na,[174] K,[174,175] Ag,[175] Cs,[176] Ca[174,177] (also at 123 K[178]), Sr,[174] Ba,[179] Cd,[179] Mn,[180] Co,[181] and Cu;[181a] *dehydrated and observed at room temperature*, exchanged with Cs,[176] Ag,[182] Ca,[183,184] Mn,[180] Co,[181] and Cu;[181a] NH_4-exchanged, converted to H form, pretreated at 593 and 873 K after steaming;[185] *complexes* with chlorine[186] and CO.[187] K-exchanged *ZK-14*, with faults,[187a] was studied at high temperature.[188] Some large monovalent ions are gatekeepers in 8-rings, but most other species allow three-dimensional access to the cages. An Fe-rich chabazite, analyzed at 293 and 573 K, showed similar changes to Fe-poor ones.[189] A synthetic aluminosilicophosphate, $H_3O \cdot Al_4SiP_3O_{16} \cdot nH_2O$, has ordered Al and (Si,P).[190]

DAC. The rare mineral *dachiardite* has a wide range of Na, K, Ca, and Cs,[5] and the ideal crystal structure[191,192] is complicated by stacking faults,[192a] especially in the variety *svetlozarite*.[119] No data on dehydrated structure.

EDI. The mineral *edingtonite*, ideally $Ba_2Al_4Si_6O_{20} \cdot 8H_2O$, has ordered[193,194] and disordered Al,Si arrangements[195,195a] and some water loss at room temperature.[194] No structural data on dehydrated variety. The synthetic zeolite *K-F*, $K_{13}Al_{10}Si_{10}O_{40}(OH)_3(H_2O)_{13}$, the Na-exchanged variety, and the Rb analogue *Rb-D* also have the channels spanned by cations and water molecules.[196,197] *Kalborskite*, an anhydrous analogue, has K, Cl, and $B(OH)_4$ in the channels.[198]

EPI. *Epistilbite*, near $Ca_{2.5}Na_{0.8}K_{0.2}Al_6Si_{18}O_{48} \cdot 16H_2O$,[199] has partial Si,Al order, a domain texture, and variable stacking disorder which affects the channel system.[200–202]

ERI. *Erionite*, variable composition,[5] including $Na_{0.9}K_{2.0}Mg_{0.7}Ca_{2.4}Al_9Si_{27}O_{72} \cdot 28H_2O$, tends to have faults related to offretite and sodalite.[109,204,205] During dehydration, internal ion exchange[206] occurs as Ca moves into the *canc* unit and K leaves to go into an 8-ring.[207–209] Four 8-rings of the *erio* cage remain open. A low-accuracy structure[210] is available for Linde T synthetic zeolite.

FAU. The rare mineral *faujasite*[5] contains 52–68 Al per cell and a wide range of Ca (10–20), Na (8–35), Mg (3–9), and K (1–6). Synthetic materials in the *Linde X* and *Y* series, and dealuminated varieties, range from Si/Al = 1 down to near zero. Because the micropores are accessible in 3D by 12-rings and because only minor changes of window size occur, the details of framework geometry are relatively unimportant for loading of the *fauj* cages. The *to* cages, however, are accessible only when the 6-rings are unblocked. The following papers contain details of framework geometry and cation sites from diffraction evidence: review up to 1970;[210a] data on faujasite;[210b,c] *ion-exchanged faujasite*, including Ca-,[210d] La-,[210e] and Ce-;[211] *dehydrated ion-exchanged faujasite*, including Ca-,[212] Ni-,[213] La-,[214,214a] La- at 693 K,[215] Ce-,[211] and H-;[216] *varieties of Linde Y*, hydrated and dehydrated as-synthesized Na- at various temperatures,[217,217a] Pd and H reduction, benzene adsorption, and dehydrogenation,[218] dehydrated La-deuteriated-,[219] hydrated and dehydrated Na-, K-, and Ag-,[220] benzene complex,[221] partly hydrogen-exchanged,[222,222a] Ce,H-exchanged,[223] partly and strongly dehydrated Co-exchanged,[224] Ni complexes,[225,226] Cu complex with ammonia and pyridine,[227] oxidation and reduction of Ag-,[228] dehydrated Li-exchanged with considerable tetrahedral rotation;[229] hydrated and dehydrated K-,[230–232] dehydrated Cr-,[233] dehydrated and oxidized Fe-,[234] benzene complexes of K-, Ca-, and Sr- at various temperatures;[235] *varieties of Linde X*, progressive dehydration of as-synthesized Na-,[236–238] La- at 298, 698, and 1008 K,[239] hydrated as-synthesized Na-,[240] hydrated $Ge_{27}Na_7$,[241] hydrated and partly dehydrated Cd-,[242] dehydrated Li-,[229] hydrated and dehydrated K,[230,231] hydrated as-synthesized Na-,[243] dehydrated Cr-,[233] dehydrated Ca-,[244] hydrated and dehydrated as-synthesized Na-,[245] *complexes of faujasite*, Mn-exchanged and 1-chlorobutane,[246] Ni-exchanged and *m*-dichlorobenzene;[247] *dealuminated-Y*, AlO_4 species in *to* cage;[248] *dehydrated Na,Ga-Y* and *-X*.[249,250]

FER. *Ferrierite* is a high-silica zeolite mineral[5] with 5–7 Al and variable Mg (0.4–3.0), Na (0.1–3.1), K (0.4–1.6), and Ca (0–1) atoms/cell. The basic crystal structure[251,252] is slightly distorted in a monoclinic variety,[253] and the channel system is modified by stacking faults.[114a,192a,254] Structural data are lacking on cation sites and framework geometry after dehydration; probably the 2D channel system will remain open.

GIS. This framework topology occurs in *gismondine*, $Ca_4Al_8Si_8O_{32} \cdot 18H_2O$, with an ordered Al,Si framework and partly disordered water molecules,[255–257] *amicite*, $K_4Na_4Al_8Si_8O_{32} \cdot 10H_2O$, with ordered Al,Si and K,Na,[258] *gobbinsite*, $Ca_{0.6}Na_{2.6}K_{2.2}Al_6Si_{10}O_{32} \cdot 12H_2O$,[259] *garronite*, a domain-disordered variety[260] of gismondine, and synthetic *Na-P1*[261] and *TMA-gismondine*.[262] Cations will probably block some windows in dehydrated varieties.

GME. *Gmelinite*, ideally $Na_8Al_8Si_8O_{32} \cdot 24H_2O$, has a wide composition range[5] with Na (0.8–7.6), Ca (0–2.1), and Sr (0–1.3). The cylindrical 12-ring channels in the ideal structures of Na-rich,[108,263] Ca-rich,[263] K-rich,[264] and Ba-exchanged[265] varieties have similar geometry in the hydrated varieties, but the cation positions in dehydrated ones are not known. Stacking faults block the 12-ring channels, but a synthetic variety is fault-free.[266]

GOO. Goosecreekite has ordered Si,Al and distorted 8-rings,[267] which might be partly blocked in the dehydrated variety.

HEU. There is a complex range of chemical compositions[5] between *heulandite*, near $(Na,K)Ca_4Al_9Si_{27}O_{72}\cdot 24H_2O$, and *clinoptilolite*, near $(Na,K)_6Al_6Si_{30}O_{72}\cdot 2H_2O$, with Al (6–9), Na (0–4), K (0.2–2.6), Ca (0.1–3.6), Sr (0–2), and Ba (0–1). The structural changes during dehydration are complex and become irreversible; natural heulandites,[268–272] natural clinoptilolites;[273–275] heated heulandites;[272,276,277] clinoptilolite at 623 K;[278] ion-exchanged varieties, heated Ca-, Na-, K-, and Rb-,[279] Ag-,[280,281] K- at 293, 373, and 593 K,[282] partly NH_4- at 483 K,[283] Rb-,[271] and Ba-.[284]

LAU. Laumontite, ideally $Ca_4Al_8Si_{16}O_{48}\cdot 16H_2O$, dehydrates under low humidity to *leonhardite* with 14 H_2O.[5] The complex details of the early structure work[285–287] are extended by further studies.[288,289] The fully dehydrated structure is unknown.

LEV. Levynite has a complex distribution of Ca, Na, and K[290] in the characteristic framework.[291] The dehydrated structure is unknown, but cations should move to 6-rings by analogy with chabazite.

LIO. Liottite is a feldspathoid stuffed with SO_4, CO_3, Cl, and OH.[103]

MAZ. Mazzite[292] is apparently isostructural with synthetic zeolite *Omega*. Cations interchange during partial dehydration of mazzite at 873 K[293,294] so that $Mg(H_2O)$ spans each 6-ring, $Ca(2H_2O)$ blocks an 8-ring, and K projects into a small cage; the 12-ring channel is clear. The structure of dehydrated synthetic gallium mazzite[295] is similar. Structural faults occur.[296]

MER. The crystal structures[297,298] were determined for two samples of the very rare mineral *merlinoite*, $Na_{0.6}K_{4.2}Ca_{1.5}Ba_{0.4}Al_9Si_{23}O_{64}\cdot 23H_2O$ and $\sim$ $NaK_5Ba_3Al_{12}Si_{20}O_{64}\cdot 20H_2O$. There are no structural data on the dehydrated structure or on synthetic isotypes.

MOR. The high-silica zeolite *mordenite*, with variable Ca (1.5–2.4), Na (2–5), and K (0.1–0.8) atoms/cell,[5] and the synthetic isotypes have an ideal structure containing 1D channels bounded by nonplanar 12-rings. Side pockets, each outlined by two 4-rings, four 5-rings, and two 6-rings, are accessible through 8-rings, unless blocked by cations. Stacking faults occur.[192a] Dealumination produces encapsulated octahedral aluminum species (see later). The structural differences between large- and small-port mordenites are only partly resolved (see earlier). Structural data are available for natural mordenites;[299,300] dehydrated exchanged varieties, Ca-,[301] heated ammoniated H-,[302] Rb-,[303] Ba-,[304] Cs-,[305] K-,[306] Na-,[307] acid-exchanged H-,[308] Ca-;[309] rehydrated Ca-[310] and K-;[306] hydrated HCl treated.[311]

NAT. This structure topology is represented by the fibrous zeolites: *Natrolite*, $Na_2Al_2Si_3O_{10}\cdot 2H_2O$, in ordered and disordered varieties, *scolecite*, $CaAl_2Si_3O_{10}\cdot 3H_2O$, and *mesolite*, $Na_2Ca_2Al_6Si_9O_{30}\cdot 8H_2O$, both ordered; there is only minor chemical deviation from the ideal formulas.[312] In general, the *fi* chains rotate and kink during dehydration as the pores shrink, and the windows of nonplanar 8-rings become even more nonplanar. Recent structural data of hydrated varieties at room temperature are as follows: ordered natrolite,[313–318] disordered natrolites (including *tetranatrolite* and *gonnardite*);[319–322] scolecite,[321–326] mesolite,[327,328] heated and dehydrated natrolites.[329,330] The $Rb_2Ga_2Ge_3O_{10}$ structure is anhydrous.[331]

OFF. Offretite, $KCaMgAl_5Si_{13}O_{36}\cdot 15H_2O$, has 12-ring channels which can be blocked by stacking faults or intergrowths with erionite.[332–334] The cations move during dehydration[335,336] and block 6- and 8-rings but not the 12-ring channels; only slight changes occur upon CO adsorption.[337] A synthetic variety with encapsulated tetramethylammonium has crystallographic disorder, which explains the restricted shape-selective catalysis.[338]

PAU. The *paulingite* structure[339] is complex, and a modern refinement[340] was hampered by disorder. There is no determination of the dehydrated structure.

PHI. This topology is represented by *phillipsite* (wide composition range (atoms/cell): Al (4–6), Ca (0–2), Na (0–2), K (1–4)), *harmotome* (Al ($\sim$5), Ba ($\sim$2)), and *wellsite* (Al (4–5), Ba (0.4–1.1), K (0.7–1.0)).[5] Structure determinations of the hydrated varieties of phillipsite[341,342] and harmotome[342] have not been extended to dehydrated and ion-exchanged varieties. Some cation blockage of the channels should occur.

SOD. Natural *sodalites* are anhydrous feldspathoids with trapped cations and anions[103] and will not be described here. Some synthetic sodalites contain hydroxyls, or water molecules, or both. The most interesting one to zeolite scientists is the *hydrosodalite* $Ca_6Al_6Si_6O_{24}\cdot 8H_2O$,[343,344] but the structural data[345–355] on the hydroxyl-bearing varieties are also relevant to terminal hydroxyls of zeolites. Tetrahedral distortions in the *to* of sodalites release stress by both tilting and change of edge lengths,[356] and DLS modeling can be related to thermal expansion.[357] The silica framework of silica-sodalite[358] with encapsulated ethylene glycol crinkles at a sluggish phase transition near 200 K.[359] The position of tetramethylammonium in the *to* cage[360] is also relevant to the geometry of zeolites containing polyhedral cages.

STI. This topology is represented by *stellerite*, near $Ca_2Al_4Si_{14}O_{36}\cdot 14H_2O$, *barrerite*, near $(Na,K,Ca)_4Al_4Si_{14}O_{36}\cdot 13H_2O$, and *stilbite*, intermediate compositions.[5] The following structural data are available: stellerite[361–363] and Ca-exchanged barrerite,[364] barrerite[365] and Na-exchanged stellerite,[366] stilbite.[367–368a] The thermal behavior of ion-exchanged phases[369,370] is complex and involves[371] reversible rotation of the *brew* unit up to $\sim$460 K, conversion of some stellerites and probably some stilbites to interrupted frameworks with some terminal hydroxyls, and retention of the framework for cations with low ionic potential (Rb, K).

THO. The hydrated structure of the fibrous zeolite *thomsonite* is known,[372–374] but the structural effects of dehydration are not.

YUG. The hydrated structure[375,376] of *yugawaralite* has disordered water molecules even at 20 K.[377]

B. Synthetic Aluminosilicates with a (4;2)-3D Net

ABW. Represented by Li-A(BW),[378,379] a gallium analogue,[380] and anhydrous Rb and Cs analogues. All the Li, Al, and Si atoms are in tetrahedral coordination.[380a]

EAB. Zeolite *(Na,TMA)-E(AB)* transforms topotactically to a sodalite-type structure above 633 K.[381]

KFI. Zeolite *ZK-5*, $Na_{30}Al_{30}Si_{66}O_{192}\cdot 98H_2O$, and the Cs,K analogues show considerable changes of cation positions and framework geometry upon heating. Data are available for ZK-5 at room temperature and 423 K,[382] at room temperature for dealuminated specimens calcined at 773 and 923 K,[383] and for Cs,K analogues at 294 and 493 K.[384] The larger Cs ion prefers the planar 8-ring, and the smaller K the nonplanar 8-ring. Pore access is restricted by occupancy of the 8-rings and by encapsulated Al–O species. Barium halides and hydroxides are occluded in Ba analogues *P* and *Q*.[385]

LOS. *Losod* zeolite[386] has pores accessible only by 6-rings.

LTA. There is much literature on the cation sites and framework geometry of *Linde Type A* zeolite and related materials. It is somewhat confusing because most single-crystal studies have been made on samples with Si > Al; some as-synthesized samples and all dehydrated specimens exchanged with multivalent cations contain encapsulated Al–O species; and various technical problems involving the Si,Al ordering, space group of symmetry, and actual chemical composition have compromised the integrity of some conclusions. For the present purpose, the principal conclusions are these. The ideal composition $Na_{12}Al_{12}Si_{12}O_{48}\cdot 27H_2O$ allows occupancy of all eight 6-rings, three 8-rings, and one offset 4-ring by monovalent cations, thus blocking all access to the *grco* cages. Six divalent ions tend to be located near 6-rings, and the 8-rings are unblocked. The framework geometry is affected considerably by tetrahedral tilting in response to any distortion of a 6-ring, especially by the bonding to three oxygens by an ion with high ionic potential. Papers up to ca. 1981 on cation positions are given in ref 56. Later ones on crystal structure determinations are as follows: *hydrated at room temperature*, Ba_xNa_{12-x}- ($x = 1$–6),[387] Cu,NH_4-,[388] Ni,Na-;[388a] *dehydrated with monovalent cations*, Linde 5A with all Na,Ca at 6-rings;[389] Linde 3A with all $K_{0.63}Na_{0.37}$ at 6-rings,[390] Na- with Si/Al = 1.03, 1.09, 1.12, and 1.67, all cubic,[391–392a] Na-dehydrated at 623 K is cubic, but at 673 K is noncubic at room temperature[393] (confirmed,[394] but not rhombohedral as in ref 395–397), Tl- and Ag-,[396] Ag,H-,[398] Na_xLi_{12-x} with progressive distortion of 8-rings from K- to Na- to Li-,[399] Na,Ag, partly reduced,[400–402] Cs-,[402a] Cs,Ag with Cs in 8-rings,[403] NH_4;[404] *dehydrated with divalent cations*, Mg_2Na_8- with residual H_2O,[405] progressive dehydration of Ca-,[406] Ni,Na-,[388a] partly dehydrated Ba,Na-,[387] Ca- with AlO_4 complex in *to*,[407] Ba-,[408] Pb- and Pb hydroxyhydrate,[409] Mg-, Ca-, Ba-, and Zn-partial exchange derivatives of Ag,Na-;[410] *sorption complexes*, Co,Na–CO,[411] Na–CH_3OH,[412] *salt complex* Na–$NaNO_3$,[413] *hydrothermally treated*, Ca_4Na_4-.[413a,b]

LTL. Available structure data are for hydrated *Linde zeolite L*,[410] dehydrated L,[414] the Ga analogue,[415] the pyridine complex of the Ga analogue,[416] the deuteriobenzene complex of L.[416a] There is no obvious structural fault that would block the 12-rings, and most cations should enter the walls. The new mineral *perlialite* may be an isotype,[417] based on X-ray powder diffraction and infrared data.

LTN. The *Linde Type N* zeolite has access only through 6-rings.[418,419]

MEL. There are no accurate structure analyses of the Mobil *ZSM-11* high-silica zeolite, but the computer-generated framework geometry[98] should be generally correct.

MFI. The early structure refinements of Mobil *ZSM-5* high-silica zeolite[99] and the Union Carbide *silicalite*[97a] were hampered by small crystal size and twinning. A precise analysis[420] of an excellent crystal of the as-synthesized ZSM-5 with encapsulated tetrapropylammonium confirms the general geometrical features of the earlier analyses (including ref 420a–422) and demonstrates how the TPA lies in two different conformations in the channels. After calcination, the ZSM-5 silicalite specimens may adopt monoclinic symmetry with the transition from orthorhombic symmetry depending in a complex way on the bulk chemical composition and physical conditions (e.g., ref 423 and 424). Intergrowths between ZSM-5 and ZSM-11 types of stacking of pentasil units have been described theoretically[96] and observed (e.g., ref 425 and 426); twinning of MFI materials may be related. Three types of positions were found for deuteriobenzene molecules in ZSM-5 zeolite at 77 K using neutron powder diffraction.[426a] *p*-Xylene and benzene were located by X-ray powder studies of pentasil materials containing B.[427–429] Because of the strong "bracing" of the T–T linkages in the MFI net and because there are few exchangeable cations, it is likely that the channel system will vary only a little from one variety to another.

MTN. This is represented by the silica compounds Mobil *ZSM-39* high-silica zeolite,[430] the *dodecasil 3C* clathrasil,[431] and the Union Carbide *holdstite*.[432] The geometry is only pseudocubic,[431,433] and the framework will probably change shape in response to chemical and physical treatment.

MTT. The framework geometry of the Mobil *ZSM-23* high-silica zeolite[116] is based on a distance-least-squares model, and the details may change; however, the channel dimensions should be accurate within a few tenths of an angstrom.

MTW. A similar comment as above applies to the framework geometry[434] of Mobil *ZSM-12* high-silica material.

RHO. The principal structure variation in zeolite *Rho* is the change of the 8-ring from a circular shape when hydrated[434a] to an elliptical shape when dehydrated.[435,436] Other changes occur as a result of variation in cation content,[437] dealumination,[438] and adsorption of Xe.[439,440] A mineral isotope, *pahasapaite*, has been discovered.[441]

TON. The structure was determined from powder data of *Theta-1*[112,113] and *ZSM-22*[114] and from a single crystal of a silica polymorph.[442]

C. Synthetic Aluminophosphates with a (4;2)-3D Net and Related Materials

This section can be brief since there are recent reviews of the chemical features of 1:1 aluminophosphate molecular sieves and new generations of materials that incorporate one or more of an additional 13 elements from the periodic table into the $AlPO_4$ framework.[18,51,443,444] The review of the structural features[52] is supplemented here with brief descriptions of new structure types. Aluminum is bonded to four oxygen species, each also bonded to P to generate a (4;2)-3D net. Some Al atoms are also bonded to one or two additional oxygen species in the as-synthesized materials, as shown by diffraction and resonance[445] studies. Upon calcination, some materials become $AlPO_4$ molecular sieves with alternating Al and P atoms at the vertices of a (4;2)-3D net. Many aluminum phosphates not based on such a net are listed in ref 52, and others are given in a review of orthophosphates.[446] The following list is in numerical sequence of the Union Carbide numerical code.

AFI. The cylindrical channels of as-synthesized $AlPO_4$-5[447] change only slightly upon calcination.[448]

AEL. The geometrical details of this structure with elliptical channels[67] have been determined for calcined $AlPO_4$-11,[449,450] as-synthesized MnAPO-11, $Al_9Mn_1P_{10}O_{40}\cdot C_6H_{16}N$,[451] and a silicoaluminophosphate.[452]

No ST Code. $AlPO_4$-12[453] is based on an interrupted net.[52]

No ST Code. $GaPO_4$-14[454] and its analogue $AlPO_4$-14 are based on net 399 with an *odc* chain.[52]

No ST Code. $AlPO_4$-15[455,456] is based on net 400 with *odc* structural units.[52]

AST. $AlPO_4$-16[457] is related to the zunyite structure[458] and has a complete (4;2)-3D net instead of the isolated Si_5O_{16} units of the latter.

ERI. As-synthesized $AlPO_4$-17[459] has OH bridges across pairs of Al atoms in hexagonal prisms of the erionite structure.

SOD. $AlPO_4$-20 has the sodalite structure,[51] but no geometrical details have been published.

ATF. As-synthesized $AlPO_4$-21[460,461] is based on net 401,[52] and it is *presumed* that the hydroxyl bridges are removed during calcination to $AlPO_4$-25 without rearrangement of the framework topology. No detailed structure of $AlPO_4$-25 has been published.

ANA. $AlPO_4$-24 has the analcime structure,[51] but no structural details have been published. See preceding section for a silicoaluminophosphate.[146]

ATT. $AlPO_4$-33 is an isotype of $AlPO_4$-12-TAMU, whose structure[462] is based on net 102.[66] To avoid confusion with $AlPO_4$-12,[463] the structure code is based on $AlPO_4$-33, which was synthesized before $AlPO_4$-12-TAMU.

CHA. $CoAlPO_4$-34, $CoAlPO_4$-44, $CoAlPSiO_4$-47, and $MeAlPSiO_4$-47 have alternation of P and (Al, Co, or other metal) on vertices of a chabazite-type net.[18,51,96c] The structure of an aluminosilicophosphate contains a nonplanar, near-circular 8-ring.[464]

LEV. $SiAlPO_4$-35 has an X-ray powder pattern with the hexagonal characteristic of levyne.[444]

FAU. $SiAlPO_4$-37 has the characteristic X-ray pattern of a faujasite structure,[444] and the substitution mechanism was determined from NMR data.[465]

LTA. The cubic X-ray powder pattern[444] of $SiAlPO_4$-42 is indicative of the type A net.

GIS. The gismondine net[18] of $Mg_{0.25}Al_{0.75}PO_4$-43 has been confirmed by a single-crystal X-ray study.[466]

AFS. The new net[96c] of the MAPSO-46 structure is shown in Figure 1.

AFY. The new net[96c] of the CoAlPO-50 structure is shown in Figure 1.

APC. The as-synthesized structure[467,468] of the H_3 variety of $AlPO_4\cdot 1.5H_2O$ is based on net 24a.[52] Partial dehydration to $AlPO_4$-C[469] is reversible, and the net topology is retained as the coordination is reduced.

APD. Further dehydration to $AlPO_4$-D is irreversible, and there is a topotactic transformation to a new net[469] to be numbered 41a in Table 3 of ref 65. The topologic description is ScScCcCc, 16, $(4^26^28^2)_1(4.6^5)_1$, *Acam*, 32, 9.5, 20, 8; *Pcab* for Al, P alternation on vertices.

No ST Code. The *$AlPO_4$-EN3* structure[470] is based on net 402.[52]

No ST Codes. The *variscite*[471] and *metavariscite*[472] polymorphs of $AlPO_4\cdot 2H_2O$ are based[52] on nets 5 and 3[64] (Figures 1 and 8).

No ST Codes. The $AlPO_4$ analogue of quartz is known as *berlinite*[473] and is based on net 90[66] (Figure 14). Two other silica polymorphs, *cristobalite* and *tridymite* (nets 1 and 2[64]), are represented by $AlPO_4$ analogues.[474,475]

D. Silica Polymorphs Classified As Clathrasils

The essential topological information is summarized in Table Ie an a review.[35] References to the structures are as follows: *silica-sodalite*,[358,359] *dodecasil 1H*,[476,477] *decadodecasil 3R*,[128] *melanophlogite*,[478,479] *nonasil*,[480] *dodecasil 3C*.[430–432]

E. Aluminosilicates with Interrupted Frameworks Based Mainly on a (4;2)-3D Net

The essential information on seven aluminosilicates with interrupted nets is given in Table If; the last two also contain Be in the framework. Stereoviews of the first three are given in the draft for the revised *Atlas of Zeolite Structure Types*.[33] The *quasitectosilicate* family was reviewed.[95] References to the structures are as follows: *parthéite*,[481] *roggianite*,[482] *wenkite*,[483,484] *sarcolite*,[485] *ussingite*,[486] *bavenite*,[487] *leifite*,[488] *chiavennite*;[489] see also $RbSi_{10}O_{23}$,[490] *tuhualite*,[491] $AlPO_4$-12.[52] Interruptions should occur during topological transformations of zeolites upon heating.[492]

F. Materials with Open Frameworks That Do Not Fall in the Above Classifications

This section signals the existence of some materials with open frameworks that have zeolitic properties (sensu lato) or might do so. It is designed to trigger off synthesis and characterization of new types of useful microporous materials. Other interesting porous materials have been reviewed.[492a]

Lovdarite, $K_4Na_{12}Be_8Si_{28}O_{72}\cdot 18H_2O$, and its synthetic equivalent are based on a remarkable (4;2)-3D net[90,93,493] (LOV; stereoview in revised edition[33]) in which each vertex of each 4-ring is connected by an edge to a vertex of two spiro-5 units (pair of vertex-shared 3-rings). The net contains a 4^26^4 unit obtained by removing two opposing edges of a cube (e.g., pg and es of the cube in column 2, Figure 3).

Cavansite and *pentagonite* dimorphs of $Ca(VO)Si_4O_{10}\cdot 4H_2O$ have structures[494] in which the V and Si atoms lie at the vertices of two (4;2)-3D nets, related respectively to the gismondine and paracelsian nets. Three water molecules are removed from cavansite at 493 K without loss of the framework,[495] but collapse occurs at 673 K. A key geometrical feature is that the four linkages from each T to adjacent Si atoms nearly form the diagonals of a rectangle (stereoview of cavansite,

Figure 1). This geometrical distinction from the more tetrahedral geometry of zeolite nets allows invention of a new family[496] of 4-connected nets that are geometrically plausible for vanadyl silicates and topochemically related materials.

Verplanckite, $[(Mn,Ti,Fe)_6(OH,O)_2(Si_4O_{12})_3]Ba_{12}Cl_9\{(OH,H_2O)_7\}$, has a framework with triple units of (Mn, Ti, Fe) in square-pyramidal coordination and 4-rings of Si tetrahedra.[497] The voids have a free diameter of 7 Å, but no measurements were made of possible zeolitic properties. *Muirite*, $Ba_{10}(Ca,Mn,Ti)_4Si_8O_{24}(Cl,OH,O)_{12}\cdot 4H_2O$, has edge-sharing trigonal prisms and 8-rings of SiO_4,[498] and a synthetic barium chloroaluminosilicate is a salt complex.[499]

The widest channel in a framework is in *cacoxenite*, a highly hydrated basic ferric oxyphosphate mineral, with an ideal chemical composition from the structure analysis[500] of $[AlFe_{24}O_6(OH)_{12}(PO_4)_{17}(H_2O)_{24}]\cdot\sim 51H_2O$. The moiety in brackets forms walls of vertex- and edge-sharing Fe and Al octahedra and Al and P tetrahedra which outline cylindrical channels in a manner analogous to the nets in Figure 18. Each channel is filled with unlocated water molecules, which must be strongly disordered as in faujasite. The formal value of the free diameter is 14 Å between the oxygen atoms of framework water molecules. There are no published data on the structural stability of the framework as water molecules are removed. Perhaps the most important implication from cacoxenite is the knowledge that Nature can build larger channels than those currently used in molecular sieve technology. Whether cacoxenite or related materials (liskeardite, challantite?) can be exploited in new industrial processes, probably near ambient temperature to preserve framework integrity, is an intriguing question.

Ashcroftine, $K_{10}Na_{10}(Y,Ca)_{24}(OH)_4(CO_3)_{16}(Si_{56}O_{140})\cdot 16H_2O$, has unlocated water molecules.[500a]

Pillared clays have large pores,[501] but are not true frameworks.

Cordierite, $(Na, etc.)_{0.1}(Mg, etc.)_2Si_5Al_4O_{18}\cdot 0.5H_2O$, has a (4;2)-connected framework of $Si_5Al_4O_{18}$ containing small pores, which encapsulate H_2O, CO_2, Ar, etc., and 6-rings which allow diffusion at high temperature;[502–509] it could be called a *high-temperature molecular sieve*.

Petarasite, $Na_5Zr_2Si_6O_{18}(Cl,OH)\cdot 2H_2O$, has a (4,6;2)-3D framework[510] in which each oxygen is connected to either two Si or one Si and one Zr and in which Si_6O_{18} rings are vertex-shared to ZrO_6 octahedra. Access to the micropores is through 6-rings. There are no published data on zeolitic properties.

Chlorotile, $(rare\ earth)_1Cu_6(AsO_4)_3(OH)_6\cdot 3H_2O$, has a complex framework[511] of AsO_4 tetrahedra and $Cu(OH)_2O_3$ square pyramids with H_2O as a sixth ligand. Water lies in cylindrical channels circumscribed by crown-shaped 12-rings of potential free diameter 6.9 Å. *Mixite* has Bi replacing rare earths. There are no published data on zeolitic properties.

Vinogradovite, $Na_4Ti_4(Si_2O_6)_2(Si_4O_{10})O_4\cdot nH_2O$, is a (4,6;2)-3D framework,[512] except for one oxygen connected to one Si and two octahedral Ti. Narrow channels are defined by 8-rings.

Cadmium trimetaphosphate 14-hydrate has a 4-connected framework[513] of 3-rings of PO_4 tetrahedra joined by $CdO_4(H_2O)_2$ octahedra. Four water molecules were not located in the channels.

Wightmanite, $Mg_5(O)(OH)_5[BO_3]\cdot nH_2O$, has an elliptical channel[514] with free diameter 6.0 × 4.0 Å. The 8-ring channels of the original simple model[515] of *gageite*, $(Mn,Mg)_7(O)(OH)_8(Si_2O_6)$, are blocked by disordered SiO_4-chains.[515a]

Some frameworks containing *heteropoly complexes* have loosely bound water not located in the structure analysis.[516–518]

Montregianite, $Na_2K_2Y_2Si_{16}O_{38}\cdot 10H_2O$, has a framework[519] of SiO_4 and YO_6 which encloses H_2O in micropores.

Pharmacosiderite, $KFe_4(AsO_4)_3(OH)_4\cdot 7H_2O$, has disordered water molecules in micropores of a framework[520] of AsO_4 tetrahedra and edge-sharing Fe octahedra.

Other hydrated materials with complexly connected frameworks are *catapleiite*,[521] *elpidite*,[522] *nenadkevichite*,[523] *lemoynite*,[524] and *stokesite*.[525]

Acknowledgments. This review is dedicated to the late Donald W. Breck, whose ideas have been so helpful in development of the theory and practice of zeolite science, and to the late William H. Taylor, who started the structural chemistry of zeolite minerals. Many thanks indeed to co-workers, especially Lesley Dent Glasser, J. Michael Bennett, Joseph J. Pluth, Wilfrid M. Mortier, Romano Rinaldi, John L. Schlenker, Gilberto Artioli, Frank C. Hawthorne, Åke Kvick, and James W. Richardson, Jr. The collaboration with Edith M. Flanigen and her group of innovative synthesizers of new materials continues to be crucial to the development of new ideas on the topochemistry of zeolites and related materials. Considerable assistance was obtained from the members of the Structure Commission of the International Zeolite Association, particularly Walter M. Meier and David H. Olson; in particular, many of the stereoplots in Figure 1 are reprinted from the Atlas. Helpful reviews were supplied by Glauco Gottardi, Walter Meier, Joseph Pluth, and James Richardson. Financial support over the past three decades from the National Science Foundation (currently Grant CHE 86-18041), Union Carbide Corp., ACS Petroleum Research Fund, and Mobil Foundation is gratefully acknowledged. Nancy Weber efficiently prepared the manuscript.

References

(n) Breck, D. W. *Zeolite Molecular Sieves. Structure, Chemistry, and Use*; Wiley-Interscience: New York, 1974.
(2) Barrer, R. M. *Zeolites and Clay Minerals as Sorbents and Molecular Sieves*; Academic: New York, 1978.
(3) Barrer, R. M. *Hydrothermal Chemistry of Zeolites*; Academic: New York, 1982.
(4) Rabo, J. A., Ed. *Zeolite Chemistry and Catalysis*; ACS Monograph 171; American Chemical Society: Washington, DC, 1976.
(5) Gottardi, G.; Galli, E. *Natural Zeolites*; Springer: Berlin, 1985. (a) Gottardi, G. *Pure Appl. Chem.* **1986**, *58*, 1343.
(6) *Molecular Sieves*; Society of Chemical Industry: London, 1968. (a) Flanigen, E. M.; Sand, L. B., Eds.; *Molecular Sieve Zeolites. I.*; Advances in Chemistry 101; American Chemical Society: Washington, DC, 1971.
(7) Meier, W. M.; Uytterhoeven, J. B., Eds. *Molecular Sieves*; Advances in Chemistry 121; American Chemical Society: Washington, DC, 1973.
(8) Uytterhoeven, J. B., Ed. *Molecular Sieves*; Leuven University Press: Leuven, 1973.
(9) Katzer, J. R., Ed. *Molecular Sieves. II*; ACS Symposium Series 40; American Chemical Society: Washington, DC, 1977.
(10) Sand, L. B.; Mumpton, F. A., Eds. *Natural Zeolites. Occurrence, Properties, Use*; Pergamon: Oxford, 1978.

(11) Rees, L. V. C. Ed. *Proceedings of the Fifth International Conference on Zeolites, Naples, Italy, 2–6 June 1980*; Heyden: London, 1980.
(12) Stucky, G. D.; Dwyer, F. G., Eds. *Intrazeolite Chemistry*; ACS Symposium Series 218; American Chemical Society: Washington, DC, 1983.
(13) Olson, D.; Bisio, A. *Proceedings of the Sixth International Zeolite Conference, Reno, 10–15 July 1983*; Butterworths: Guilford, 1984.
(14) Drzaj, B.; Hocevar, S.; Pejovnik, S., Eds. *Zeolites. Synthesis, Structure, Technology and Application*; Elsevier: Amsterdam, 1985.
(15) Murakami, Y.; Iijima, A.; Ward, J. W., Eds. *New Developments in Zeolite Science Technology*; Kodansha: Tokyo, 1986.
(16) Smith, E. F. *Chemistry in America. Chapters from the History of the Science in the United States*; C. Appleton and Co.: New York, 1914.
(17) Thackray, A.; Sturchio, J. L.; Carroll, P. T.; Bud, R. *Chemistry in America 1876–1976. Historical Indicators*; Reidel: Dordrecht, 1985.
(18) Flanigen, E. M.; Lok, B. M.; Patton, R. L.; Wilson, S. T. *Pure Appl. Chem.* **1986**, *58*, 1351.
(19) Smith, J. V. *Feldspar Minerals*; Springer: Berlin, 1974. Revised edition (with W. L. Brown) in press. (a) Brown, W. L., Ed. *Feldspars and Feldspathoids*; Reidel: Dordrecht, 1983.
(20) Cronstedt, A. F. *Kongl Vetenskaps Acad. Handl. Stockholm* **1756**, *17*, 120.
(21) Damour, A. *Ann. Mines* **1840**, *17*, 191.
(22) Friedel, G. *Bull. Soc. Fr. Mineral. Cristallogr.* **1896**, *14*, 96.
(23) Grandjean, F. *C. R. Seances Acad. Sci.* **1909**, *149*, 866.
(24) Taylor, W. H. *Z. Kristallogr.* **1930**, *74*, 1.
(25) Taylor, W. H.; Jackson, R. *Z. Kristallogr.* **1933**, *86*, 53.
(26) Taylor, W. H.; Meek, C. A.; Jackson, W. W. *Z. Kristallogr.* **1933**, *84*, 373.
(27) Taylor, W. H. *Mineral. Mag.* **1935**, *24*, 208.
(28) Pauling, L. *Proc. Natl. Acad. Sci. U.S.A.* **1930**, *16*, 453.
(29) Weigel, O.; Steinhoff, E. *Z. Kristallogr.* **1925**, *61*, 125.
(30) McBain, J. W. *The Sorption of Gases and Vapors by Solids*; Routledge and Sons: London, 1932.
(31) Eichhorn, H. *Ann. Phys. Chem. Poggendorff* **1858**, *105*, 126.
(32) Liebau, F. *Zeolites* **1983**, *3*, 191.
(33) Meier, W. M.; Olson, D. H. *Atlas of Zeolite Structure Types* (Structure Commission of the International Zeolite Association); Juris Press: Zürich, 1978. Revised edition in press.
(34) Smith, J. V. *Zeolites* **1984**, *4*, 309.
(35) Liebau, F.; Gies, H.; Gunawardane, R. P.; Marler, B. *Zeolites* **1986**, *6*, 373.
(36) Smith, J. V. *Mineral. Soc. Am. Spec. Pap.* **1963**, *1*, 281.
(37) Wells, A. F. *Structural Inorganic Chemistry*, 4th ed.; Clarendon: Oxford, 1975.
(38) Zoltai, T. *Am. Mineral.* **1960**, *45*, 960.
(39) Belov, N. V. *Crystal Chemistry of Large Cation Silicates*; Consultants Bureau: New York, 1959.
(40) Bragg, W. L.; Claringbull, G. F.; Taylor, W. H. *Crystal Structures of Minerals*; Cornell University Press: Ithaca, NY, 1965.
(41) Povarennykk, A. S. *Crystal Chemical Classification of Minerals* (2 vols.); Plenum: New York, 1972.
(42) Liebau, F. *Structural Chemistry of Silicates. Structure, Bonding, and Classification*; Springer: Berlin, 1985.
(43) Flanigen, E. M.; Bennett, J. M.; Grose, R. W.; Cohen, J. P.; Patton, R. L.; Kirchner, R. M.; Smith, J. V. *Nature* (*London*) **1978**, *271*, 512.
(44) Kokotailo, G. T.; Lawton, S. L.; Olson, D. H.; Meier, W. M. *Nature* (*London*) **1978**, *272*, 437.
(45) von Ballmoos, R.; Gubser, R.; Meier, W. M. *Reference* 13, p 803.
(46) Smith, J. V.; Steele, I. M. *Neues Jahrb. Mineral. Mh.* **1984**, 137.
(47) Chester, A. W.; Chu, Y. F.; Dessau, R. M.; Kerr, G. T.; Kresge, C. T. *J. Chem. Soc., Chem. Commun.* **1985**, 289.
(48) Nagy, J. B.; Gabelica, Z.; Derouane, E. G. *Chem. Lett.* **1985**, 1105.
(49) Woolery, G. L.; Alemany, L. B.; Dessau, R. M.; Chester, A. W. *Zeolites* **1986**, *6*, 14.
(50) Ward, J. W. *Reference* 4, p 118.
(51) Wilson, S. T.; Lok, B. M.; Messina, C. A.; Cannan, T. R.; Flanigen, E. M. *J. Am. Chem. Soc.* **1982**, *104*, 1146.
(52) Bennett, J. M.; Dytrych, W. J.; Pluth, J. J.; Richardson, J. W., Jr.; Smith, J. V. *Zeolites* **1986**, *6*, 349.
(53) Felsche, J.; Luger, S.; Fischer, P. *Acta Crystallogr., Sect. C* **1987**, *C43*, 809.
(54) Zhdanov, S. P.; Buntar, N. N.; Egorova, E. N. *Dokl. Akad. Nauk. SSSR* **1964**, *154*, 419.
(55) Bibby, D. M.; Dale, M. P. *Nature* (*London*) **1985**, *317*, 157.
(56) Mortier, W. M. *Compilation of Extra Framework Sites in Zeolites*; Butterworths: Guildford, 1982.
(57) von Ballmoos, R. *Collection of Simulated XRD Powder Patterns for Zeolites*; Butterworths: Guildford, 1984.
(58) Wells, A. F. *Three-Dimensional Nets and Polyhedra*; Wiley: New York, 1977.
(59) Wells, A. F. *Further Studies of Three-Dimensional Nets*; *Am. Cryst. Assoc. Monog. No. 8*, 1979.
(60) Smith, J. V. *Structural and Geometrical Crystallography*; Wiley: New York, 1982.
(61) Baerlocher, C.; Hepp, C.; Meier, W. M. *DLS-76 Manual*; Institut für Kristallographie und Petrographie: ETH, Zürich, 1977 (revised 1978).
(62) Gramlich-Meier, R.; Meier, W. M. *J. Solid State Chem.* **1982**, *44*, 41.
(63) Niggli, A. *Schweiz Mineral. Petrol. Mitt.* **1967**, *47*, 279.
(64) Smith, J. V. *Am. Mineral.* **1977**, *62*, 703.
(65) Smith, J. V. *Am. Mineral.* **1978**, *63*, 960.
(66) Smith, J. V. *Am. Mineral.* **1979**, *64*, 551.
(67) Smith, J. V.; Bennett, J. M. *Am. Mineral.* **1981**, *66*, 777.
(68) Smith, J. V.; Bennett, J. M. *Am. Mineral.* **1984**, *69*, 104.
(69) Smith, J. V. *Z. Kristallogr.* **1983**, *165*, 191.
(70) Bennett, J. M.; Smith, J. V. *Z. Kristallogr.* **1985**, *171*, 65.
(71) Smith, J. V.; Dytrych, W. J. *Nature* (*London*) **1984**, *309*, 607.
(72) Hawthorne, F. C.; Smith, J. V. *Z. Kristallogr.* **1986**, *175*, 15.
(73) Smith, J. V.; Dytrych, W. J. *Z. Kristallogr.* **1986**, *175*, 31.
(74) Hawthorne, F. C.; Smith, J. V. *Z. Kristallogr.*, in press.
(75) Hawthorne, F. C.; Smith, J. V. *Can. Mineral.* **1986**, *24*, 643.
(76) Hawthorne, F. C.; Smith, J. V. *Z. Kristallogr.*, submitted.
(77) Brunner, G. O.; Laves, F. *Wiss. Z. Tech. Univ. Dresden* **1971**, *20*, 387. (a) Sato, M. *J. Phys. Chem.* **1987**, *91*, 4675.
(78) Meier, W. M.; Moeck, H. J. *J. Solid State Chem.* **1979**, *27*, 349.
(79) Meier, W. M. Reference 6, p 10.
(80) Merlino, S. *R. Soc. Ital. Mineral. Petrol.* **1975**, *31*, 513.
(81) Meier, W. M. Reference 7, p 39.
(82) Sherman, J. D.; Bennett, J. M. Reference 7, p 52.
(83) Shoemaker, D. P.; Robson, H. E.; Broussard, L. Reference 8, p 138.
(84) Gottardi, G. Reference 10, p 31.
(85) Meier, W. M. Reference 10, p 99.
(86) Smith, J. V. Reference 11, p 194.
(87) Wilson, S. T.; Lok, B. M.; Messina, C. A.; Cannan, T. R.; Flanigen, E. M. Reference 12, p 79.
(88) Wilson, S. T.; Lok, B. M.; Messina, C. A.; Flanigen, E. M. Reference 13, p 97.
(89) Rinaldi, R. Reference 13, p 570.
(90) Merlino, S. Reference 13, p 747.
(91) Kokotailo, G. T. Reference 13, p 760.
(92) Sato, M. Reference 13, p 851.
(93) Meier, W. M. Reference 15, p 13.
(94) Alberti, A. *Am. Mineral.* **1979**, *64*, 1188.
(95) Rossi, G. *R. Soc. Ital. Mineral. Petrol.* **1975**, *31*, 541.
(96) Kokotailo, G. T.; Meier, W. M. *Chem. Soc. Spec. Publ.* **1980**, *33*, 133. (a) Hansen, S.; Fälth, L.; Andersson, S. *J. Solid State Chem.* **1981**, *39*, 137. (b) McCusker, L. B.; Meier, W. M.; Rechsteiner, H. *Mater. Res. Bull.* **1987**, *22*, 1203. (c) Bennett, J. M.; Marcus, B. K. Preprint, Innovations in Zeolite Materials Science Conference, Nieuwpoort, Belgium, Sept 28–30, 1987.
(97) Smith, J. V. Reference 6, p 28. (a) Price, G. D.; Pluth, J. J.; Smith, J. V.; Bennett, J. M.; Patton, R. L. *J. Am. Chem. Soc.* **1982**, *104*, 5761.
(98) Kokotailo, G. T.; Chu, P.; Lawton, S. L.; Meier, W. M. *Nature* (*London*) **1978**, *275*, 119.
(99) Olson, D. H.; Kokotailo, G. T.; Lawton, S. L.; Meier, W. M. *J. Phys. Chem.* **1981**, *85*, 2238.
(100) O'Keeffe, M.; Hyde, B. G. *Philos. Trans. R. Soc. London, A*: **1980**, *295*, 38.
(101) Wells, A. F. *Philos. Trans. R. Soc. London, A*: **1986**, *319*, 291.
(102) Gregorkiewitz, M.; Schäfer, H. *6th European Cryst. Mtg.* **1980**, 155.
(103) Merlino, S. Reference 19a, p 435.
(104) Klaska, R.; Selker, P. *Z. Kristallogr.* **1983**, *162*, 131.
(105) Pluth, J. J.; Smith, J. V. *Nature* (*London*) **1985**, *318*, 165.
(106) Keller, E. B. Doctoral thesis, ETH, Zürich, 1987.
(107) Dent, L. W.; Smith, J. V. *Nature* (*London*) **1958**, *181*, 1794. (a) Smith, J. V. Reference 13, p 56.
(108) Fischer, K. *Neues Jahrb. Mineral. Mh.* **1966**, 1.
(109) Bennett, J. M.; Gard, J. A. *Nature* (*London*) **1967**, *214*, 1005.
(110) Barrer, R. M.; Villiger, H. *Z. Kristallogr.* **1969**, *128*, 352.
(111) Hansen, S.; Fälth, L. *Zeolites* **1982**, *2*, 162.
(112) Barri, S. A. I.; Smith, G. W.; White, D.; Young, D. *Nature* (*London*) **1984**, *312*, 533.
(113) Highcock, R. M.; Smith, G. W.; Wood, D. *Acta Crystallogr., Sect.* **1985**, *C41*, 1391.
(114) Kokotailo, G. T.; Schlenker, J. L.; Dwyer, F. G.; Valyocsik, E. W. *Zeolites* **1985**, *5*, 349. (a) Gramlich-Meier, R.; Meier, W. M.; Smith, B. K. *Z. Kristallogr.* **1984**, *169*, 201.
(115) Hawthorne, F. C.; Smith, J. V. *Z. Kristallogr.*, to be submitted.

(116) Rohrman, A. C., Jr.; LaPierre, R. B.; Schlenker, J. L.; Wood, J. D.; Valyocsik, E. W.; Rubin, M. K.; Higgins, J. B.; Rohrbaugh, W. J. *Zeolites* **1985**, *5*, 352.
(117) Kerr, I. S. *Nature* (*London*) **1963**, *197*, 1194.
(118) Merlino, S. *Izvj. Jugoslav. Cent. Krist. Zagreb* **1976**, *11*, 19.
(119) Gellens, L. R.; Price, G. D.; Smith, J. V. *Mineral. Mag.* **1982**, *45*, 157.
(120) Dent Glasser, L. S.; Henderson, A. P.; Howie, R. A. *Acta Crystallogr., Sect. B* **1982**, *B38*, 24.
(121) Andreini, A. *Soc. Ital. Sci., Mem. Math. Fis.* **1907**, *Ser. 3 14*, 75.
(122) Treacy, M. M. H.; Newsam, J. M.; Beyerlein, R. A.; Leonowicz, M. E.; Vaughan, D. E. W. *J. Chem. Soc., Chem. Commun.* **1986**, 1211.
(123) Kokotailo, G. T.; Ciric, J. *Adv. Chem. Ser.* **1971**, *No. 101*, 109.
(124) Thomas, J. M.; Audier, M.; Klinowski, J. *J. Chem. Soc., Chem. Commun.* **1981**, 1221.
(125) Jeffrey, G. A. In Atwood, J. L.; Davies, J. E.; McNicol, D. D., Eds.; *Hydrate Inclusion Compounds*, Academic: London, 1984; p 135.
(126) Johnson, N. W. *Can. J. Math.* **1965**, 169.
(127) Brunner, G. O. *Z. Kristallogr.* **1981**, *156*, 295.
(128) Gies, H. *Z. Kristallogr.* **1986**, *175*, 93.
(129) Barrer, R. M.; Peterson, D. *Proc. R. Soc. London, A* **1964**, *280*, 466.
(130) Sand, L. B. Reference 6, p 71.
(131) Raatz, F.; Freund, E.; Marcilly, C. *J. Chem. Soc., Faraday Trans. 1* **1985**, *81*, 299. (a) Davis, M. E. Unscheduled presentation, Innovations in Zeolite Materials Science Conference, Nieuwpoort, Belgium, Sept 28–30, 1987.
(132) Buser, O.; Aufdermaur, A. N. *J. R. Meteorol. Soc.* **1973**, *99*, 388.
(133) Heesch, H.; Laves, F. *Z. Kristallogr.* **1933**, *85*, 43.
(134) Fischer, W. *Z. Kristallogr.* **1976**, *143*, 140.
(135) Melmore, S. *Nature* (*London*) **1942**, *149*, 412, 669.
(136) Melmore, S. *Mineral. Mag.* **1949**, *28*, 479.
(137) Slack, G. A. *Z. Kristallogr.* **1983**, *165*, 1.
(138) Brunner, G. O. *J. Solid State Chem.* **1979**, *29*, 41. (a) Cannillo, E.; Mazzi, F.; Rossi, G. *Acta Crystallogr.* **1975**, *31*, 541.
(139) Bariand, P.; Cesbron, F.; Giraud, R. *Bull. Soc. Fr. Mineral. Cristallogr.* **1968**, *91*, 34.
(140) Hazen, R. M.; Finger, L. W. *Phase Transitions* **1979**, *1*, 1.
(141) Beattie, I. R. *Acta Crystallogr.* **1954**, *7*, 357.
(142) Calleri, M.; Ferraris, G. *Atti Accad. Sci. Torino* **1964**, *98*, 821.
(143) Knowles, C. R.; Rinaldi, F. F.; Smith, J. V. *Indian Mineral.* **1965**, *6*, 127.
(144) Ferraris, G.; Jones, D. W.; Yerkess, J. *Z. Kristallogr.* **1972**, *135*, 240.
(145) Takêuchi, Y.; Mazzi, F.; Haga, N.; Galli, E. *Am. Mineral.* **1979**, *64*, 993. (a) Dyer, A.; Enamy, H.; Wilson, O. M.; Foy, H. *Zeolites* **1987**, *7*, 284.
(146) Artioli, G.; Pluth, J. J.; Smith, J. V. *Acta Crystallogr., Sect.* **1984**, *C40*, 214.
(147) Peacor, D. R. *Z. Kristallogr.* **1968**, *127*, 213.
(148) Mazzi, F.; Galli, E.; Gottardi, G. *Am. Mineral.* **1976**, *61*, 108.
(149) Kosorukov, A. A.; Nadel, L. G. *Kristallografiya* **1986**, *31*, 252.
(150) Klaska, R. *Naturwissenschaften* **1978**, *65*, 592.
(151) Beger, R. M. *Z. Kristallogr.* **1969**, *129*, 280.
(152) Torres-Martinez, L. M.; Gard, J.; Howie, R. A.; West, A. R. *J. Solid State Chem.* **1984**, *51*, 100.
(153) Torres-Martinez, L. M.; West, A. R. *Z. Kristallogr.* **1986**, *175*, 1.
(154) Section of Crystal Structure Analysis, Academy of Geological Sciences, Academia Sinica. *Acta Geol. Sin.* (*Engl. Transl.*) **1973**, *2*, 226.
(155) Kocman, V.; Gait, R. I.; Rucklidge, J. *Am. Mineral.* **1974**, *59*, 71.
(156) Bissert, G.; Liebau, H. *Neues Jahrb. Mineral. Mh.* **1986**, 241.
(157) Annehed, H.; Fälth, L. *Z. Kristallogr.* **1984**, *166*, 301.
(158) Schlenker, J. L.; Pluth, J. J.; Smith, J. V. *Acta Crystallogr., Sect. B* **1977**, *B33*, 2907.
(159) Artioli, G.; Smith, J. V.; Kvick, Å. *Acta Crystallogr., Sect. C* **1985**, *C41*, 492.
(160) Jarchow, O. *Z. Kristallogr.* **1965**, *122*, 407.
(161) Smolin, Yu. I.; Shepelev, Yu. E.; Butikova, I. K.; Kobyakov, I. B. *Sov. Phys.—Crystallogr.* (*Engl. Transl.*) **1981**, *26*, 33.
(162) Émiraliev, A.; Yamzin, I. I. *Sov. Phys.—Crystallogr.* (*Engl. Transl.*) **1982**, *27*, 27.
(163) Grundy, H. D.; Hassan, I. *Can. Mineral.* **1982**, *20*, 239.
(164) Kanepit, V. N.; Nozik, Yu. Z. *Geokhimiya* **1985**, 1058.
(165) Klaska, R.; Jarchow, O. *Naturwissenschaften* **1977**, *64*, 93. (a) Peacor, D. A.; Rouse, R. C.; Ahn, J.-H. *Ann. Mineral.* **1987**, *72*, 816.
(166) Sokolov, Yu. A.; Maksimov, B. A.; Galiulin, R. V.; Ilyukhin, V. V.; Belov, N. V. *Kristallografiya* **1981**, *26*, 287. (a) Beloneva, E. L.; Uvarova, T. G.; Dem'yanets, L. N. *Sov. Phys.—Crystallogr.* (*Engl. Transl.*) **1986**, *31*, 516.
(167) Bresciani Pahor, N.; Calligaris, M.; Nardin, G.; Randaccio, L. *Acta Crystallogr., Sect. B* **1982**, *B38*, 893.
(168) Rinaldi, R.; Wenk, H. R. *Acta Crystallogr., Sect. A* **1979**, *A35*, 825.
(169) Passaglia, E. *Am. Mineral.* **1970**, *55*, 1278.
(170) Peacor, D. R.; Dunn, P. J.; Simmons, W. B.; Tillmans, E.; Fisher, R. X. *Am. Mineral.* **1984**, *69*, 186.
(171) Tillmans, E.; Fischer, R. *Z. Kristallogr.* **1982**, *159*, 125.
(172) Smith, J. V. *J. Chem. Soc.* **1964**, 3759.
(173) Calligaris, M.; Nardin, G.; Randaccio, L.; Comin Chiaramonti, P. *Acta Crystallogr., Sect. B* **1982**, *B38*, 602.
(174) Alberti, A.; Galli, E.; Vezzalini, G.; Passaglia, E.; Zanazzi, P. F. *Zeolites* **1982**, *2*, 303.
(175) Calligaris, M.; Nardin, G.; Randaccio, L. *Zeolites* **1983**, *3*, 205.
(176) Calligaris, M.; Mezzeti, A.; Nardin, G.; Randaccio, L. *Zeolites* **1986**, *6*, 137.
(177) Smith, J. V.; Rinaldi, F.; Dent Glasser, L. S. *Acta Crystallogr.* **1963**, *16*, 45.
(178) Smith, J. V.; Knowles, C. R. *Acta Crystallogr.* **1964**, *17*, 374.
(179) Calligaris, M.; Nardin, G. *Zeolites* **1982**, *2*, 200.
(180) Calligaris, M.; Mezzetti, A.; Nardin, G.; Randaccio, L. *Zeolites* **1985**, *5*, 317.
(181) Calligaris, M.; Nardin, G.; Randaccio, L. *Zeolites* **1984**, *4*, 251. (a) Pluth, J. J.; Smith, J. V.; Mortier, W. J. *Mater. Res. Bull.* **1977**, *12*, 1001.
(182) Calligaris, M.; Mezzetti, A.; Nardin, G.; Randaccio, L. *Zeolites* **1984**, *4*, 323.
(183) Smith, J. V. *Acta Crystallogr.* **1962**, *15*, 835.
(184) Mortier, W. J.; Pluth, J. J.; Smith, J. V. *Mater. Res. Bull.* **1977**, *12*, 97.
(185) Mortier, W. J.; King, G. S. D.; Sengier, L. *J. Phys. Chem.* **1979**, *83*, 2263.
(186) Fang, J. H.; Smith, J. V. *J. Chem. Soc.* **1964**, 3749.
(187) Mortier, W. J.; Pluth, J. J.; Smith, J. V. *Mater. Res. Bull.* **1977**, *12*, 103. (a) Cartlidge, S.; Wessicken, R.; Nissen, H. U. *Phys. Chem. Mineral.* **1983**, *9*, 139.
(188) Cartlidge, S.; Keller, E. B. *Zeolites* **1984**, *4*, 226.
(189) Belokoneva, E. L.; Maksimov, B. A.; Verin, I. A.; Sirota, M. I.; Voloshin, A. V.; Pakhomovskii, Ya. A. *Sov. Phys.—Crystallogr.* (*Engl. Transl.*) **1985**, *30*, 507.
(190) Ito, M.; Shimoyama, Y.; Saito, Y.; Tsurita, Y.; Otake, M. *Acta Crystallogr., Sect. C* **1985**, *C41*, 1698.
(191) Gottardi, G.; Meier, W. M. *Z. Kristallogr.* **1963**, *119*, 53.
(192) Vezzalini, G. *Z. Kristallogr.* **1984**, *166*, 63. (a) Sanders, J. V. *Zeolites* **1985**, *5*, 81.
(193) Galli, E. *Acta Crystallogr., Sect. B* **1976**, *B32*, 1623.
(194) Kvick, Å.; Smith, J. V. *J. Chem. Phys.* **1983**, *79*, 2356.
(195) Mazzi, F.; Galli, E.; Gottardi, G. *Neues Jahrb. Mineral. Mh.* **1984**, 373. (a) Nadezhina, T. N.; Pobedimskaya, E. A.; Khomyakov, A. P. *Mineral. Zh.* **1984**, *6*, 56.
(196) Tambuyzer, E.; Bosmans, H. J. *Acta Crystallogr., Sect. B* **1976**, *B32*, 1714.
(197) Baerlocher, C.; Barrer, R. M. *Z. Kristallogr.* **1974**, *140*, 10.
(198) Malinovskii, Yu. A.; Belov, N. V. *Dokl. Adad. Nauk SSSR* **1980**, *252*, 611.
(199) Galli, E.; Rinaldi, R. *Am. Mineral.* **1974**, *59*, 1055.
(200) Kerr, I. S. *Nature* (*London*) **1964**, *202*, 589.
(201) Perrotta, A. J. *Mineral. Mag.* **1967**, *36*, 480.
(202) Slaughter, M.; Kane, W. T. *Z. Kristallogr.* **1969**, *130*, 68.
(203) Alberti, A.; Galli, E.; Vezzalini, G. *Z. Kristallogr.* **1985**, *173*, 257.
(204) Kokotailo, G. T.; Sawruk, S.; Lawton, S. L. *Am. Mineral.* **1972**, *57*, 439.
(205) Millward, G. R.; Thomas, J. M.; Terasaki, O.; Watanabe, D. *Zeolites* **1986**, *6*, 91.
(206) Kokotailo, G. T.; Lawton, S. L. U.S. Patent 3 640 680, 1972.
(207) Kawahara, A.; Curien, H. *Bull. Soc. Fr. Mineral. Cristallogr.* **1969**, *92*, 250.
(208) Gard, J. A.; Tait, J. M. Reference 8, p 94.
(209) Schlenker, J. L.; Pluth, J. J.; Smith, J. V. *Acta Crystallogr., Sect. B* **1977**, *B33*, 3265.
(210) Glonti, O. A.; Shishakov, N. A. *Izv. Akad. Nauk SSSR, Ser. Khim.* **1965**, 1275. (a) Smith, J. V. Reference 6a, p 171. (b) Bergerhoff, G.; Baur, W. H.; Nowacki, W. *Neues Jahrb. Mineral. Mh.* **1958**, 193. (c) Baur, W. H. *Am. Mineral.* **1964**, *49*, 697. (d) Bennett, J. M.; Smith, J. V. *Mater. Res. Bull.* **1968**, *3*, 933. (e) Bennett, J. M.; Smith, J. V. *Mater. Res. Bull.* **1969**, *4*, 343.
(211) Olson, D. H.; Kokotailo, G. T.; Charnell, J. F. *J. Colloid Interface Sci.* 1968, *28*, 305.
(212) Bennett, J. M.; Smith, J. V. *Mater. Res. Bull.* **1968**, *3*, 633.
(213) Olson, D. H. *J. Phys. Chem.* **1968**, *72*, 4366.
(214) Bennett, J. M.; Smith, J. V. *Mater. Res. Bull.* **1968**, *3*, 865. (a) Lee, Y.; Rees, L. V. C. *Zeolites* **1987**, *7*, 143.
(215) Bennett, J. M.; Smith, J. V. *Mater. Res. Bull.* **1969**, *4*, 7.
(216) Olson, D. H.; Dempsey, E. *J. Catal.* **1969**, *13*, 221.
(217) Mortier, W. J.; Van den Bossche, E.; Uytterhoeven, J. B. *Zeolites* **1984**, *4*, 41. (a) Beagley, B.; Dwyer, J.; Fitch, F. R.; Zanjanchi, M. A. *J. Inclusion Phenom.* **1985**, *3*, 143.
(218) Bergeret, G.; Tran Manh Tri; Gallezot, P. *J. Phys. Chem.* **1983**, *87*, 1160.

(219) Cheetham, A. K.; Eddy, M. M.; Thomas, J. M. *J. Chem. Soc., Chem. Commun.* **1984**, 1337.
(220) Eulenberger, G. R.; Shoemaker, D. P.; Keil, J. G. *J. Phys. Chem.* **1967**, *71*, 1812.
(221) Fitch, A. N.; Jobic, H.; Renouprez, A. *J. Phys. Chem.* **1986**, *90*, 1311.
(222) Gallezot, P.; Imelik, B. *J. Chim. Phys. Physicochim. Biol.* **1971**, *68*, 816. (a) Jiraz, Z.; Vratislav, S.; Bosacek, V. *J. Phys. Chem. Solids* **1980**, *41*, 1089.
(223) Gallezot, P.; Imelik, B. *J. Chim. Phys. Physicochim. Biol.* **1971**, *68*, 34.
(224) Gallezot, P.; Imelik, B. *J. Chim. Phys. Physicochim. Biol.* **1974**, *71*, 155.
(225) Gallezot, P.; Ben Taarit, Y.; Imelik, B. *J. Catal.* **1972**, *26*, 481.
(226) Gallezot, P.; Ben Taarit, Y.; Imelik, B. *J. Phys. Chem.* **1973**, *77*, 2556.
(227) Gallezot, P.; Ben Taarit, Y.; Imelik, B. *J. Catal.* **1972**, *26*, 295.
(228) Gellens, L. R.; Mortier, W. J.; Uytterhoeven, J. B. *Zeolites* **1981**, *1*, 85.
(229) Herden, H.; Einicke, W. D.; Schoellner, R.; Mortier, W. J.; Gellens, L. R.; Uytterhoeven, J. B. *Zeolites* **1982**, *2*, 131.
(230) Mortier, W. J.; Bosmans, H. J.; Uytterhoeven, J. B. *J. Phys. Chem.* **1971**, *75*, 3327.
(231) Mortier, W. J.; Bosmans, H. J.; Uytterhoeven, J. B. *J. Phys. Chem.* **1972**, *76*, 650.
(232) Mortier, W. J.; Bosmans, H. J.; Uytterhoeven, J. B. *J. Phys. Chem.* **1973**, *77*, 2880.
(233) Pearce, J. R.; Mortier, W. J. *J. Chem. Soc., Faraday Trans. 1* **1981**, *77*, 1935.
(234) Pearce, J. R.; Mortier, W. J.; Uytterhoeven, J. B.; Lunsford, J. H. *J. Chem. Soc., Faraday Trans. 1* **1981**, *77*, 937.
(235) Van Dun, J. J. I.; Mortier, W. J.; Uytterhoeven, J. B. *Zeolites* **1985**, *5*, 257.
(236) Beagley, B.; Dwyer, J. *Zeolites* **1981**, *1*, 69.
(237) Beagley, B.; Dwyer, J.; Evmerides, N. P.; Hawa, A. I. F.; Ibrahim, T. K. *Zeolites* **1982**, *2*, 167.
(238) Al-Ajdah, G. N. D.; Al-Rished, A. A.; Beagley, B.; Dwyer, J.; Fitch, F. R.; Ibrahim, T. K. *J. Inclusion Phenom.* **1985**, *3*, 135.
(239) Bennett, J. M.; Smith, J. V. *Mater. Res. Bull.* **1969**, *4*, 77.
(240) Calestani, G.; Bacca, G.; Andreeti, G. D. *Zeolites* **1987**, *71*, 54.
(241) Calestani, G.; Bacca, G.; Andreeti, G. D. *Zeolites* **1987**, *71*, 59.
(242) Calligaris, M.; Nardin, G.; Randaccio, L.; Zangrando, E. *Zeolites* **1986**, *6*, 439.
(243) Olson, D. H. *J. Phys. Chem.* **1970**, *74*, 2758.
(244) Pluth, J. J.; Smith, J. J. *Mater. Res. Bull.* **1972**, *7*, 1311.
(245) Smolin, Yu. I.; Shepelev, Yu. F.; Butikova, I. K.; Petranovskii, V. P. *Kristallografiya* **1983**, *28*, 72.
(246) Simpson, H. D.; Steinfink, H. *J. Am. Chem. Soc.* **1969**, *91*, 6229.
(247) Simpson, H. D.; Steinfink, H. *J. Am. Chem. Soc.* **1969**, *91*, 6225.
(248) Parise, J. B.; Corbin, D. R.; Abrams, L.; Cox, D. E. *Acta Crystallogr., Sect. C* **1984**, *C40*, 1493.
(249) Newsam, J. M.; Jacobson, A. J.; Vaughan, D. E. W. *J. Phys. Chem.* **1986**, *90*, 6858.
(250) Newsam, J. M.; Vaughan, D. E. W. Reference 15, p 457.
(251) Kerr, I. S. *Nature (London)* **1966**, *210*, 294.
(252) Vaughan, P. A. *Acta Crystallogr.* **1966**, *21*, 983.
(253) Gramlich-Meier, R.; Gramlich, V.; Meier, W. M. *Am. Mineral.* **1985**, *70*, 619.
(254) Smith, B. K. *Am. Mineral.* **1986**, *71*, 989.
(255) Fischer, K. *Am. Mineral.* **1963**, *48*, 664.
(256) Rinaldi, R.; Vezzalini, G. *Stud. Surf. Sci. Catal.* **1985**, *24*, 481.
(257) Artioli, G.; Rinaldi, R.; Kvick, Å.; Smith, J. V. *Zeolites* **1986**, *6*, 361.
(258) Alberti, A.; Vezzalini, G. *Acta Crystallogr., Sect. B* **1979**, *B35*, 2866.
(259) McCusker, L. B.; Baerlocher, C.; Nawaz, R. *Z. Kristallogr.* **1985**, *171*, 281.
(260) Gottardi, G.; Alberti, A. *Mineral. Mag.* **1974**, *39*, 898.
(261) Baerlocher, C.; Meier, W. M. *Z. Kristallogr.* **1972**, *135*, 339.
(262) Baerlocher, C.; Meier, W. M. *Helv. Chim. Acta* **1970**, *53*, 1285.
(263) Galli, E.; Passaglia, E.; Zanazzi, P. F. *Neues Jahrb. Mineral. Mh.* **1982**, 145.
(264) Malinowski, Yu. A. *Sov. Phys.—Crystallogr. (Engl. Transl.)* **1984**, *29*, 256.
(265) Vigdorchik, A. G.; Malinovskii, Yu. A. *Sov. Phys.—Crystallogr. (Engl. Transl.)* **1986**, *31*, 519.
(266) Kerr, G. T.; Rollmann, L. D. U.S. Patent 4 061 717, 1977.
(267) Rouse, R. C.; Peacor, D. R. *Am. Mineral.* **1986**, *71*, 1494.
(268) Alberti, A. *Tschermaks Mineral. Petrog. Mitt.* **1972**, *18*, 129.
(269) Bresciani-Pahor, N.; Callegaris, M.; Nardin, G.; Randaccio, L.; Comin-Chiaramonti, P. *J. Chem. Soc., Dalton Trans.* **1980**, *1511*.
(270) Merkle, A. B.; Slaughter, M. *Am. Mineral.* **1968**, *53*, 1120.
(271) Sugiyama, K.; Takêuchi, Y. *Stud. Surf. Sci. Catal.* **1986**, *28*, 449.
(272) Hambley, T. W.; Taylor, J. C. *J. Solid State Chem.* **1984**, *54*, 1.
(273) Alberti, A. *Tschermaks Mineral. Petrog. Mitt.* **1975**, *22*, 25.
(274) Koyama, K.; Takêuchi, Y. *Z. Kristallogr.* **1977**, *145*, 216.
(275) Petrov, O.; Karameneva, T.; Kirov, G. *Dokl. Bolg. Akad. Nauk* **1984**, *37*, 785.
(276) Alberti, A.; Vezzalini, G.; Cariati, F.; Erre, L.; Piu, P. *Zeolites* **1985**, *5*, 289.
(277) Alberti, A.; Vezzalini, G. *Tschermaks Mineral. Petrog. Mitt.* **1983**, *31*, 259.
(278) Kudoh, Y.; Takêuchi, Y. *Mineral. J. Jpn.* **1983**, *11*, 392.
(279) Alberti, A.; Gottardi, G.; Poppi, L. *Tschermaks Mineral. Petrog. Mitt.* **1974**, *21*, 291.
(280) Bresciani-Pahor, N.; Calligaris, M.; Nardin, G.; Rondaccio, L.; Comin-Chiaramonti, P. *J. Chem. Soc., Dalton Trans.* **1980**, 1511.
(281) Bresciani-Pahor, N.; Calligaris, M.; Nardin, G.; Randaccio, L. *J. Chem. Soc., Dalton Trans.* **1981**, 2288.
(282) Galli, E.; Gottardi, G.; Mayer, H.; Preisinger, A.; Passaglia, E. *Acta Crystallogr., Sect. B* **1983**, *B39*, 189.
(283) Mortier, W. J.; Pearce, J. R. *Am. Mineral.* **1981**, *66*, 309.
(284) Petrov, O.; Filizova, L.; Kirov, G. *Dokl. Bolg. Akad. Nauk* **1985**, *38*, 603.
(285) Bartl, H.; Fischer, K. F. *Neues Jahrb. Mineral. Mh.* **1967**, 33.
(286) Schramm, V.; Fischer, K. F. Reference 69, p 259.
(287) Amirov, S. T.; Ilynkhin, V. V.; Belov, N. V. *Dokl. Acad. Sci. USSR Earth Sci. Sect.* **1967**, *174*, 121.
(288) Yakubovich, O. V.; Simonov, M. A. *Kristallografiya* **1985**, *30*, 1072.
(289) Artioli, G.; Smith, J. V.; Kvick, Å., in preparation.
(290) Merlino, S.; Galli, E.; Alberti, A. *Tschermaks Mineral. Petrogr. Mitt.* **1975**, *22*, 117.
(291) Barrer, R. M.; Kerr, I. S. *Trans. Faraday Soc.* **1959**, *55*, 1915.
(292) Galli, E. *Cryst. Struct. Commun.* **1974**, *3*, 339.
(293) Rinaldi, R.; Pluth, J. J.; Smith, J. V. *Acta Crystallogr., Sect. B* **1975**, *B31*, 1603.
(294) Alberti, A.; Vezzalini, G. *Bull. Mineral.* **1981**, *104*, 5.
(295) Newsam, J. M.; Jarman, R. H.; Jacobson, A. J. *Mater. Res. Bull.* **1985**, *20*, 125.
(296) Terasaki, O.; Thomas, J. M.; Millward, G. R. *Proc. R. Soc. London, A:* **1984**, *395*, 153.
(297) Galli, E.; Gottardi, G.; Pongiluppi, D. *Neues Jahrb. Mineral. Mh.* **1979**, 1.
(298) Baturin, S. V.; Malinovskii, Yu. A.; Bunova, I. B. *Mineral. Zh.* **1985**, *7*, 67.
(299) Meier, W. M. *Z. Kristallogr.* **1961**, *115*, 439.
(300) Alberti, A.; Davoli, P.; Vezzalini, G. *Z. Kristallogr.* **1986**, *175*, 249.
(301) Mortier, W. J.; Pluth, J. J.; Smith, J. V. *Mater. Res. Bull.* **1975**, *10*, 1037.
(302) Mortier, W. J.; Pluth, J. J.; Smith, J. V. *Mater. Res. Bull.* **1975**, *10*, 1319.
(303) Schlenker, J. L.; Pluth, J. J.; Smith, J. V. *Mater. Res. Bull.* **1978**, *13*, 77.
(304) Schlenker, J. L.; Pluth, J. J.; Smith, J. V. *Mater. Res. Bull.* **1978**, *13*, 169.
(305) Schlenker, J. L.; Pluth, J. J.; Smith, J. V. *Mater. Res. Bull.* **1978**, *13*, 901.
(306) Mortier, W. J.; Pluth, J. J.; Smith, J. V. Reference 10, p 53.
(307) Schlenker, J. L.; Pluth, J. J.; Smith, J. V. *Mater. Res. Bull.* **1979**, *14*, 751.
(308) Schlenker, J. L.; Pluth, J. J.; Smith, J. V. *Mater. Res. Bull.* **1979**, *14*, 849.
(309) Schlenker, J. L.; Pluth, J. J.; Smith, J. V. *Mater. Res. Bull.* **1979**, *14*, 961.
(310) Mortier, W. J.; Pluth, J. J.; Smith, J. V. *Mater. Res. Bull.* **1976**, *11*, 15.
(311) Saito, Y. *Bull. Chem. Soc. Jpn.* **1985**, *58*, 3035.
(312) Alberti, A.; Pongiluppi, D.; Vezzalini, G. *Neues Jahrb. Mineral. Abh.* **1982**, *143*, 231.
(313) Meier, W. M. *Z. Kristallogr.* **1960**, *113*, 430.
(314) Torrie, B. H.; Brown, I. D.; Petch, H. E. *Can. J. Phys.* **1964**, *42*, 229.
(315) Pechar, F. *Acta Crystallogr., Sect. B* **1981**, *B37*, 1909.
(316) Pechar, F.; Schäfer, W.; Will, G. *Z. Kristallogr.* **1983**, *164*, 19.
(317) Artioli, G.; Smith, J. V.; Kvick, Å. *Acta Crystallogr., Sect. C* **1984**, *C40*, 1658.
(318) Kirfel, A.; Orthen, M.; Will, G. *Zeolites* **1984**, *4*, 140.
(319) Alberti, A.; Vezzalini, G. *Acta Crystallogr., Sect. B* **1981**, *B37*, 781.
(320) Hesse, K.-F. *Z. Kristallogr.* **1983**, *163*, 69.
(321) Mazzi, F.; Larsen, A. O.; Gottardi, G.; Galli, E. *Neues Jahrb. Mineral. Mh.* **1986**, 219.
(322) Mikheeva, M. G.; Pushcharovskii, D. Yu.; Khomyakov, A. P.; Yamnova, N. A. *Kristallografiya* **1986**, 434.
(323) Fälth, L.; Hansen, S. *Acta Crystallogr., Sect. B* **1979**, *B35*, 1877.
(324) Pechar, F. *Acta Mont.* **1982**, *60*, 121.
(325) Joswig, W.; Bartl, H.; Fuess, H. *Z. Kristallogr.* **1984**, *170*, 220.
(326) Kvick, Å.; Stahl, K.; Smith, J. V. *Z. Kristallogr.* **1985**, *171*, 141.
(327) Pechar, F. *Acta Mont.* **1982**, *59*, 143.

(328) Artioli, G.; Smith, J. V.; Pluth, J. J. *Acta Crystallogr., Sect. C* **1986**, *C42*, 937.
(329) Peacor, D. R. *Am. Mineral.* **1973**, *58*, 676.
(330) Alberti, A.; Vezzalini, G. *Neues Jahrb. Mineral. Mh.* **1983**, 135.
(331) Klaska, K. H.; Jarchow, O. *Z. Kristallogr.* **1985**, *172*, 167.
(332) Rinaldi, R.; Smith, J. V.; Jung, G. *Neues Jahrb. Mineral. Mh.* **1975**, 443.
(333) Rinaldi, R. *Neues Jahrb. Mineral. Mh.* **1976**, 145.
(334) Millward, G. R.; Thomas, J. M. *J. Chem. Soc., Chem. Commun.* **1984**, 77.
(335) Gard, J. A.; Tait, J. M. Reference 8, p 94.
(336) Mortier, W. J.; Pluth, J. J.; Smith, J. V. *Z. Kristallogr.* **1976**, *143*, 319.
(337) Mortier, W. J.; Pluth, J. J.; Smith, J. V. *Z. Kristallogr.* **1976**, *144*, 32.
(338) Chen, N. Y.; Schlenker, J. L.; Garwood, W. E.; Kokotailo, G. T. *J. Catal.* **1984**, *86*, 24.
(339) Gordon, E. K.; Samson, S.; Kamb, W. B. *Science (Washington, D.C.)* **1966**, *154*, 1004.
(340) Pluth, J. J.; Price, G. D.; Smith, J. V., in preparation.
(341) Steinfink, H. *Acta Crystallogr.* **1962**, *15*, 644.
(342) Rinaldi, R.; Pluth, J. J.; Smith, J. V. *Acta Crystallogr., Sect. B* **1974**, *B30*, 2426.
(343) Felsche, J.; Luger, S.; Baerlocher, C. *Zeolites* **1986**, *6*, 367.
(344) Felsche, J.; Luger, S.; Fischer, P. *Acta Crystallogr., Sect. C* **1987**, *C43*, 809.
(345) Bondareva, O. S.; Malinovskii, Yu. A. *Sov. Phys.—Crystallogr. (Engl. Transl.)* **1983**, *28*, 273.
(346) Bukin, V. I.; Makarov, Ye. S. *Geochem. Int.* **1967**, *4*, 19.
(347) Emiraliev, A.; Yamzin, I. I. *Sov. Phys.—Crystallogr. (Engl. Transl.)* **1978**, *23*, 27.
(348) Galitskii, V. Yu.; Shcherbakov, V. N.; Gabuda, S. P. *Sov. Phys.—Crystallogr. (Engl. Transl.)* **1974**, *18*, 620.
(349) Hassan, I.; Grundy, H. D. *Acta Crystallogr., Sect. C* **1983**, *C39*, 3.
(350) Kanepit, V. N.; Nozik, Yu. Z.; Fizkin, L. Ye. *Geochem. Int.* **1984**, *21*, 134.
(351) Luger, S.; Felsche, J.; Fischer, P. *Acta Crystallogr., Sect. C* **1987**, *C43*, 1.
(352) McCusker, L. B.; Meier, W. M.; Suzuki, K.; Shin, S. *Zeolites* **1986**, *6*, 388.
(353) Sahl, K. *Z. Kristallogr.* **1980**, *152*, 13.
(354) Sturua, G. I.; Belokoneva, E. L.; Simonov, M. A.; Belov, N. V. *Sov. Phys. Dokl.* **1978**, *23*, 703.
(355) Belokoneva, E. L.; Uvarova, T. G.; Dem'yanets, L. N. *Sov. Phys.—Crystallogr. (Engl. Transl.)* **1985**, *30*, 465.
(356) Depmeier, W. *Acta Crystallogr., Sect. B* **1984**, *B40*, 185.
(357) Dempsey, M. J.; Taylor, D. *Phys. Chem. Mineral.* **1980**, *6*, 197.
(358) Bibby, D. M.; Dale, M. P. *Nature (London)* **1985**, *317*, 157.
(359) Richardson, J. W., Jr.; Pluth, J. J.; Smith, J. V.; Dytrych, W. J. *J. Phys. Chem.*, in press.
(360) Baerlocher, C.; Meier, W. M. *Helv. Chim. Acta* **1969**, *52*, 1853.
(361) Galli, E.; Alberti, A. *Bull. Fr. Mineral. Crystallogr.* **1975**, *98*, 11.
(362) Miller, S. A.; Taylor, J. C. *Zeolites* **1985**, *5*, 7.
(363) Pechar, F.; Mattern, G. *Cryst. Res. Technol.* **1986**, *21*, 1029.
(364) Sacerdoti, M.; Gomedi, I. *Bull. Mineral.* **1984**, *107*, 799.
(365) Galli, E.; Alberti, A. *Bull. Fr. Mineral. Crystallogr.* **1975**, *98*, 331.
(366) Passaglia, E.; Sacerdoti, M. *Bull. Mineral.* **1982**, *105*, 338.
(367) Galli, E. *Acta Crystallogr., Sect. B* **1971**, *B27*, 833.
(368) Slaughter, M. *Am. Mineral.* **1970**, *55*, 387. (a) Quartieri, S.; Vezzalini, G. *Zeolites* **1987**, *7*, 163.
(369) Passaglia, E. *Tschermaks Mineral. Petrogr. Mitt.* **1980**, *27*, 67.
(370) Mortier, W. J. *Am. Mineral.* **1983**, *68*, 414.
(371) Alberti, A.; Vezzalini, G. Reference 13, p 834.
(372) Alberti, A.; Vezzalini, G.; Tazzoli, V. *Zeolites* **1981**, *1*, 91.
(373) Pechar, F. *Cryst. Res. Technol.* **1982**, *17*, 1141.
(374) Pluth, J. J.; Smith, J. V.; Kvick, Å. *Zeolites* **1985**, *5*, 73.
(375) Kerr, I. S.; Williams, D. J. *Acta Crystallogr., Sect B* **1969**, *B25*, 1183.
(376) Leimer, H. W.; Slaughter, M. *Z. Kristallogr.* **1969**, *130*, 88.
(377) Kvick, Å.; Artioli, G.; Smith, J. V. *Z. Kristallogr.* **1986**, *174*, 265.
(378) Kerr, I. S. *Z. Kristallogr.* **1974**, *139*, 186.
(379) Norby, P.; Nörlund Christensen, A.; Krogh Anderson, I. G. *Acta Chem. Scand., Ser. A*: **1986**, *A40*, 500.
(380) Newsam, J. M. *J. Chem. Soc., Chem. Commun.* **1986**, 1295. (a) Andersen, E. K.; Plough-Sorensen, G. *Z. Kristallogr.* **1986**, *176*, 67.
(381) Meier, W. M.; Groner, M. *J. Solid State Chem.* **1981**, *37*, 204.
(382) Meier, W. M.; Kokotailo, G. T. *Z. Kristallogr.* **1965**, *121*, 211.
(383) Fischer, R. X.; Baur, W. H.; Shannon, R. D.; Staley, R. H.; Vega, A. J.; Abrams, L.; Prince, E. *Zeolites* **1986**, *6*, 378.
(384) Parise, J. B.; Shannon, R. D.; Prince, E.; Cox, D. E. *Z. Kristallogr.* **1983**, *165*, 175.
(385) Barrer, R. M.; Robinson, D. J. *Z. Kristallogr.* **1972**, *135*, 374.
(386) Sieber, W.; Meier, W. M. *Helv. Chim. Acta* **1974**, *57*, 1533.
(387) Kim, Y.; Subramanian, V.; Firor, R. L.; Seff, K. *Am. Chem. Soc. Symp. Ser.* **1980**, *No. 135*, 137.
(388) Lee, H. S.; Cruz, W. V.; Seff, K. *J. Phys. Chem.* **1982**, *86*, 3562. (a) Heo, N. H.; Cruz-Patalinghug, W. V.; Seff, K. *J. Phys. Chem.* **1986**, *90*, 3931.
(389) Adams, J. M.; Haselden, D. A. *J. Solid State Chem.* **1984**, *51*, 83.
(390) Adams, J. M.; Haselden, D. A. *J. Solid State Chem.* **1983**, *47*, 123.
(391) Adams, J. M.; Haselden, D. A. *J. Chem. Soc., Chem. Commun.* **1982**, 822.
(392) Adams, J. M.; Haselden, D. A.; Hewat, A. W. *J. Solid State Chem.* **1982**, *44*, 245. (a) Eddy, M. M.; Cheetham, A. K.; David, W. I. F. *Zeolites* **1987**, *6*, 449.
(393) Belbeoch, B.; Roulliay, M.; Kahn, R.; Cohen de Lara, E. *Zeolites* **1983**, *3*, 99.
(394) Richardson, J. W., Jr.; Pluth, J. J.; Smith, J. V., in preparation.
(395) Bennett, J. M.; Blackwell, C. S.; Cox, D. E. Reference 12, p 143.
(396) Cheetham, A. K.; Eddy, M. M. Reference 12, p 131.
(397) Rayment, T.; Thomas, J. M. *Zeolites* **1983**, *3*, 2.
(398) Gellens, L. R.; Smith, J. V.; Pluth, J. J. *J. Am. Chem. Soc.* **1983**, *105*, 51.
(399) Jirak, Z.; Bosacek, V.; Vratislav, S.; Herden, H.; Schoellner, R.; Mortier, W. J.; Gellens, L.; Uytterhoeven, J. B. *Zeolites* **1983**, *3*, 255.
(400) Kim, Y.; Seff, K. *Bull. Korean Chem. Soc.* **1984**, *5*, 135.
(401) Kim, Y.; Seff, K. *Bull. Korean Chem. Soc.* **1985**, *6*, 202.
(402) Kim, Y.; Seff, K. *Bull. Korean Chem. Soc.* **1986**, *7*, 190. (a) Heo, N. H.; Dejsupa, C.; Seff, K. *J. Phys. Chem.* **1987**, *91*, 3943.
(403) Kim, Y.; Seff, K. *Bull. Korean Chem. Soc.* **1984**, *5*, 117.
(404) McCusker, L. B.; Seff, K. *J. Am. Chem. Soc.* **1981**, *103*, 3441.
(405) Adams, J. M.; Rees, L. V. C. *J. Solid State Chem.* **1986**, *62*, 184.
(406) De Roy, G.; Vansant, E. F.; Mortier, W. J.; Uytterhoeven, J. B. Reference 11, p 214.
(407) Pluth, J. J.; Smith, J. V. *J. Am. Chem. Soc.* **1983**, *105*, 1192.
(408) Pluth, J. J.; Smith, J. V. *J. Am. Chem. Soc.* **1983**, *105*, 2621.
(409) Ronay, C.; Seff, K. *J. Phys. Chem.* **1985**, *89*, 1965.
(410) Schoellner, R.; Gellens, L. R.; Mortier, W. J.; Uytterhoeven, J. B. *Zeolites* **1983**, *3*, 149.
(411) Adams, J. B.; Haselden, D. A. *J. Solid State Chem.* **1984**, *55*, 209.
(412) Cheng, M. Y.; Lee, H. S.; Seff, K. *Zeolites* **1983**, *3*, 348.
(413) Dimitrijevic, R.; Petranovic, N.; Krstanovic, I.; Susic, M.; Mioc, U. *Stud. Surf. Sci. Catal.* **1985**, *24*, 453. (a) Siegal, H.; Schöllner, R.; Staudte, B.; Van Dun, J. J.; Mortier, W. J. *Zeolites* **1987**, *7*, 372. (b) Siegel, H.; Schoellner, R.; Van Dun, J. J.; Mortier, W. J. *Zeolites* **1987**, *7*, 148.
(414) Newsam, J. *J. Chem. Soc., Chem. Commun.* **1987**, 123.
(415) Newsam, J. M. *Mater. Res. Bull.* **1986**, *21*, 661.
(416) Wright, P. A.; Thomas, J. M.; Cheetham, A. K.; Nowak, A. K. *Nature (London)* **1986**, *318*, 611. (a) Newsam, J. M.; Silbernagel, B. G.; Garcia, A. R.; Hulme, R. *J. Chem. Soc., Chem. Commun.* **1987**, 664.
(417) Men'shikov, Yu. P. *Zap. Vses. Mineral. Ova* **1984**, *113*, 607.
(418) Fälth, L.; Andersson, S. *Z. Kristallogr.* **1982**, *160*, 313.
(419) Shepelev, Yu. F.; Smolin, Yu. I.; Butikova, I. K.; Tarasov, V. I. *Dokl. Akad. Nauk SSSR* **1983**, *272*, 1133.
(420) van Koningsveld, H.; van Bekkum, H.; Jansen, J. C. *Acta Crystallogr., Sect. B* **1987**, *B43*, 127. (a) Baerlocher, C. Reference 13, p 823.
(421) Lermer, H.; Draeger, M.; Steffen, J.; Unger, K. K. *Zeolites* **1985**, *5*, 131.
(422) Chao, K. J.; Lin, J. C.; Wang, Y.; Lee, G. H. *Zeolites* **1986**, *6*, 35.
(423) Hay, D. G.; Jaeger, H.; West, G. W. *J. Phys. Chem.* **1985**, *89*, 1070.
(424) Fyfe, C. A.; Kennedy, G. J.; Kokotailo, G. T.; Lyerla, J. R.; Fleming, W. W. *J. Chem. Soc., Chem. Commun.* **1985**, 740.
(425) Milward, G. R.; Ramdas, S.; Thomas, J. M.; Barlow, M. T. *J. Chem. Soc., Faraday Trans. 2* **1983**, *79*, 1075.
(426) Jablonski, G. A.; Sand, L. B.; Gard, J. A. *Zeolites* **1986**, *6*, 396. (a) Taylor, J. C. *Zeolites* **1987**, *7*, 311.
(427) Mentzen, B. F. *C. R. Seances Acad. Sci., Ser. B* **1986**, *303*, 681.
(428) Mentzen, B. F. *Mater. Res. Bull.* **1987**, *22*, 337.
(429) Mentzen, B. F.; Vigne-Maeder, F. *Mater. Res. Bull.* **1987**, *22*, 309.
(430) Schlenker, J. L.; Dwyer, F. G.; Jenkins, E. E.; Rohrbaugh, W. J.; Kokotailo, G. T.; Meier, W. M. *Nature (London)* **1981**, *294*, 340.
(431) Gies, H. *Z. Kristallogr.* **1984**, *167*, 73.
(432) Smith, J. V.; Blackwell, C. S. *Nature (London)* **1983**, *303*, 223.
(433) Pluth, J. J.; Smith, J. V., unpublished.
(434) LaPierre, R. B.; Rohrman, A. C., Jr.; Schlenker, J. J.; Wood, J. D.; Rubin, M. K.; Rohrbaugh, W. J. *Zeolites* **1985**, *5*, 346.

(a) Robson, H. E.; Shoemaker, D. P.; Ogilvie, R. A.; Manor, P. C. Reference 7, p 106.
(435) Parise, J. B.; Gier, T. E.; Corbin, D. R.; Cox, D. E. *J. Phys. Chem.* **1984**, *88*, 1635.
(436) McCusker, L. B.; Baerlocher, C. Reference 13, p 812.
(437) Parise, J. B.; Prince, E. *Mater. Res. Bull.* **1983**, *18*, 841.
(438) Fischer, R. X.; Baur, W. H.; Shannon, R. D.; Staley, R. H. *J. Phys. Chem.* **1987**, *91*, 2227.
(439) Wright, P. A.; Thomas, J. M.; Ramdas, S.; Cheetham, A. K. *J. Chem. Soc., Chem. Commun.* **1984**, 1338.
(440) Gameson, I.; Wright, P. A.; Rayment, T.; Thomas, J. M. *Chem. Phys. Lett.* **1986**, *123*, 145.
(441) Rouse, R. C.; Peacor, D. R.; Dunn, P. J.; Campbell, T. J.; Roberts, W. L.; Wicks, F. J.; Newbury, D. *Neues Jahrb. Mineral. Mh.*, in press.
(442) Marler, B. *Z. Kristallogr.* **1986**, *173*, 141. Also: *Zeolites*, in press.
(443) Flanigen, E. M.; Lok, B. M.; Patton, R. L.; Wilson, S. T. *Stud. Surf. Sci. Catal.* **1986**, *28*, 103.
(444) Lok, B. M.; Messina, C. A.; Patton, R. L.; Gajek, R. T.; Cannan, T. R.; Flanigen, E. M. *J. Am. Chem. Soc.* **1984**, *106*, 6092.
(445) Blackwell, C. S.; Patton, R. L. *J. Phys. Chem.* **1984**, *88*, 6135.
(446) Kniep, R. *Angew. Chem., Int. Ed. Engl.* **1986**, 525.
(447) Bennett, J. M.; Cohen, J. P.; Flanigen, E. M.; Pluth, J. J.; Smith, J. V. Reference 12, p 109.
(448) Richardson, J. W., Jr.; Pluth, J. J.; Smith, J. V. *Acta. Crystallogr., Sect. C* **1987**, *C43*, 1469.
(449) Bennett, J. M.; Richardson, J. W., Jr.; Pluth, J. J.; Smith, J. V. *Zeolites* **1987**, *7*, 160.
(450) Richardson, J. W., Jr.; Pluth, J. J.; Smith, J. V. *Acta Crystallogr.*, in press.
(451) Pluth, J. J.; Smith, J. V.; Richardson, J. W., Jr. *J. Phys. Chem.*, in press.
(452) Mentzen, B. F.; Vedrine, J. C.; Khouzami, R. *C. R. Seances Acad. Sci., Ser. B* **1987**, *304*, 11.
(453) Parise, J. B. *J. Chem. Soc., Chem. Commun.* **1984**, 1449.
(454) Parise, J. B. *J. Chem. Soc., Chem. Commun.* **1985**, 606.
(455) Pluth, J. J.; Smith, J. V.; Bennett, J. M.; Cohen, J. P. *Acta Crystallogr., Sect. C* **1984**, *C40*, 2008.
(456) Parise, J. B. *Acta Crystallogr., Sect. C* **1984**, *C40*, 1641.
(457) Bennett, J. M., personal communication.
(458) Kamb, W. B. *Acta Crystallogr.* **1960**, *13*, 15.
(459) Pluth, J. J.; Smith, J. V.; Bennett, J. M. *Acta Crystallogr., Sect. C* **1986**, *C42*, 283.
(460) Bennett, J. M.; Cohen, J. M.; Artioli, G.; Pluth, J. J.; Smith, J. V. *Inorg. Chem.* **1985**, *24*, 188.
(461) Parise, J. B.; Day, C. S. *Acta Crystallogr., Sect. C* **1985**, *C41*, 515.
(462) Rudolf, P. R.; Saldarriaga-Molina, C.; Clearfield, A. *J. Phys. Chem.* **1986**, *90*, 6122.
(463) Smith, J. V.; Pluth, J. J.; Bennett, J. M. *Zeolites*, to be submitted.
(464) Ito, M.; Shimoyama, Y.; Saito, Y.; Tsurita, Y.; Otake, M. *Acta Crystallogr., Sect. C* **1985**, *C41*, 1698.
(465) Saldarriaga, L. S. de; Saldarriaga, C.; Davis, M. E. *J. Am. Chem. Soc.* **1987**, *109*, 2686.
(466) Pluth, J. J.; Smith, J. V. *Acta Crystallogr., Sect. C*, in preparation.
(467) Pluth, J. J.; Smith, J. V. *Nature (London)* **1985**, *318*, 165.
(468) Pluth, J. J.; Smith, J. V. *Acta Crystallogr., Sect. C* **1986**, *C42*, 1118.
(469) Keller, E. B. Doctoral Thesis, ETH, Zürich, 1987.
(470) Parise, J. B. Reference 14, p 271.
(471) Kniep, R.; Mootz, D.; Vegas, A. *Acta Crystallogr., Sect. B* **1977**, *B33*, 263.
(472) Kniep, R.; Mootz, D. *Acta Crystallogr., Sect. B* **1973**, *B29*, 2292.
(473) Schwarzenbach, D. *Z. Kristallogr.* **1966**, *123*, 161.
(474) Wright, A. F.; Leadbetter, A. J. *Philos. Mag.* **1975**, *31*, 1391.
(475) Arnold, H.; Brüggemann, W.; Müllner, M. *Z. Kristallogr.* **1982**, *159*, 10.
(476) Gerke, H.; Gies, H.; Luebau, F. *Z. Kristallogr.* **1982**, *159*, 52.
(477) Gies, H. *J. Inclusion Phenom.* **1986**, *4*, 85.
(478) Kamb, W. B. *Science (Washington, D.C.)* **1965**, *148*, 232.
(479) Gies, H. *Z. Kristallogr.* **1983**, *164*, 247.
(480) Marler, B.; Dehnbostel, N.; Eulert, H.-H.; Gies, H.; Liebau, F. *J. Inclusion Phenom.* **1986**, *4*, 339.
(481) Engel, N.; Yvon, K. *Z. Kristallogr.* **1984**, *169*, 165.
(482) Galli, E. Reference 11, p 205.
(483) Wenk, H. R. *Z. Kristallogr.* **1973**, *137*, 113.
(484) Merlino, S. *Acta Crystallogr., Sect. B* **1974**, *B30*, 1262.
(485) Guiseppetti, G.; Mazzi, F.; Tadini, C. *Tschermaks Mineral. Petrol. Mitt.* **1977**, *24*, 1.
(486) Rossi, G.; Tazzoli, V.; Ungaretti, L. *Am. Mineral.* **1974**, *59*, 335.
(487) Cannillo, E.; Coda, A.; Fagnani, G. *Acta Crystallogr.* **1966**, *20*, 301.
(488) Coda, A.; Ungaretti, L.; Giusta, A. D. *Acta Crystallogr., Sect. B* **1974**, *B30*, 396.
(489) Domeneghetti, M. C.; Rossi, G.; Tazzoli, V. R. *Soc. Ital. Mineral. Petrol.* **1981**, *37*, 994.
(490) Schichl, H.; Vollenkle, H.; Wittman, A. *Monatsh. Chem.* **1973**, *104*, 854.
(491) Merlino, S. *Science (Washington, D.C.)* **1974**, *166*, 1399.
(492) Alberti, A.; Vezzalini, G. Reference 13, p 834. (a) Barrer, R. M. *Pure Appl. Chem.* **1986**, *58*, 1317.
(493) Merlino, S. *Acta Crystallogr., Sect. C* **1981**, *C37*, Suppl. 189.
(494) Evans, H. T., Jr. *Am. Mineral.* **1973**, *58*, 412.
(495) Rinaldi, R.; Pluth, J. J.; Smith, J. V. *Acta Crystallogr., Sect. B* **1975**, *B31*, 1598.
(496) Smith, J. V., in preparation.
(497) Kampf, A. R.; Khan, A. A.; Baur, W. H. *Acta Crystallogr., Sect. B* **1973**, *B29*, 2019.
(498) Khan, A. A.; Baur, W. H. *Science (Washington, D.C.)* **1971**, *173*, 916.
(499) Solov'eva, L. P.; Borisov, S. V.; Bakakin, V. V. *Sov. Phys.—Crystallogr. (Engl. Transl.)* **1972**, *16*, 1035.
(500) Moore, P. B.; Shen, J. *Nature (London)* **1983**, *306*, 356. (a) Moore, P. B.; Gupta, P. K.; Schlemper, E. O.; Merlino, S. *Am. Mineral.*, submitted.
(501) Vaughan, D. E. W.; Lussier, R. J. Reference 11, p 94.
(502) Smith, J. V.; Schreyer, W. *Mineral. Mag.* **1962**, *33*, 226.
(503) Goldman, D. S.; Rossman, G. R.; Dollase, W. A. *Am. Mineral.* **1977**, *62*, 1144.
(504) Cohen, J. P.; Ross, F. K.; Gibbs, G. V. *Am. Mineral.* **1977**, *62*, 67.
(505) Hochella, M. F., Jr.; Brown, G. E., Jr.; Ross, F. K.; Gibbs, G. V. *Am. Mineral.* **1979**, *64*, 337.
(506) Carson, D. G.; Rossman, G. R.; Vaughan, R. W. *Phys. Chem. Minerals* **1982**, *8*, 14.
(507) Johannes, W.; Schreyer, W. *Am. J. Sci.* **1981**, *281*, 299.
(508) Armbruster, T. *Phys. Chem. Minerals* **1985**, *12*, 233.
(509) Schreyer, W. *Bull. Mineral.* **1985**, *108*, 273.
(510) Ghose, S.; Wan, C.; Chao, C. Y. *Can. Mineral.* **1980**, *18*, 503.
(511) Hess, H. *Neues Jahrb. Mineral. Mh.* **1983**, 385.
(512) Rastsvetaeva, R. K.; Simonov, V. I.; Belov, N. V. *Dokl. Akad. Nauk SSSR* **1967**, *177*, 832.
(513) Averbuch-Pouchot, M. T.; Durif, A.; Guitel, G. C. *Acta Crystallogr., Sect. B* **1976**, *B32*, 1533.
(514) Moore, P. B.; Araki, T. *Nature (London), Phys. Sci.* **1972**, *239*, 25.
(515) Moore, P. B. *Am. Mineral.* **1969**, *54*, 1005. (a) Ferraris, G.; Mellini, M.; Merlino, S. *Am. Mineral.* **1987**, *72*, 382.
(516) Kobayashi, A.; Sasaki, Y. *Chem. Lett. Jpn.* **1975**, 1123.
(517) Strandberg, R. *Acta Chem. Scand., Ser. A:* **1975**, *A29*, 359.
(518) Evans, H. T., Jr.; Konnert, J. A. *Am. Mineral.* **1978**, *63*, 863.
(519) Ghose, S.; Sen Gupta, P. K.; Campana, C. F. *Am. Mineral.* **1987**, *72*, 365.
(520) Buerger, M. J.; Dollase, W. A.; Garaycochea-Wittke, I. *Z. Kristallogr.* **1967**, *125*, 92.
(521) Ilyshin, G. D.; Voronkov, A. A.; Ilyushin, V. V.; Nevskii, N. N.; Belov, N. V. *Sov. Phys. Dokl.* **1981**, *26*, 808.
(522) Cannillo, E.; Rossi, G.; Ungaretti, L. *Am. Mineral.* **1973**, *58*, 106.
(523) Perrault, G.; Boucher, C.; Vicat, J.; Cannillo, E.; Rossi, G. *Acta Crystallogr., Sect. B* **1973**, *B29*, 1432.
(524) Blinov, V. A.; Voronkov, A. A.; Ilyukhin, V. V.; Belov, N. V. *Sov. Phys. Dokl.* **1975**, *19*, 397.
(525) Vorma, A. *Mineral. Mag.* **1963**, *33*, 615.